Pure and Mixed Strategies in Cyclic Competition: Extinction, Coexistence, and Patterns

Ben Frederick Martir Intoy

Dissertation submitted to the Faculty of the
Virginia Polytechnic Institute and State University
in partial fulfillment of the requirements for the degree of

Doctor of Philosophy
in
Physics

Michel J. F. Pleimling, Chair
Giti A. Khodaparast
Leo E. Piilonen
Uwe C. Täuber

March 25, 2015
Blacksburg, Virginia

Keywords: Evolutionary Game Theory, Population Dynamics, Non-Equilibrium Statistical Physics, Pattern Formation

Pure and Mixed Strategies in Cyclic Competition: Extinction, Coexistence, and Patterns

Ben Frederick M. Intoy

(ABSTRACT)

We study game theoretic ecological models with cyclic competition in the case where the strategies can be mixed or pure. For both projects, reported in [49] and [50], we employ Monte Carlo simulations to study finite systems.

In chapter 3 the results of a previously published paper [49] are presented and expanded upon, where we study the extinction time of four cyclically competing species on different lattice structures using Lotka-Volterra dynamics. We find that the extinction time of a well mixed system goes linearly with respect to the system size and that the probability distribution approximately takes the shape of a shifted exponential. However, this is not true for when spatial structure is added to the model. In that case we find that instead the probability distribution takes on a non-trivial shape with two characteristic slopes and that the mean goes as a power law with an exponent greater than one. This is attributed to neutral species pairs, species who do not interact, forming domains and coarsening.

In chapter 4 the results of [50] are reported and expanded, where we allow agents to choose cyclically competing strategies out of a distribution. We first study the case of three strategies and find through both simulation and mean field equations that the probability distributions of the agents synchronize and oscillate with time in the limit where the agents probability distributions can be approximated as continuous. However, when we simulate the system on a one-dimensional lattice and the probability distributions are small and discretized, it is found that there is a drastic transition in stability, where the average extinction time of a strategy goes from being a power law with respect to system size to an exponential. This transition can also be observed in space time images with the emergence of tile patterns. We also look into the case of four cyclically competing strategies and find results similar to that of [49], such as the coarsening of neutral domains. However, the transition from power law to exponential for the average extinction time seen for three strategies is not observed, but we do find a transition from one power law to another with a different slope.

This work was supported by the United States National Science Foundation through grants DMR-0904999 and DMR-1205309.

Dedication

Dedicated to my aunt, who always supported
the education of my sisters and me:

Melinda P. Intoy
October 22, 1959 - September 12, 2013

"Your education can never be taken away from you."

Acknowledgments

First and foremost, I would like to thank my advisor Professor Michel Pleimling, who always found time in his busy schedule to meet and discuss, and whose advice, insight, and guidance made all this possible. I am also very thankful for his support in letting me pursue my own ideas.

Thanks to Professor Uwe Täuber for his advice and suggestions, as well as discussions with my committee members Professors Giti Khodaparast and Leo Piilonen.

A special thanks to the administrative and support staff of the physics department: The previous graduate program coordinator, Chris Thomas (may she rest in peace), and the current, Betty Wilkins, and the previous program support technician, Betty Wilkins, and the current, Sarah Sullivan. Thanks to Roger Link and Travis Heath for allowing me to use the physics department's computational resources, helping me whenever I had computer trouble, and forgiving me whenever I broke and/or slowed the network and/or computer systems.

I also thank the many students (graduate and undergraduate) I have met while at Virginia Tech who helped me out one way or another (and not necessarily in research). In no particular order they are Nasrin Afzal, Hiba Assi, Brandon Bear, Nicholas Borchers, Adam Bowman, Bart Brown, Kristen Brown, Carter Chamberlain, Eric Christensen, Harshwardhan Chaturvedi, Sheng Chen, Ulrich Dobramysl, Sven Dorosz, Wade Duvall, Shadi Esmaeili, Nicholas Gray, Qian He, Patrick Jaffke, Shivakumar Jolad, Hyunju Kim, Zachary Lewis, James Mayberry, Michael Meeker, Shahir Mowlaei, Curtis Ogle, Matthew Raum, Yoh Yamamoto and many others.

I thank my parents, Bienvenido and Joann, and siblings, Janis and Erika, for their support and escape from graduate school life.

Contents

List of Figures

List of Tables

Chapter 1

Introduction

We begin this thesis by briefly going over topics that the reader may be unfamiliar with. These topics will help motivate the research and results in latter chapters. In the final section of this chapter a summary of the thesis is given to further prepare the reader.

1.1 Overviews

In this section brief overviews of topics relevant to this thesis are given, mainly Population Dynamics, Game Theory, and Evolutionary Game Theory.

1.1.1 Population Dynamics

Population dynamics was first started around the late 1700's and was predominately used in demography, specifically to understand the changes in population over time. A well known example are the studies of Thomas Robert Malthus and his book *An Essay on the Principle of Population* [66], first published in 1798 and revised many times. Malthus formulated one of the first growth models where the rate of growth of a population is proportional to the current population. This is known as Malthusian growth and results in exponential growth. Mathematical biologists later used population dynamics to study ecological systems, and formulated predator prey models. One of the better known examples is the Lotka-Volterra equations, also known as the predator-prey equations. Alfred J. Lotka formulated them in the 1920's for oscillating chemical reactions [63] and later used them as an approximation of predator prey models in his book [64]. Vito Volterra used them to describe fish in the Adriatic sea [118]. The Lotka-Volterra equations have many biological examples, including hares and lynxes [61], and marine phages [33]. This model has been extensively studied in physics [20–23, 70–72, 109, 110, 122].

1.1.2 Game Theory

Game theory developed into a field of its own in the late 1920s with a publication and book by John von Neumann [77, 119] and became popular to mathematicians in the 1950s. It is a rational form of decision making that maximizes the gains of an individual. However, optimizing the gains of the individual does not necessarily optimize the gains of the system as a whole. We use the following well known example known as the prisoner's dilemma to illustrate this.

The prisoner's dilemma was originally framed by Merrill Flood and Melvin Dresher working at the RAND Corporation in 1950 [83]. Later Albert Tucker formalized the game as follows:

> Two members of a criminal gang are arrested and imprisoned. Each prisoner is in solitary confinement with no means of speaking to or exchanging messages with the other. The police admit they don't have enough evidence to convict the pair on the principal charge. They plan to sentence both to a year in prison on a lesser charge. Simultaneously, the police offer each prisoner a Faustian bargain. If he testifies against his partner, he will go free while the partner will get three years in prison on the main charge. Oh, yes there is a catch . . . If *both* prisoners testify against each other, both will be sentenced to two years in jail. [83]

	Silent (Cooperate)	Testify (Defect)
Silent (Cooperate)	-1,-1	-3,0
Testify (Defect)	0,-3	-2,-2

Table 1.1: The normal form representation of the prisoner's dilemma game. The left column represents the decisions the first prisoner can make and the upper row represents the decisions the second prisoner can make. For each pair of decisions there is a pair of values that represent the payoffs to the first and second prisoners respectively.

In table 1.1 we present this version of the prisoner's dilemma in normal form. The game theoretic method to solve this game is take the perspective of the first prisoner and assume that the second prisoner has made a decision. If the first prisoner assumes the second prisoner has made the decision to stay silent then we may either stay silent as well, which gives a payoff of -1 (for one year in prison), or testify, which gives a payoff of zero (no years in prison). Comparing payoffs $0 > -1$, so if the second prisoner stays silent then the decision for the first prisoner should be to testify. If the first prisoner assumes the second prisoner has made the decision to testify then we may either stay silent, which gives a payoff of -3, or testify, which has a payoff of -2. Comparing payoffs $-2 > -3$, so if the second prisoner testifies then the decision of the first prisoner should be to also testify. It is now concluded

that the first prisoner should testify regardless of what decision the second prisoner makes, the same is also true for the second prisoner. The system is now at an equilibrium state where both prisoners choose to testify and both have a payoff of -2. However, there exists a configuration which is better off for both parties, and that is for the both of them to remain silent which gives them both a payoff of -1. It is because of this that the prisoner's dilemma has been used to study cooperation in economics and the behavioral sciences [3–5, 11, 32, 57]. Table 1.2 is the generalized prisoner's dilemma where there are arbitrary values for the reward (R), punishment (P), sucker (S) and temptation (T) payoff values and obey the condition $T > R > P > S$. We mentioned that both prisoners testifying (defecting) was an equilibrium. Specifically this is called a Nash equilibrium, whose brief definition is that no player can profitably deviate given the actions of the other players [82].

	Cooperate	Defect
Cooperate	R,R	S,T
Defect	T,S	P,P

Table 1.2: The normal form representation of the generalized prisoner's dilemma game, where $T > R > P > S$. The left column represents the decisions the first player can make and the upper row represents the decisions the second player can make. For each pair of decisions there is a pair of values that represent the payoffs to the first and second players respectively.

In the prisoner's dilemma we found that both players should defect and only defect. The act of playing a single strategy is known as a pure strategy in game theory. Instead of playing the same strategy every single time the game is played, the player can choose either to cooperate or defect randomly with possibly different probabilities. Choosing a strategy out of a probability distribution is known as a mixed strategy [82], and if there is no pure strategy Nash equilibrium in a game there is usually a mixed strategy Nash equilibrium.

1.1.3 Evolutionary Game Theory

Evolutionary game theory was introduced by John Maynard Smith and George R. Price in their publication [101] and better formalized by J. M. Smith in his book [99]. In the 1970s mathematical biologists started using evolutionary game theory and applying it to ecological models. In essence evolutionary game theory is the combination of game theory and population dynamics. The way it is implemented is different from game theory in that an agent's strategy is inherent, like a phenotype/genes, which changes with reproduction. The offsprings strategy differs from its parent(s) by a perturbation by mutation, and/or its strategy is a mixture of its parent's strategies (if the offspring has multiple parents). An agent's strategy then determines its fitness in a given environment. Agents that are more fit tend to survive and reproduce, and thus over time the system fills with agents

whose strategies have great fitness. However, not only do agents have to deal with the environment, but also with other agents. The fitness of an agent now not only depends on the environment, but also on the fitnesses and strategies of the other agents in the system. More about evolutionary game theory can be found in J. M. Smiths book [99], chapter 7 of [28], as well as other books written on the subject [25, 117].

Much like there is a notion of an equilibrium in game theory (Nash equilibrium), there is also notion of an equilibrium in evolutionary game theory called an evolutionary stable strategy (ESS). An ESS is supposed to be robust rather than optimal, much like Nash equilibria. If there is a population whose strategy is evolutionary stable it should be able to expunge invaders of a differing strategy. An ESS should also be able to invade populations of a differing strategy. Many of these facts are attributed to the fact that not only should an ESS do well when interacting with different strategies it should also do well when pitted against itself, as the number of agents with the ESS will grow. Most of the time the Nash equilibrium and ESS coincide, such is the case in the prisoner's dilemma. More about ESS can be found in the references that also discuss evolutionary game theory.

1.2 Examples of Cyclic Competition

Cyclic competition is a set of strategies that compete with each other in a non-transitive way. In terms of predator prey ecological systems this is rarely, or never, seen as usually food chains have an apex predator. The following are examples of cyclic competition that are given for motivation, although all of them have three species/strategies.

At this point in time there are no real systems which have four cyclically competing strategies. However we motivate the system as it is the minimal number of species where it is the case that there are species/strategies which do not interact/react, which is commonplace in complex food webs/chains.

1.2.1 In Nature

In nature the notable examples of cyclic competition are the lizard mating strategies in California [97, 98, 100], competing bacterial strains [52, 53, 55, 73, 76, 80], and plant systems [8,60,112]. Brief explanations of the lizard and bacterial systems, each having three "species" whose interactions are like that of the game Rock-Paper-Scissors (RPS), follow.

Side-blotched Lizards

Side-blotched lizards, scientific name *Uta stansburiana*, are abundant and commonly observed in the deserts of western North America. There are three distinctive males each with

different colored throats and different testosterone levels [92]. The orange throated males have the highest level of testosterone and are the most aggressive. They have the largest territories and thus, control the most females. The blue throated males have moderate testosterone and medium aggression. They control a small territory that contains only one female which they guard and form a pair bond with. Finally, the yellow throated lizards have the lowest level of testosterone and, rather than having a territory of their own, sneak around other lizards' territories.

The cyclic competition interactions come into play through the different male mating strategies. Orange beats blue, because the orange males are strong enough to take away the blue's female. Yellow beats orange, because the yellow males look like and mimic females, fool the orange, and mate with the orange's females. Blue beats yellow, because, due to the strong pair bond, the blue's female remains faithful.

The populations of the three different males were recorded from 1990-95 at the inner Coast Range of California and an oscillation was observed [97]. An explanation of why the populations might oscillate will be given in the background chapter.

Bacterial Strains

In [53] experiments were done using three strains of *Escherichia coli*. The three strains are colicin-producing, colicin-resistant, and colicin-sensitive. The colicin-sensitive strain does not produce the toxic colicin nor the immunity protein needed for resistance, it thus has more resources to devote towards reproduction and reproduces the fastest. The colicin-resistant strain has to use some resources to produce the immunity protein, and has a reproduction rate slower than the colin-sensitive. Finally the colicin-producing strain produces both the toxic colicin and the immunity protein (so it does not die by its own toxin), so it has the least resources for reproduction, and thus has the slowest reproduction rate of the three strains.

From what they produce and their reproduction rates we get a cyclic competition interaction. The colicin-producing defeats the colicin-sensitive, because the colicin toxin kills the sensitive strain. The colicin-resistant defeats the colicin-producing, because the resistant survives and outgrow the producing. Finally the colicin-sensitive defeats the colicin-resistant, because the sensitive outgrows the resistant.

It is important for coexistence of the three strains that there is a spatial structure (such as a petri dish) as the colicin-sensitive strain will quickly die in a well mixed system (beaker with a stirrer) if there is any colicin-producing strain [73].

1.2.2 In Social and Economic Systems

In this subsection we provide examples in social and economic systems which have cyclic competition. We start by looking at social systems, for which the only provided example is

people playing Rock-Paper-Scissors [120,121,127], and then economic systems. The economic system exemplified is a modified version of the public goods game. Originally the public goods games is much like that of the prisoner's dilemma, however adding another strategy can give rise to Rock-Paper-Scissor type dynamics.

Rock-Paper-Scissors

People playing Rock-Paper-Scissors is the most trivial social system example which has cyclic competition. Rock-paper-scissors is a hand game of Asian origin usually played by two people, where players simultaneously form one of three gestures with an outstretched hand [124]. The three hand gestures are rock, paper, and scissors, and the objective of the game is to select a gesture which defeats that of the opponent(s). Rock defeats scissors, scissors defeat paper, and paper defeats rock. If both players choose the same gesture the game is tied and the game is played again. With its intransitive strategies and simple rules it is used to test learning and intelligence algorithms [18, 84, 93].

In economics and game theory much theoretic work has been done [6,62,115], the main result being that the mixed strategy of choosing rock, paper, and scissors with equal probability is an equilibrium solution. However it is possible to see oscillations in the probabilities if one incorporates a delay or other dynamics in their system [46, 79]. Social scientists and theoretical physicists have even collaborated to perform experiments in which participants played RPS [120, 121, 127]. They even observed oscillations in the individual strategies.

Public Goods Game

The Public Goods game is a model most used to study cooperation. It was made famous in 1965 with the publication of Mancur Olsons book *The Logic of Collective Action* [81]. In this game players can contribute a portion of their resources to the group or keep it to themselves. The contributed resources are then combined, possibly increased depending on the model, and redistributed equally among the players regardless if they contributed or not [57, 81]. Although the optimal solution for the entire system is for everyone to contribute, that is not the case in game theory. In game theory if everyone contributed an individual can maximize their gains by not contributing at all and receiving the community share. If all players thought this way, soon there would be nobody contributing resources and everybody would keep their own resources for themselves. Someone who does not contribute to the community yet benefits from it is called a "free rider", and is also associated with the economic and social dilemma known as "The Tragedy of the Commons" [12, 35, 57].

Although in the Public Goods game a player can contribute any fraction of their resources to the group, in most models it is simplified by giving the player just two actions. The first action is to contribute all their resources. A player who does this is known as a cooperator. The second is to contribute nothing at all, and that kind of player is known as a defector.

Simplifying the public goods game like this makes it similar to the prisoner's dilemma [57]. By adding a different third strategy it is possible to induce Rock-Paper-Scissors type dynamics, and in all cases cooperators are always beaten/invaded by defectors.

One strategy that some models added was a rewarding strategy. In [107] the authors Attila Szolnoki and Matjaž Perc added a rewarding cooperator strategy, which offers additional reward resources to all cooperators around them at an additional cost. In their spatial simulations they found that the cyclic dominance is as follows. Defectors can invade cooperators, as is normal. Rewarding cooperators can outperform defectors, if the reward is large. Cooperators can spread through rewarding cooperators, as cooperators enjoy the benefits of rewarding cooperators but do not pay a cost.

The third strategy can also be volunteering. In [38, 103] Christoph Hauert et al. added a loner strategy. An agent who chooses the loner strategy refuses to participate and relies on a small fixed income. The loner strategy is thus risk-averse as they would not have to worry if there are many defectors in the system, however they do not get the benefits if the system is instead full of cooperators. The cyclic dominance is as follows. Again, defectors defeat cooperators. If the system is too full of defectors players can instead abstain from playing via the loner strategy. If there are almost no participants (mostly loners), small groups can form and it is beneficial to return to cooperation. A social experiment has been done using these dynamics by Bin Xu and Zhijian Wang [126] and saw a significant number of individuals cycle from cooperate, to defect, to loner, and back to cooperate.

Lastly, a third strategy that is seen in the literature is the joker strategy. In references [2,89] the authors have added a destructive strategy termed the joker strategy, named after the comic character the Joker seen in the Hollywood movie *The Dark Knight* (2008). An agent who chooses the joker strategy does not participate in the public good, destroys public goods and damages a common enterprise. The motivation for adding a destructive strategy is the notion that cooperation can be driven by fighting a common enemy/danger and is seen in both society and nature (see introduction of [2]). The cyclic dominance is as follows. As always, defectors defeat cooperators. Jokers outperform defectors, as defectors now receive negative benefits from being near a joker. Cooperators outperform jokers, as they can overcome the negative effects of the destructive jokers.

1.3 Thesis Summary

A brief summary of the thesis is written in this section, accentuating the main results for the body chapters.

In the first chapter of this thesis brief descriptions of topics relevant to motivation are given. The topics included are population dynamics, game theory, evolutionary game theory, and examples of cyclic competition.

In the second chapter of this thesis the background of this project is explored and relevant results of previous work in the field are overviewed. It is more technical than the introduction chapter and will help clarify and motivate techniques used in latter parts of this thesis. Topics and techniques relevant are mean field techniques, pattern formation, extinction and coexistence.

The third chapter of this thesis presents the results of a previously published paper [49] on the extinction of four cyclically competing species. The main results are as follows: (1) With four species competing cyclically with symmetric rates, we find that with no spatial structure the probability distribution it takes for a neutral species pair to dominate the system can be approximated as a shifted exponential with a characteristic slope. This shifted exponential is attributed to the system performing a random walk in population density space and is similar to a one-dimensional random walk on a finite line with an absorbing boundary on one end and a reflecting boundary on the other. (2) When spatial structure is added it is found that the probability distribution for domination takes on a nontrivial shape with two characteristic slopes. The two slopes correspond to systems that are short lived and systems that are long lived. It is found that the short lived states are those that are similar to that of a well mixed system where individual species domains die out. The long lived systems are those in which the neutral species form domains and the system coarsens, yielding a slower domain growth and coexistence. (3) Information about system dynamics is lost if one only looks at mean extinction times, which is common in the literature, and the probability distributions give more insight to the dynamics of the system.

The fourth chapter contains results of my recent work in mixed strategies in cyclic competition. It is different from the third chapter as we now allow agents to pick their strategy from a probability distribution, however the way the agents change their distributions is through reactions similar to that of Lotka-Volterra. The main results are as follows: (1) We find that depending on how discretized that probability distributions are for the agents, the stability of the system can possibly change. For three strategies we find that there is a clear transition from neutrally stable coexistence to stable coexistence. With four strategies the system always is neutrally stable, however the system now has two different regimes of neutrally stable coexistence. (2) Using same techniques used to mathematically analyze ecological systems, we find that the agents within our system synchronize the oscillations of their probability densities. This is shown to be the case by studying simple cases and comparing numerical integration of derived differential equations to numerical simulation. (3) All of these properties are observed when looking at space-time plots where pattern formation of tiles and oscillations appear when studying the one-dimensional system. The material is currently being reviewed for publication in Physical Review E, but has been submitted to arXiv [50].

In the final chapter we conclude the thesis with a brief summary of the body chapters as well as possible future work. In the appendices results for smaller projects are presented. These include the study of the period of oscillations for a different system dynamics scheme and relations between spatial covariances in the case of symmetric cyclic competition.

Chapter 2

Background

In this chapter we briefly and broadly go over what physicists have done and techniques used in modeling and analyzing ecological systems. A subset of these topics relevant to this thesis are then delved into, specifically mean field equations, pattern formation, extinction and coexistence.

2.1 Broad Overview

Due to its non-transitivity of strategies and interesting results, cyclic competition has been an interest of physicists. Many a dissertation has been written in the simple case of RPS interactions [40, 104, 125], and a plethora of results have been published.

A review of cyclic competition was recently published by Attila Szolnoki et al. [106]. Their review mostly focuses on pattern formation, the role and effects of mobility, and the spontaneous emergence of cyclic dominance, although they do touch upon other aspects as well, such as phase transitions, mean field equations, and mapping spatial mean field partial differential equations to the complex Ginzburg-Landau equations.

There are also non-equilibrium aspects to studying biological models, and a review by Edo Kussell and Marjia Vuceljia was recently published [59]. They take a more physical view and look at techniques and intuition gained from studying these systems. The non-equilibrium aspects they focus on are the impacts of noise and fluctuations on the systems, stability properties, and diversity. For some of the models they even present related biological experiments and encourage physicists to engage with experimental biologists.

The results of studying ecological models have also been proposed to be used in medical research, an example being the study of cancer tumors [58, 69].

The following sections in this chapter delve deeper in the results, techniques, and interests of

physicists. Specifically mean field equations, pattern formation, and extinction, coexistence, and biodiversity will be discussed.

2.2 Mean Field Equations

In this section we introduce a standard technique for deriving mean field equations for ecological systems. This technique is used to derive all mean field equations seen in this thesis. In terms of ecological and biological modeling this approach is used extensively [9,45,56,67,75]. The Lotka Volterra Rock-Paper-Scissor (RPS) model is discussed as a quick example, where [26] is used as a guide. We then motivate why and how these mean field equations become exact when the total system size becomes large.

2.2.1 Lotka Volterra RPS Well Mixed Mean Field Derivation

The Lotka Volterra RPS Well Mixed model is a simple urn model where we have N balls labeled A, B, and C which represent different particle types/species. For an elementary time step we randomly select two balls out of the urn and try to perform one of the following reactions.

$$\begin{aligned} A + B &\xrightarrow{p_a} A + A \\ B + C &\xrightarrow{p_b} B + B \\ C + A &\xrightarrow{p_c} C + C \end{aligned} \tag{2.1}$$

where A, B, and C correspond to particle types/species and the p_i's are probabilities. Since every reaction uses an input of two particles and outputs two particles the total number of particles is conserved in the system:

$$N_A + N_B + N_C = N \tag{2.2}$$

where N_i is the total number of species i.

With equations 2.1 we can easily write down the master equation for $P(\{N_m\}, \tau)$, which is

the probability to find the system in a particular configuration at time τ.

$$\begin{aligned} P(N_m;\tau+1) - P(N_m;\tau) = \\ =&\frac{p_a(N_A-1)(N_B+1)}{N(N-1)/2}P(N_A-1,N_B+1,N_C;\tau) \\ &+\frac{p_b(N_B-1)(N_C+1)}{N(N-1)/2}P(N_A,N_B-1,N_C+1;\tau) \\ &+\frac{p_c(N_C-1)(N_A+1)}{N(N-1)/2}P(N_A+1,N_B,N_C-1;\tau) \\ &-\frac{p_aN_AN_B+p_bN_BN_C+p_cN_CN_A}{N(N-1)/2}P(N_A,N_B,N_C;\tau) \end{aligned} \tag{2.3}$$

In mean field theory we are interested in the evolution of the averages, so we now define population densities to be:

$$\begin{aligned} A(\tau) \equiv \langle N_A/N\rangle_\tau \equiv \sum_{\{N_m\}}(N_A/N)P(N_m;\tau) \\ B(\tau) \equiv \langle N_B/N\rangle_\tau \quad , \quad C(\tau) \equiv \langle N_C/N\rangle_\tau \end{aligned} \tag{2.4}$$

We derive the differential equations of the averages by looking at the quantity $A(\tau+1)-A(\tau)$, etc., and plugging in the master equation 2.3. We neglect correlations by assuming $\langle N_iN_j\rangle = \langle N_i\rangle\langle N_j\rangle$ for $i \neq j$. Finally we take the limit for large population size ($N \to \infty$), defining $t \equiv \tau/N$, which can be regarded as continuous, and let $A(\tau+1) - A(\tau) \to (1/N)\partial_t A(t)$. This results in the mean field equations:

$$\begin{aligned} \partial_t A &= [k_aB - k_cC]A \\ \partial_t B &= [k_bC - k_aA]B \\ \partial_t C &= [k_cA - k_bB]C \end{aligned} \tag{2.5}$$

where we have made the substitution $k_i = 2p_i$. It can also be shown that there is a time conserved quantity, $A^{k_b}B^{k_c}C^{k_a}$, and that the system exhibits oscillations in the densities of A, B, and C if the system does not start at a fixed point.

For an analysis of these differential equations, we refer the reader to references [31,45]. In the case of many species and their mean field treatment we refer the reader to references [56,130].

Although not touched upon in this document, there are also advanced mathematical methods to describe ecological systems. Other techniques are using a complex Ginzberg-Landau approach [74, 106], field theory approaches [95, 110, 111, 113], and mapping to a quantum system [1].

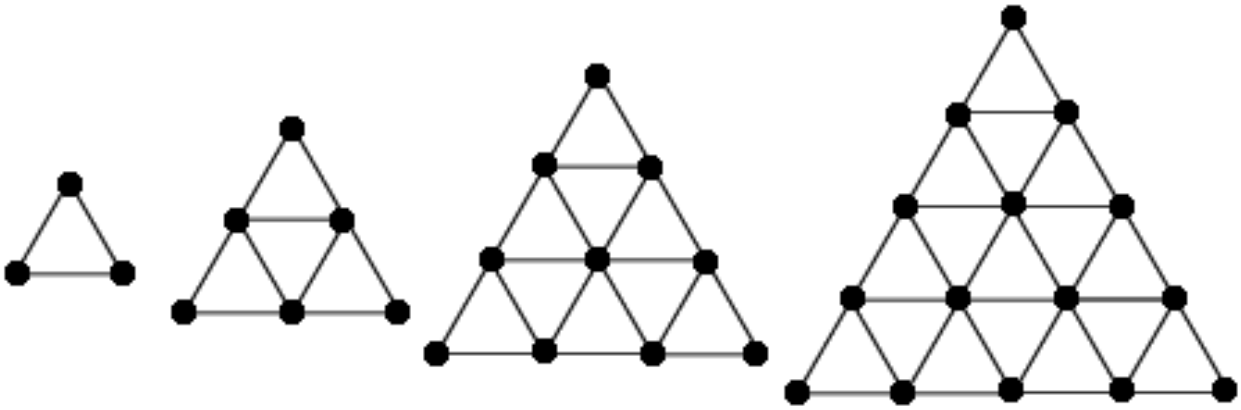

Figure 2.1: The state space for the well mixed Lotka-Volterra RPS for different values of the total population. From left to right $N = 1 \to 4$. The vertices represent states and the links represent pathways to and from states. The extreme corners represent absorption states where there is only one species left, and the extreme edges represent transient states.

2.2.2 Large System Size Limit for Mean Field Equations

In this section we motivate why the mean field equations for the well mixed Lotka Volterra model become exact as the system size goes to infinity. We will use our previous example of Rock Paper Scissors (RPS), but the reasoning can also be applied to models with greater numbers of species.

For the RPS well mixed Lotka Volterra model we have a conserved quantity, the total number of particles as seen in equation 2.2. So knowing the population of two species automatically tells us the population of the third, given that we know the total population. That means one would only need to know the population of two species to fully describe what state the system is in and thus the state space would be a plane, or more specific a 2-simplex (triangle). Figure 2.1 represents the state space in the case of RPS for different total populations N. As you increase N the number of states within the triangle increase. The reactions in equation 2.1, which take one state to a nearby state (either moving clockwise or counter-clockwise, depending on how each species correspond to a corner of the triangle), yield trajectories that look much like a random walk on the simplex. Recall the diffusion equation for a random walker with drift:

$$\partial_t P(x,t) = D\partial_x^2 P(x,t) - v\partial_x P(x,t) \tag{2.6}$$

where $P(x,t)$ is the probability density to find the random walker at location x at time t, D is the diffusivity constant, and v is the drift velocity. We can view the RPS system to be much like a random walk, as is done in reference [86]. However, this assumes that the Kramers-Moyal expansion terminates after two terms and that temporal correlations are small enough to be safely neglected. If for the state space we use $(N_a/N, N_b/N, N_c/N)$,

instead of using coordinates (N_a, N_b, N_c) then the distance between states would be $1/N$. When we derived the mean field equations, we changed the time variable to $t = \tau/N$, so a reaction would advance t by $1/N$. If we look at the units of the diffusivity constant, it is distance squared over time. As stated before, the distance per step goes as $1/N$ with time $1/N$ so distance squared over time would also go as $1/N$. So as $N \to \infty$ the diffusion term goes away and we are left with just the drift term, which yields the periodic orbits in configuration space.

The argument is more qualitative and will give insight into the well mixed system in the next chapter. It is seen in the literature that mean field equations approximate stochastic simulations of the well mixed system in the case of a large number of particles for the case of cyclically competing species [10, 24, 27]. However, there are cases when that is not the case and as an example we refer the reader to [22], where stochastic fluctuations drive the system from oscillations to the fixed point.

2.3 Pattern Formation

Patterns are found everywhere in nature. They appear on many length scales, from crystal structures, to snowflakes, from windswept sand dunes to clouds, and galaxy spirals [13]. There are many reviews on pattern formation in non-equilibrium physics [14, 34] as well as books [13, 19, 47]. Patterns can also be found in living systems, examples being tissue structure, slime-molds, and flocking [13, 19]. However, in this section examples of patterns found in simulations will be discussed.

In figure 2.2 several patterns that are found in the simulation of ecological models are displayed. In figure 2.2a a snapshot of the standard Lotka-Volterra predator prey system is shown. If A and B were predator and prey respectively then the reactions for this model would be:

$$\begin{aligned} A &\to \varnothing \\ A + B &\to A + A \\ B &\to B + B \end{aligned} \tag{2.7}$$

each with their own reaction rates. The first represents predators dying out, the second is a combination of predation and reproduction for the predators, and the last is reproduction for the prey. Although not displayed in reaction form, spatial diffusion is also taking place in the system. Depending on the reaction rates the Lotka-Volterra model in two dimensions could be in either an active or extinction phase. Figure 2.2a shows the system in the active phase, where there are activity fronts of reproducing prey followed by predators. This yields a spatio-temporal pattern reminiscent of fronts. More information can be found in reference [71].

Figure 2.2b is the case of four species competing cyclically on a two-dimensional lattice using May-Leonard dynamics [68]. It differs from that of Lotka-Volterra dynamics seen in equation

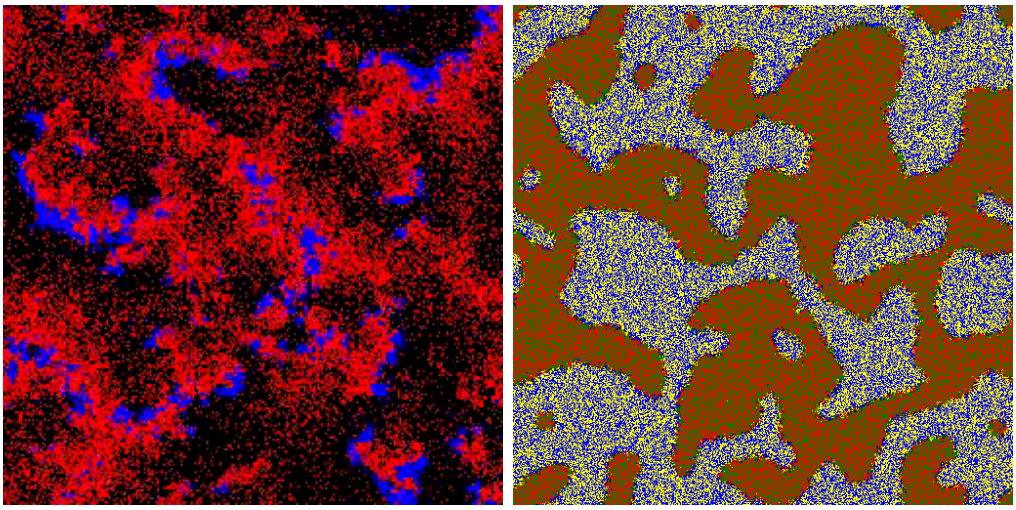

(a) Fronts. **(b)** Coarsening.

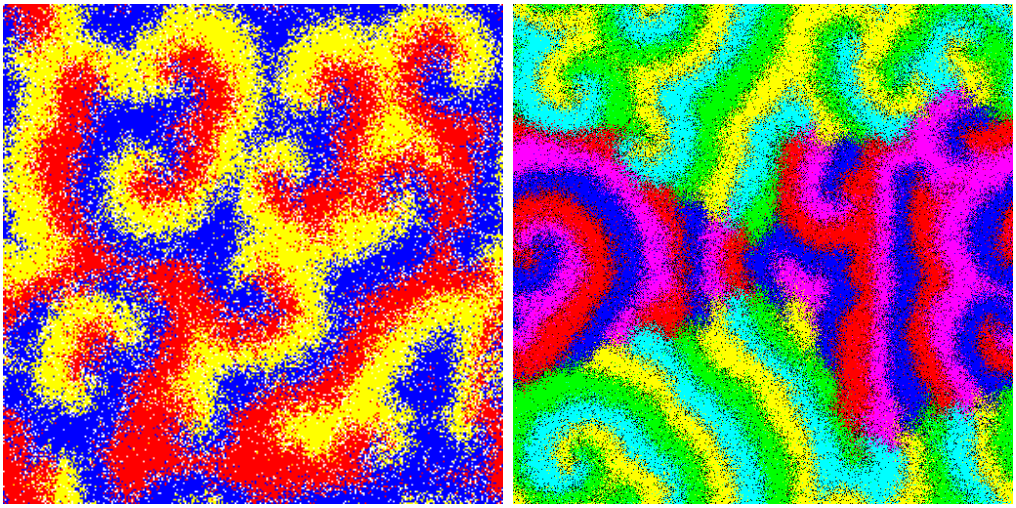

(c) Spirals. **(d)** Coarsening Spirals.

Figure 2.2: Patterns found in the simulation of ecological models. Each image is a snapshot of a two-dimensional system with differing dynamics, although in all cases black pixels denote empty sites. (a) Wave fronts Lotka-Volterra predator prey model where the blue are prey and red are predators, image credit goes to Uwe Täuber [71]. (b) Coarsening in four cyclically competing species using May-Leonard dynamics, note that each domain contains two neutral species pair, image credit goes to Bart Brown. (c) Spirals in three cyclically competing species using May-Leonard dynamics, image credit goes to Shadi Esmaeili. (d) Coarsening spirals with six cyclically competing species preying on the three ahead using May-Leonard dynamics. Notice that there are two domains each with spirals in them. Image credit goes to Shadi Esmaeili.

2.1 by particle conservation being broken during the reactions:

$$\begin{aligned} A + B &\to A\,, \quad B + C \to B \\ C + D &\to C\,, \quad D + A \to D \end{aligned} \tag{2.8}$$

where all the reaction rates are equal. There is also reproduction of the form $X \to X + X$ with its own rate, where X denotes any species. Notice that in these equations there are two species pairs that do not react with one another, AC and BD. These are called neutral species pairs and tend to form domains with one another. These domains coarsen slowly and yield long-living transient states. The image was kindly provided by Bart Brown, a graduate student advised by professor Michel Pleimling studying the dynamics of empty sites in May-Leonard cyclic competition models. For more information we refer the reader to reference [91].

Figure 2.2c is the case of three species competing cyclically on a two dimensional lattice using May-Leonard dynamics. The reactions are similar to that of equation 2.8, but instead of four species there are three. This is a very interesting case as spirals of the species chasing one another are formed. In the image the yellow chases the blue, the blue chases the red, and the red chases the yellow. A note about spirals is that they only happen with May-Leonard dynamics and do not happen with Lotka-Volterra dynamics. The image was kindly provided by Shadi Esmaeili, a graduate student advised by professor Michel Pleimling studying the effects of perturbation in the generalized cyclic competition model. More information about the spirals and their stability can be found in the following references [42, 51, 87, 88, 105].

Finally 2.2d is the case of six cyclically competing species who prey on the three species ahead of them using May-Leonard dynamics. If the species were identified as S_i where $i = 0 \to 5$, the equations would be written as:

$$\begin{aligned} S_i + S_{i+1} &\to S_i \\ S_i + S_{i+2} &\to S_i \\ S_i + S_{i+3} &\to S_i \end{aligned} \tag{2.9}$$

where the operator modulo six if the index were greater than five is applied. So species S_0 would prey upon S_1, S_2, and S_3, and etc. for the rest of the species. As you can see there are two domains, each consisting of three species, and within each domain the three species predate one another and form spirals. This image was also kindly provided by Shadi Esmaeili. More information can be found in reference [90].

Spatial Covariance, Correlation, and Correlation Length

Although spatial patterns produce beautiful images that are quite nice to look at, the snapshots do not give any quantitative data. One of the tools used to study pattern formation quantitatively are the spatial covariance and correlation functions. The spatial covariance

function between species i and j is defined as:

$$C_{i,j}(x,t) = \frac{1}{N}\sum_{y} S_i(y,t)S_j(y+x,t) - \left(\frac{1}{N}\sum_{y} S_i(y,t)\right)\left(\frac{1}{N}\sum_{y} S_j(y,t)\right) \tag{2.10}$$

where $S_i(x,t)$ is the number of species i located at position x at time t, and the sum is over all N lattice sites. Computationally the spatial covariance is usually calculated over many different runs to get an average over the realizations of the noise, also known as ensemble averaging. The spatial correlation can then be obtained by dividing both sides of equation 2.10 by the spatial variance, $C_{i,j}(t,0)$. An example for the use of spatial covariance would be the approximate determination of the width of spiral arms seen in figures 2.2c and 2.2d.

Using the spatial covariance/correlation, a correlation length $L(t)$ can be defined as the distance at which $C_{i,j}(x,t)$ drops to a portion of the value it has at $x = 0$. For times when the boundaries of domains cannot be very well defined, the correlation length is useful for approximating domain sizes and studying their growth.

2.4 Extinction and Coexistence

Although not delved into detail, the mean field equations in chapter 2.2.1 give oscillatory solutions in presence of a constant of motion. Even when there are exponential decay solutions for different reaction dynamics the system never reaches zero after a finite time due to the species populations being continuous variables. However in stochastic simulation, due to having a finite population, it is possible to reach extinction because of fluctuations. This is also true of real systems: although populations in nature may be very large, they still have a finite size.

For stochastic simulations the statistics of extinction, and complementary coexistence, gives insight into the stability of the system. In reference [24] the authors define different stability properties depending on how the mean extinction time, T_{ext}, scales with the population size, N. The system is considered to have stable coexistence if $T_{\text{ext}} \propto e^{aN}$, where a is a positive constant. Stable coexistence occurs when in deterministic dynamics (such as mean field equations) the coexistence state is an attractor, and extinction is driven by large rare fluctuations. Neutrally stable coexistence is the case where $T_{\text{ext}} \propto N^{\gamma}$, where γ is a positive number. This occurs when the deterministic dynamics predicts closed orbits corresponding to a constant of motion. Unstable coexistence, where $T_{\text{ext}} \propto \log N$, occurs when the deterministic solutions approaches, but does not go to, extinction and weak fluctuations bring the system to extinction.

As will later be explored in this thesis, pattern formation and average extinction times are related. In general adding spatial structure to an ecological model gives the possibility of domain formation, which usually increases survivability. In biology it is common that individual prey group together to reduce risk of predation, such as shoaling in fish [44].

There have also been experiments looking into the signs preceding the extinction and/or the collapse of a population strain of yeast playing the public goods game [16, 17, 94].

Chapter 3

Extinction in Cyclic Competition

In this chapter the results of my first publication [49] are presented.

3.1 Model and Algorithm

In this chapter we use the Lotka-Volterra reaction scheme for cyclic competition seen in the literature [10, 26, 27] which is:

$$\begin{aligned} A + B &\xrightarrow{\mu} A + A\,, \quad B + C \xrightarrow{\mu} B + B \\ C + D &\xrightarrow{\mu} C + C\,, \quad D + A \xrightarrow{\mu} D + D \end{aligned} \tag{3.1}$$

Our model is considered symmetric as all the reactions have the same rate/probability μ. We perform these reactions for the well mixed case (balls in an urn), in 1D with closed (line) and periodic (circle) boundary conditions, in 2D with closed (square) and periodic (torus) boundary conditions, and on a fractal called the Sierpinski Triangle shown in figure 3.1. The Sierpinski Triangle, also known as the Sierpinski Gasket or Sierpinski Sieve, is a fractal

Figure 3.1: The Sierpinski triangle after m iterations. From left to right: $m = 0 \to 4$.

with Haussdorff dimension $\log(3)/\log(2) \approx 1.585$. It is obtained by repeatedly dividing each triangular plaquette into four solid triangular plaquettes and removing the center. Since

we must have a finite number of lattice points in our simulation, I define the depth of a Sierpinski Triangle to be the number of times the triangle has been subdivided and the centers removed. Examples of how this depth refers to the Sierpinski Triangle is shown in figure 3.1. Notice that the total number of plaquettes is 3^m, where m is the depth, and that all plaquettes have three neighbors with the exception of the ones on the extreme corners which have two. This lattice structure implies a hierarchy of bottlenecks, i.e. lattice points through which one has to go when crossing from one part of the system to another. From this point of view the Sierpinski triangle is intermediate between the chain, where every lattice site can be viewed as being such a bottleneck, and the regular square lattice, where one has many equivalent paths between different parts of the system.

If not stated otherwise we prepare the system in an initial state where every lattice site is occupied with the same probability by one of the four species with no empty sites. For our algorithm we first randomly choose a lattice site and its neighbor. We then swap with rate/probability σ, which we set equal to $1 - \mu$ for computational efficiency. If the particles fail to swap and are able to perform a reaction seen in equation 3.1, they do so. However, if the particles picked are a neutral pair and fail to swap, nothing happens. We increase time by one unit (Monte Carlo time step) after N proposed updates, where N is the number of sites/individuals in the system. We stop the simulation when one neutral species pair, either AC or BD, is occupying the whole system. The time at which this happens is then taken as our lattice domination time. This domination time is closely related to the extinction time at which the first species goes extinct, as once a species dies out the prey of its prey, i.e. its partner, will also become extinct very rapidly.

In order to understand our results for the lattice domination time, we also study the average domain size of individual species as well as the average domain size of neutral species pairs. As shown in [91], the four species on a lattice tend to arrange themselves into domains, yielding ultimately a coarsening process of domains occupied by the mutually neutral species pairs. Study of these two different domain sizes allows us to relate the different phases of the coarsening process to the different regimes displayed by the probability distribution of the lattice domination time.

3.2 Domination Times

In this section we present lattice domination results for different lattice structures. This is adapted from my publication [49].

3.2.1 The Well Mixed Case Distributions and Means

We start by looking at the domination time τ in the simple case of a well mixed system without an underlying lattice structure. It has been shown in [24] that in the well mixed

four species case the mean extinction time increases linearly with the system size. In our simulations two particles are picked at random and allowed to perform a reaction following the scheme discussed previously. Since there is no spatial structure, we set the predation rate $\mu = 1$ (a different value of μ only rescales time). Initially, the system is filled with N particles with each assigned to one of the four species with equal probability.

The probability distribution $P(\tau)$ of the domination time is shown in figure 3.2a for different system sizes. Starting from a random mix, a non-zero minimum amount of time is needed for one of the neutral species pairs to dominate. Consequently, the probability distribution rises for small times until it reaches a maximum. The decaying part is well described by a shifted exponential distribution:

$$\tilde{P}(\tau) = \beta \mathrm{e}^{-\beta(\tau-\tau_0)}\Theta(\tau-\tau_0) \tag{3.2}$$

where Θ is the step function, with the shift τ_0 and the parameter β. This exponential distribution is a consequence of the fact that the system essentially performs an unbiased random walk in configuration space. The extinction of a species (which rapidly yields the extinction of its partner) can be viewed as a 1D random walk with a reflecting and absorbing boundary that starts at the reflecting boundary. Equation 3.2 captures this behavior and takes into account the fact that it takes some time for a species pair to dominate when starting from a random mix.

From the probability distribution we obtain how the mean and standard deviation of the domination time scale with system size:

$$\begin{aligned} \frac{T}{N} = \left\langle \frac{\tau}{N} \right\rangle &= \sum_{\tau=0}^{\infty} \frac{\tau}{N} P(\tau) \approx 0.2515(1) \\ \frac{\sigma_T}{N} &= \frac{\sqrt{\langle \tau^2 \rangle - \langle \tau \rangle^2}}{N} \approx 0.13967(2) \end{aligned} \tag{3.3}$$

see the inset of figure 3.2a. From equation 3.2 the relationships $\tau_0 = T - \sigma_T$ and $\beta = 1/\sigma_T$ also follow, from which one immediately deduces that the shift τ_0 is a linear function of N, whereas the parameter β varies inversely proportional to N.

It also follows from the shifted exponential distribution that data from different system sizes should collapse on a master curve when scaled properly. Indeed, exploiting directly the size dependence of the mean, $T = T_\infty N$, and the standard deviation, $\sigma_T = \sigma_\infty N$, as well as their relationships with τ_0 and β, equation 3.2 can be recast in the scaling form:

$$\tilde{P}'(\tau/N) = \frac{1}{\sigma_\infty} \mathrm{e}^{\tau_\infty/\sigma_\infty} \mathrm{e}^{(-1/\sigma_\infty)(\tau/N)} \Theta[(\tau/N) - \tau_\infty] \tag{3.4}$$

with $\tau_\infty = T_\infty - \sigma_\infty$. As verified in figure 3.2b, this scaling indeed works well.

We previously mentioned that the extinction of a species can be viewed as a 1D random walk. Here we motivate it by looking at the population density space. In the case of Lotka-Volterra

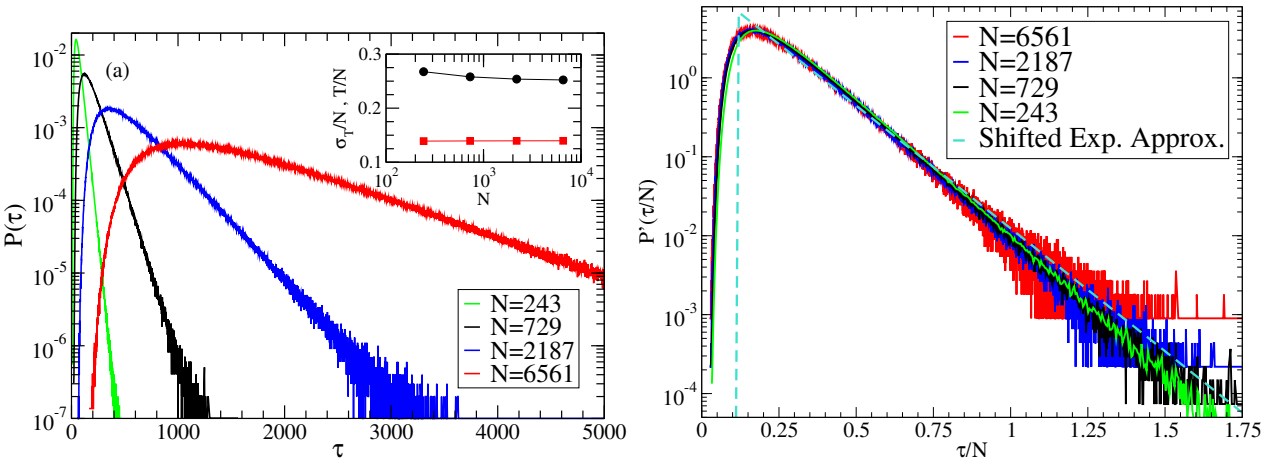

(a) Domination Distributions **(b)** Scaled Distributions

Figure 3.2: (a) Probability distribution of the domination time for different system sizes N in the well mixed case with $\mu = 1$. The inset shows that both the mean domination time T (black circles) and its standard deviation σ_T (red squares) increase linearly with the system size for not too small systems. (b) Scaling of the probability distribution with system size N as well as the shifted exponential fit, see equations 3.2 and 3.4. The probability distributions are obtained from at least seven million independent simulations.

dynamics the total population of particles is conserved and the population density state space for the Rock-Paper-Scissors model and the cyclic four species model can be portrayed in two (2-simplex) and three (3-simplex) dimensions, respectively, as seen in figure 3.3.

Approximating the orbits as circular we can represent the position of the system in population density state space by a radial and angular coordinate with respect to the fixed point, in the RPS model, or fixed line, in the case of four species. Under this scheme each deterministic orbit then has its own respective radial value. Ignoring the angular component, the system then behaves much like a random walker, going from one orbit to another, until it reaches an absorbing point, which in this case is its maximum radial distance. This thinking was also used in [86]. In order to check this approach, we simulate a random walk on a finite 1D lattice with one boundary being a reflection point and the other being an absorption point. An example of this is shown in figure 3.4a where we plot the distance from the fixed line as a function of time for a single run. Notice that it looks very much like a random walk, however the approximation of the orbits being circular breaks down as the radial distance increases and oscillations are seen. The walker starts at the reflecting point, which in the species model represents an equal population of all species, and the random walk represents the species densities going from one orbit to another. The system finally stops when the walker reaches the absorbing boundary, which represents extinction of one or more species and approximates the boundaries of the population density plots seen in figure 3.3. The

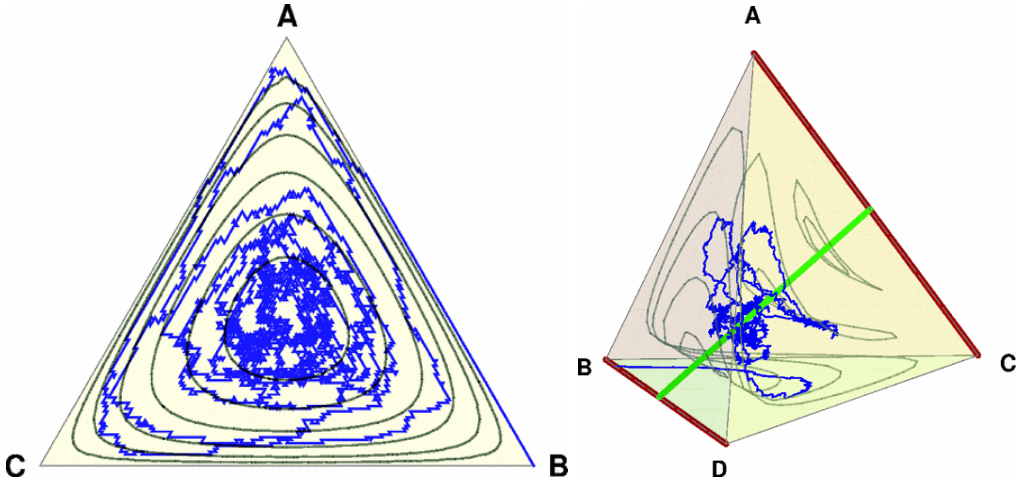

(a) Rock-Paper-Scissors. **(b)** Four Cyclically Competing Species.

Figure 3.3: (a) The population density space for the Rock-Paper-Scissors model represented as a triangle. The three corners represent absorbing points where either A, B, or C fully occupy the system. The gray lines represent the deterministic periodic orbit solutions for the mean field equations mentioned in chapter/section 2.2, and the blue line is an example of a stochastic trajectory given by simulation. (b) The population density space for the cyclic four species model represented as a tetrahedron. The four corners represent states where either A, B, C, or D fully occupy the system. Since the pairs AC and BD do not interact the absorption points lie along those lines and are represented in red. Like in (a) the gray lines represent the deterministic periodic orbit solutions for the mean field equations and the green line represents the line of fixed points. These figures were reprinted, with permission, from Alexander Dobrinevski and Erwin Frey, Physical Review E, Volume 85, published 2012 [24] Copyright 2015 by the American Physical Society.

frequency of absorbing times for the random walk system is shown in figure 3.4b. Notice that the shape is that of a shifted exponential, with the same qualitative features as those seen in figure 3.2.

1D Random Walk with an Absorbing and a Reflecting Boundary

We briefly explore the 1D random walk in this section, verify theoretical results, as well as compare it to the well mixed system.

During the 1960's there were many publications that reported theoretical findings on the absorption time of the 1D random walk with an absorbing and a reflecting boundary [7, 36, 37, 78, 123]. The probability for the walker to be absorbed at the zero boundary at time t,

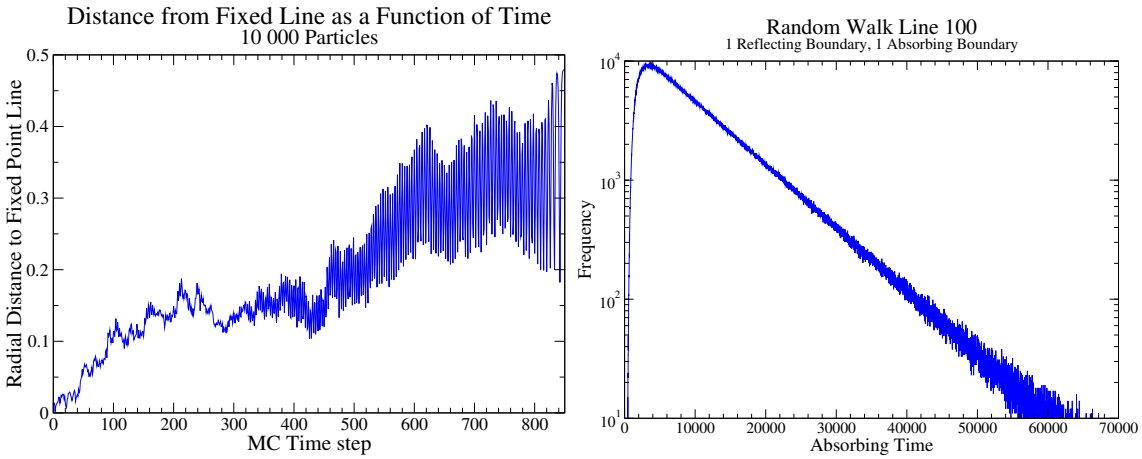

(a) Distance from Fixed Line **(b)** Random Walk

Figure 3.4: (a) A single simulation run which plots the distance from the fixed line for four species seen in figure 3.3b as a function of time. (b) The absorbing time results for an unbiased random walk on a 1D lattice of length 100 with a reflecting and an absorbing boundary.

given that at $t = 0$ the walk was at position i, is [36]:

$$q(t;i) = \frac{4p}{2b+1}\sum_{n=0}^{b-1}(-1)^n \text{ Sin}[\phi_n] \text{ Cos}[(b-i+1/2)\phi_n]\left(1-4p \text{ Sin}^2\left[\frac{\phi_n}{2}\right]\right)^{t-1} \tag{3.5}$$

Parameters in this equation are the position of the reflecting boundary (b), the probability to take a step left or right (p), and the special quantity $\phi_n = \frac{2n+1}{2b+1}\pi$, where $n = 0, 1, 2 \ldots b-1$.

We simplify equation 3.5 by assuming that the particle starts at the reflecting boundary ($i = b$) and that the particle always moves in an unbiased fashion ($p = 1/2$). Using trigonometric identities we now have the following:

$$P(t) = \frac{2}{2b+1}\sum_{n=0}^{b-1}(-1)^n \text{ Sin}[\phi_n] \text{ Cos}[\phi_n/2] \text{ Cos}^{t-1}[\phi_n] \tag{3.6}$$

We compare this equation with simulation in figure 3.5a and they agree very well. The mean and variance of the absorption time were also calculated in [37] and are given as:

$$\mu_i = i\left[\frac{1}{p} + \frac{1}{2p}(2b-i-1)\right] \tag{3.7}$$

$$\sigma_i^2 = \frac{1}{6p^2}\left\{(2b-i)(2b^2-2bi+i^2) + [6b(b-i)+2i^2+1-3p] + (2b-i)(2-3p)\right\} \tag{3.8}$$

Setting $i = b$ and taking the limit for large b gives that the mean and standard deviation go

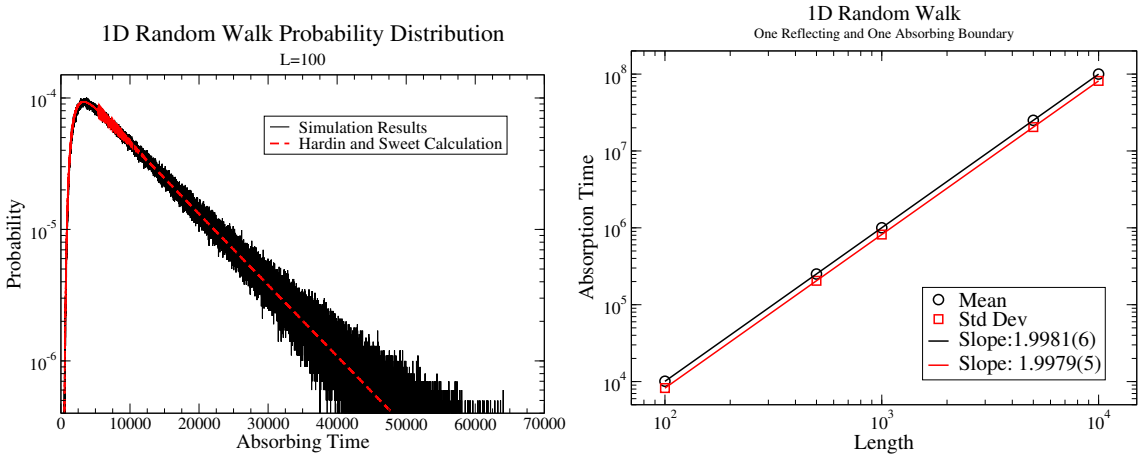

(a) Comparison of Theory and Simulation **(b)** Moments for Different Lengths

Figure 3.5: (a) The data seen in figure 3.4b compared with equation 3.5. (b) The mean and standard deviation of the absorption time.

approximately as:

$$\mu_b \approx \frac{b^2}{2p} \quad ; \quad \sigma_b \approx \frac{b^2}{p\sqrt{6}} \tag{3.9}$$

as you increase the length of the 1D line. We plot simulation results in figure 3.5 and find that for our data the mean and standard deviation indeed go as $\sim L^2$ when one increases the system size.

We notice that the mean and standard deviation of the absorbing time go as the square of the system size, whereas the mean and standard deviation of the lattice domination time go linearly with the system size. Comparing equations 3.9 and 3.3 we can identify N to be b^2, $(2p)^{-1} = 0.2525$, and $(p\sqrt{6})^{-1} = 0.13967$. Solving for p in the equations of the previous sentence gives $p = 1.9801$ and $p = 2.9229$ respectively, contradictory values so that means that the two models are not exactly alike, but qualitatively look similar (it also gives that $p > 1$, but we can rescale time so that it becomes less than one).

In figure 3.6 we compare the theoretical 1D random walk absorption distribution time with $b = 100$ (as seen in figure 3.5a) to the scaled domination time distribution for a well mixed system with $N = 243$ (as seen in figure 3.2b). We scaled the 1D random walk theoretical results by multiplying its x-axis by 0.154 (and dividing the y-axis to conserve probability) so that the slopes were equivalent which allows for a better comparison. Qualitatively the two curves seem very similar, however we see that the major difference between the two curves is during short times.

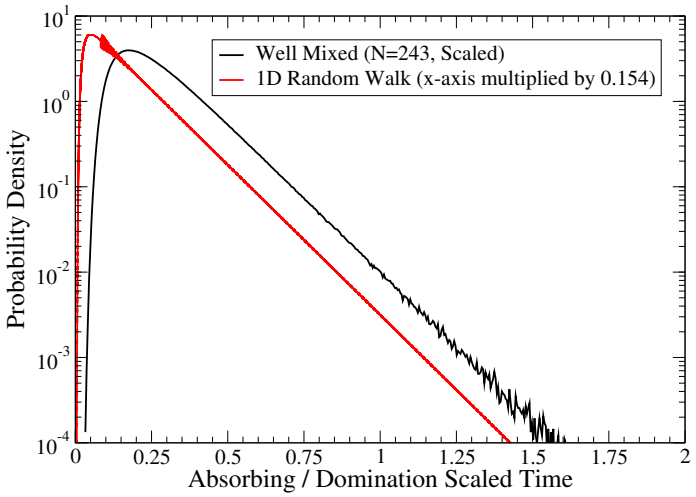

Figure 3.6: 1D random walk absorption time distribution compared to the domination distribution of a well mixed system. The 1D walk has been scaled such that the long time slopes match.

3.2.2 Domination Time Distributions for Lattice Systems

The four species cyclic game on the lattice is characterized by the competition between the two different teams composed of mutually neutral partners. As a result, coarsening of domains occupied by the different teams sets in [91]. These coarsening domains are compact and rarely contain individuals from the enemy team. In two space dimensions the domain boundaries are not very sharp due to relentless reactions (predation and swapping) taking place at these boundaries. See [91] for some configurations in one and two space dimensions. In figure 3.7 we show some snapshots from a typical run on the Sierpinski triangle. After preparing the system in a disordered initial state (a), small domains are rapidly formed (b), followed by a phase of domain growth (c). Due to the presence of bottlenecks that separate the lattice into different parts, one often observes that different parts of the lattice are occupied by different teams. This blocked situation can last for quite some time. For example, for the run shown in figure 3.7 not much is happening between the snapshots (c), taken at time $t = 510$, and (d), taken at $t = 5430$. Between these two times there are many excursions into enemy territory that fail. Eventually, one of these excursions is successful, and one of the teams takes over the whole lattice. The configuration (d) shows the beginning of that final excursion, just before the red and green species go extinct.

Team formation can also be seen in the 1D line system. Figure 3.8 has two space-time plots for the 1D line with $N = 243$. Figure 3.8a has no swapping and figure 3.8b has reaction rate $\mu = 0.6$ and swap rate $\sigma = 0.4$. For no swapping the neutral species pairs are stuck in one another and appear as stripes. However, when there is swapping the neutral species pairs diffuse into one another. The neutral domains then coarsen, as we will explain when we discuss figure 3.10 and the average domain sizes.

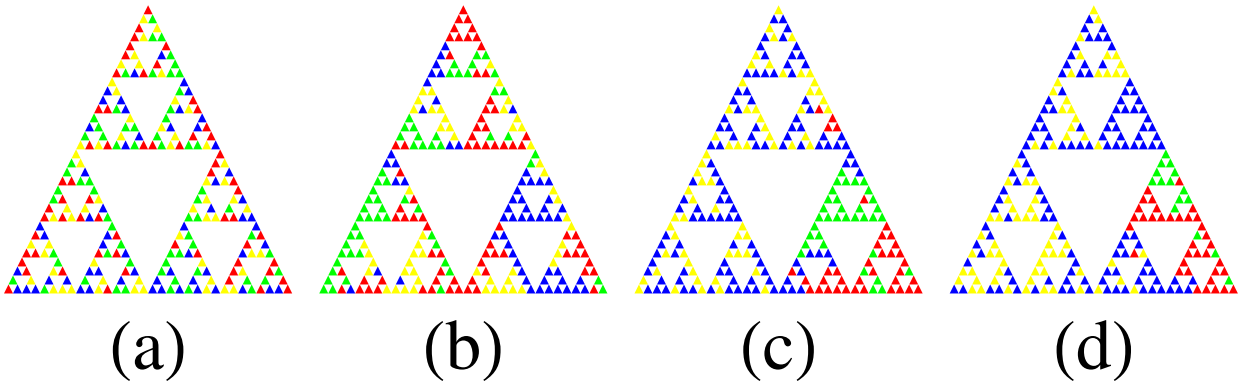

Figure 3.7: Snapshots of a simulation on the Sierpinski triangle with $\mu = 0.8$ and $\sigma = 0.2$. The system size is 243 (iteration depth $m = 5$). The snapshots are taken at times (a) $t = 0$ (initial state), (b) $t = 9$, (c) $t = 510$, and (d) $t = 5430$ (just before the yellow-blue team dominates the system). Time is measured in Monte Carlo steps. A video of this system can be seen at `http://youtu.be/afGMN6TR1Zg` and videos of other systems can be seen in reference [48].

In order to investigate species extinction in these lattice systems, we restrict ourselves to small systems. For the line and the Sierpinski triangle the sizes range from $N = 16$ to 2197, whereas in two dimensions we consider lattices from $N = 6 \times 6$ to 108×108 sites. For the studied systems we typically made millions of independent runs. We have studied one- and two-dimensional systems with both closed and periodic boundary conditions. However, as the results for periodic boundary conditions are very similar to those obtained in closed systems (there are of course quantitative differences, but qualitatively the studied quantities behave in similar ways for the different boundary conditions), we refrain from discussing in detail our results for periodic boundary conditions.

Figure 3.9 shows typical probability distributions of the domination time for the three different lattice types. While in all cases we observe an initial rise for small times and an exponential decay for long times, an additional intermediate regime is observed for the lattice systems that is absent in the well mixed case; compare with figure 3.2. Indeed, after the maximum a first exponential decaying regime is encountered before a crossover to the final exponential decay sets in. This final decay is much slower than for the well mixed case; see the inset. This intriguing shape of the probability distribution indicates the presence of two different time scales. As discussed in the following, these two different time scales correspond to two different routes to extinction.

Possible hints at the origin of these two time scales can be found in the average domain size. Due to the presence of mutually neutral species we need to distinguish between the average domain size of domains that contain individuals of only one species and the average size of the larger domains formed by neutral partners. The typical time dependences of these sizes are shown in figure 3.10 for the line containing 243 sites. Analysis of figures 3.10a and 3.10b

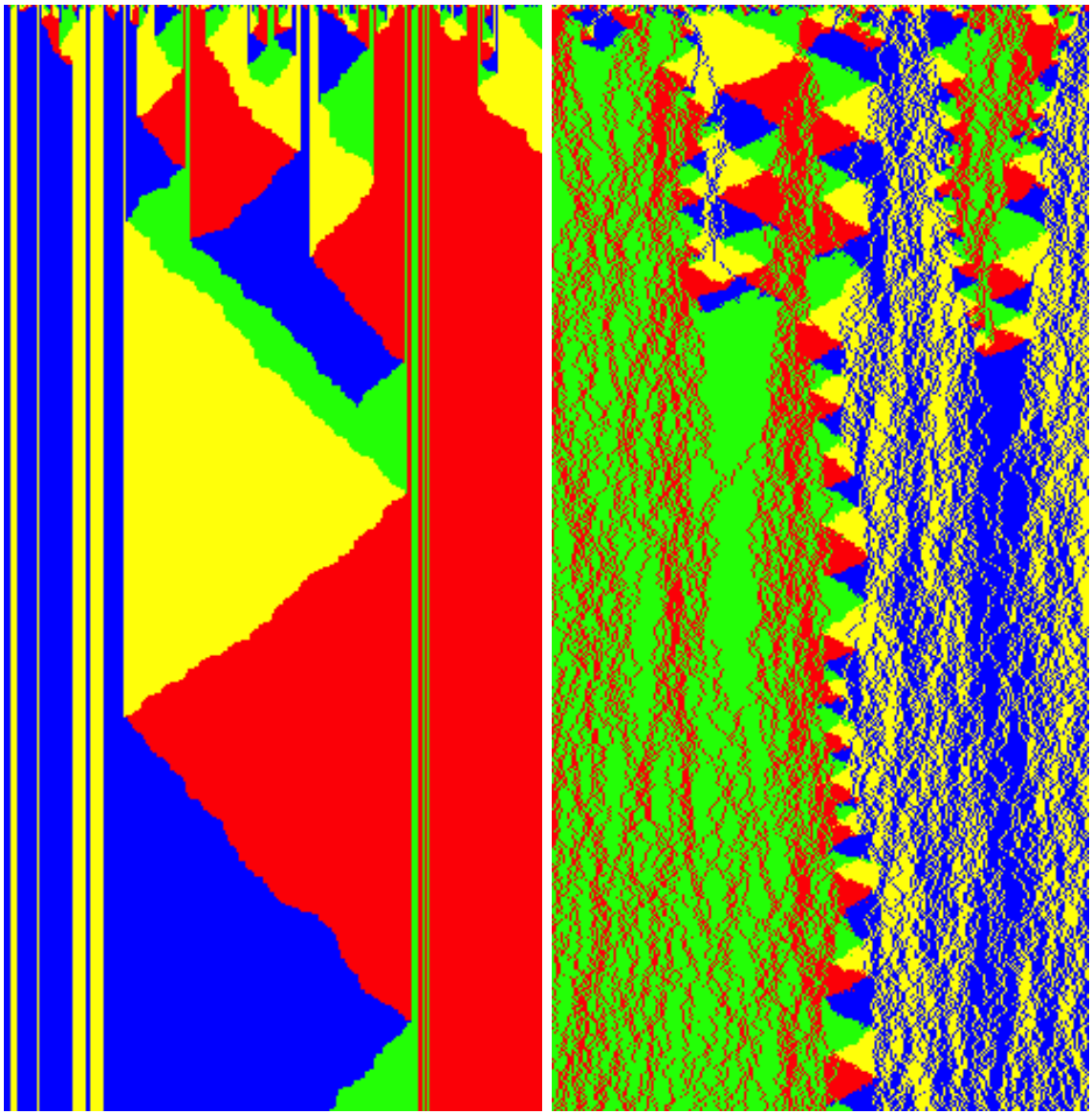

(a) $\mu = 1$ **(b)** $\mu = 0.6$

Figure 3.8: Space-time plots which show the first 500 time steps for four cyclically competing species on a 1D line lattice and $N = 243$. Space is in the horizontal direction and time increases in the downward direction. In (a) the reaction rate is set to one, so there is no swapping, the system ran for 2 414 time steps before lattice domination occurs. In (b) the reaction rate is $\mu = 0.6$ (swap rate $\sigma = 0.4$) and ran for 16 025 time steps before the lattice is dominated by one of the teams.

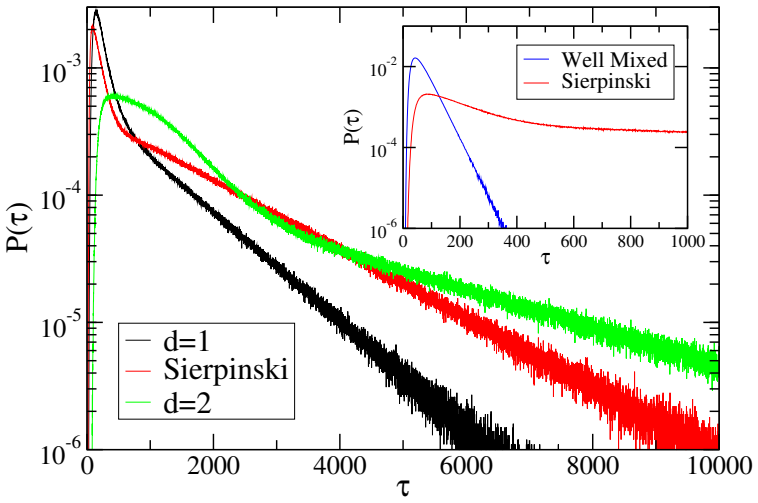

Figure 3.9: Typical probability distributions of the domination time for lattice systems. The one-dimensional chain contains $N = 81$ sites, with $\mu = 0.1$, whereas the Sierpinski triangle is formed by $N = 243$ sites, with $\mu = 0.5$. Finally, the square has $N = 45 \times 45$ sites, with $\mu = 0.6$. The swapping rates are always given by $\sigma = 1 - \mu$. Inset: comparison of the well mixed (see figure 3.2) and Sierpinski cases with the same number of individuals, $N = 243$.

reveals three different growth regimes.

As the initial preparation is a random state, many small single species domains composed of only very few individuals are formed initially. Some of them will keep growing at the expense of others. In this stochastic process species are eliminated locally, which can lead in some cases to the global extinction of one of the neutral pairs, hence the increase of the domination time probability visible in figure 3.9. The local dismissal of species will be followed by an increase in the encounters of neutral species domains, resulting in the strong increase of the neutral domain size seen in figure 3.10b as well as a decrease of the domination probability function. Concomitantly the neutral species start to diffuse into each other, yielding the decrease of the individual domain size seen in figure 3.10a. Once the neutral domains are well mixed, it becomes very difficult for a team to take over part of the system occupied by a competing team, as every species is confronted with a mixture of predators and prey. This yields a much slower domain growth, as witnessed by the change of slope in figure 3.10b, and the emergence of long-lasting transits which are revealed by the change of slope in figure 3.10c. The growing of individual domains and the coarsening of neutral domains can be seen in figure 3.8b. The simultaneity of these two events becomes obvious when including in figure 3.10b, see the circles, the domination time where the transition between the two exponential regimes in the probability takes place.

Let us add that the presence of the different regimes is a generic property of finite lattice systems, independent of system size N and the value of the reaction rate μ (that is not

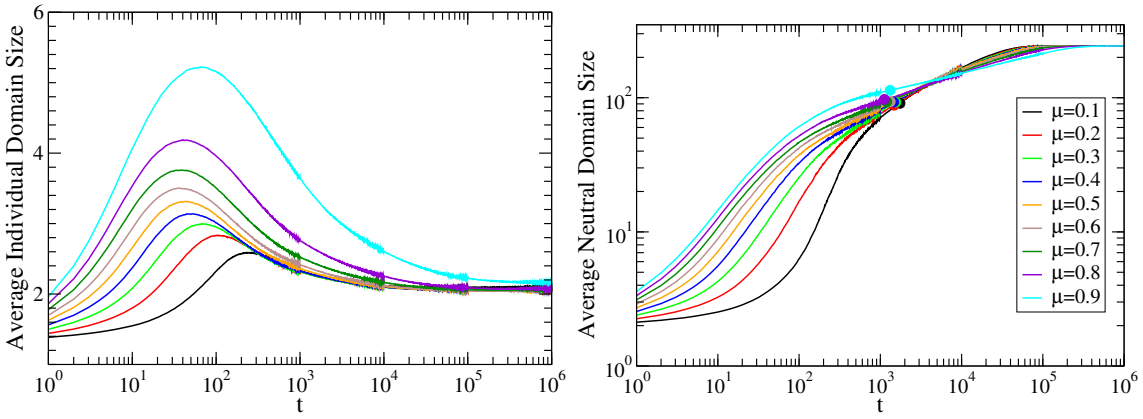

(a) Individual Domain Size **(b)** Neutral Domain Size

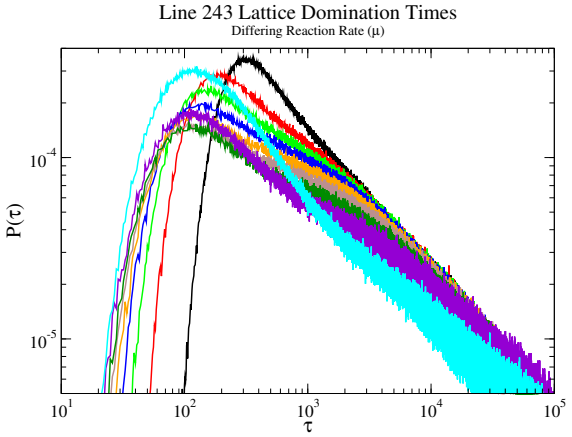

(c) 1D Dominations

Figure 3.10: (a) Average individual domain size and (b) average neutral domain size for the line composed of $N = 243$ sites. Data for different predation rates μ are shown, where the swapping rates are given by $\sigma = 1 - \mu$. The dots in (b) indicate where one passes from one exponential decaying regime to the next in the domination time distribution; see the change of slope in (c). The data result from averaging over 10 000 independent runs.

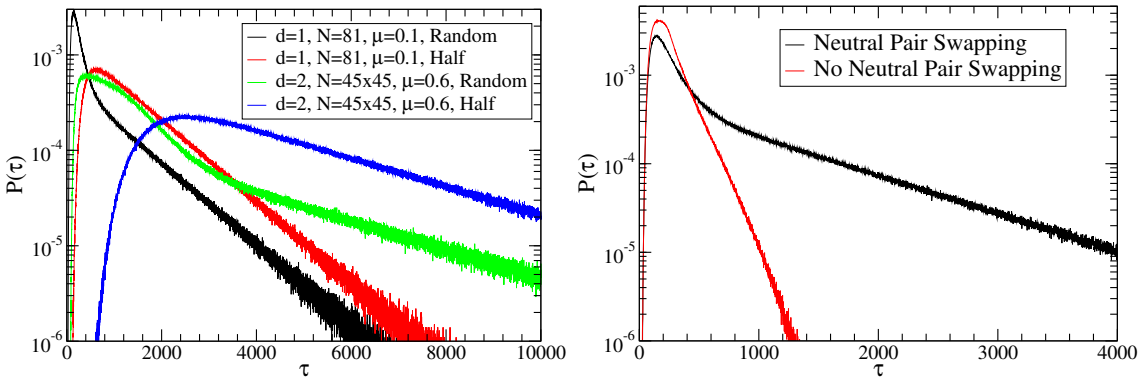

(a) Differing Initial Conditions **(b)** Neutral Swapping On and Off

Figure 3.11: Domination distributions for different initial conditions or swapping conditions. (a) Probability distributions of the domination time for the line and the square lattice with different initial conditions: random initial conditions as well as an initial state where the different teams each occupy half of the system and are arranged in such a way that every individual is surrounded by members of the partner species. (b) Probability distributions of the domination time for the line with and without neutral pair swapping. The long-lived states are absent without an efficient mixing mechanism between neutral partners. The system size is $N = 81$ and $\mu = 0.1$. The probability distributions result from more than 12 million independent runs.

exactly 0 or 1), provided that a mechanism is in place that allows partner pair domains to be well mixed. Only in the limit $\mu \ll 1$, when particles mainly swap places, is coarsening absent, and no long-lived states are encountered in the system.

Figure 3.11 provides further support for our interpretation of the processes involved. We first check in 3.11a whether these long-lived states are indeed due to the presence of well mixed neutral domains. For this we prepare the system in such a way that each half of the system is occupied by one of the partner pairs. In each half the two allying species are mixed completely by having every individual surrounded by members of the partner species (with the exception of the particles located at the interface between the two halves). For the line, this yields an initial state of the form $\cdots ACACACBDBDBD \cdots$, whereas for the square lattice we have a checkerboard of A, C and B, D particles in different halves. Figure 3.11a compares the probability distributions for the domination time obtained for these initial states with those that follow from random initial conditions. For both initial conditions the decay rate of the long-lived states is the same, indicating that these states are indeed due to the competition of a few very large well mixed domains.

In order to have well mixed domains composed of mutually neutral species, an efficient mechanism for the mixing of these species needs to be in place. This is realized in our system through swapping of neutral species with the rate $\sigma = 1 - \mu$. Without this swapping

mechanism we would expect the long-lived states to be completely absent, whereas the earlier stages of the coarsening process, that do no rely on this swapping mechanism, should be very similar. This is indeed the case; see figure 3.11b where we compare for the line with $N = 81$ sites and $\mu = 0.1$ the probability distributions with and without neutral pair swappings.

3.2.3 Lattice System Average Domination Times

The probability distributions of the domination time reveal many interesting features of the emerging spatio-temporal correlations due to the cyclic competition between species. It is obvious that much information is lost when only looking at the mean domination time (extinction time), as has been done in most recent studies. Still, because of the focus in the literature on this mean time, it is of interest to also discuss this quantity for our lattice systems.

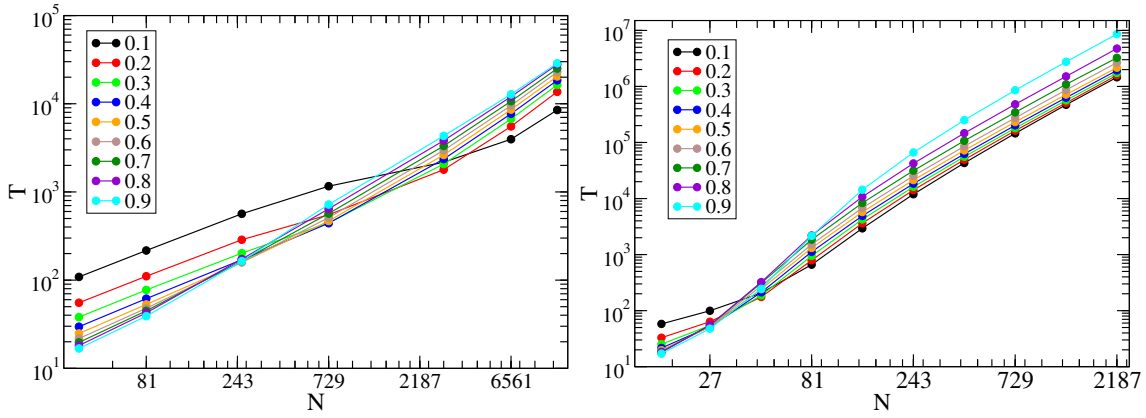

(a) 2D Square **(b)** 1D Line

Figure 3.12: The mean domination time T versus the total number of sites N for (a) the square with closed boundaries, with system sizes ranging from $N = 36 = 6 \times 6$ to $N = 11\,664 = 108 \times 108$, and (b) the line. The different data sets correspond to the different values of μ given in the legend. The swapping rates are $\sigma = 1 - \mu$. The data result from averaging over at least 100 000 independent runs.

Figure 3.12 shows the size dependence of the mean domination time T for different predation rate μ and swapping rates $\sigma = \mu - 1$. The data for the square, see figure 3.12a, clearly show a crossover between two regimes. For small system sizes the system behaves like a well mixed system, and the mean domination time increases approximately linearly with the system size. However, for the largest system sizes studied in this work spatial effects become important, and T varies algebraically, $T \sim N^{\alpha}$, with an exponent $\alpha \approx 1.45$. The same crossover is also present in the one-dimensional system, see figure 3.12b, but with a different exponent for

the larger systems. Fitting the data for the largest three system sizes to a power law yields an effective exponent $\alpha \approx 2.10$.

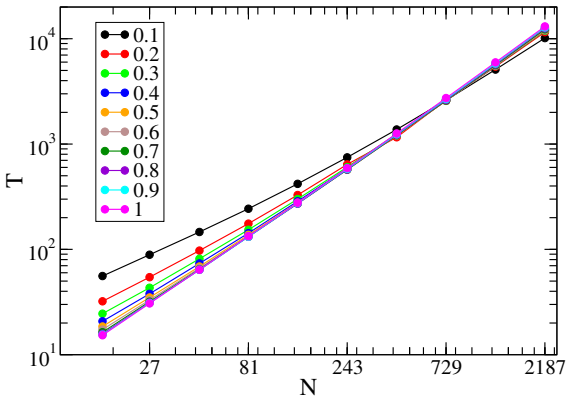

Figure 3.13: Average lattice domination times on the 1D line without neutral swapping. It is the same as figure 3.12b, but now without swapping between neutral partners. The data result from averaging over at least 100 000 independent runs.

We note that the crossover is also observed in the absence of neutral partner swappings, see figure 3.13. However, this crossover is much more gradual, presumably due to the absence of the long-lived states where well mixed domains coarsen very slowly. Another difference between this case and that of figure 3.12b is that in the absence of neutral swapping the mean domination times increases much more slowly for larger system sizes. Indeed, for large N we obtain $T \sim N^{\alpha}$ with $\alpha \approx 1.40$ for the 1D line.

Until this point for all the plots in this section we have kept the reaction rate fixed and changed the system size. We now keep the system size fixed and change the reaction/swap rate and study how it affects the mean lattice domination time as well.

In figure 3.14 we look at the means of the lattice domination time for systems with different lattice structures where the system size has been fixed and the reaction rate (μ) as well as the swapping rate ($\sigma = 1 - \mu$) are changed. Note that these plots tend to have local minima and local maxima with respect to μ which move depending on the system size. Although there are no visual minima near $\mu = 0$ for some of the plots, one has to exist, as the lattice domination time must go to infinity as μ approaches zero: In all cases the lattice domination time for $\mu = 0$ will be infinity as no reactions will take place. The μ value near zero, which corresponds to the minimum lattice domination mean, $\mu_{\min}$, asymptotically moves to zero as one increases the system size. The local maximum near $\mu = 1$, which we call $\mu_{\max}$, asymptotically increases to some value as one increases the systems size. For the 1D system (figures 3.14a and 3.14b) it is always found that $\mu = 1$ is a local minimum for any system of finite size, because of the faster coarsening in absence of a neutral pair mixing mechanism. For the 2D system $\mu = 1$ is not a local minimum. It can be seen in figures 3.14d and 3.14e that it actually becomes a local maximum when the system size increases. This transition seems to occur between $L = 16$ and 27 for the periodic 2D lattice, and between $L = 27$

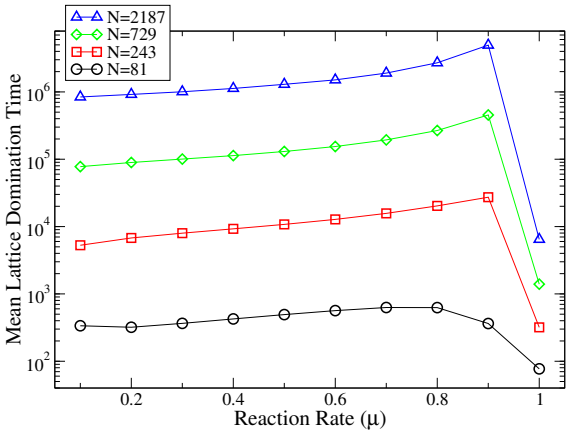

(a) 1D circle.

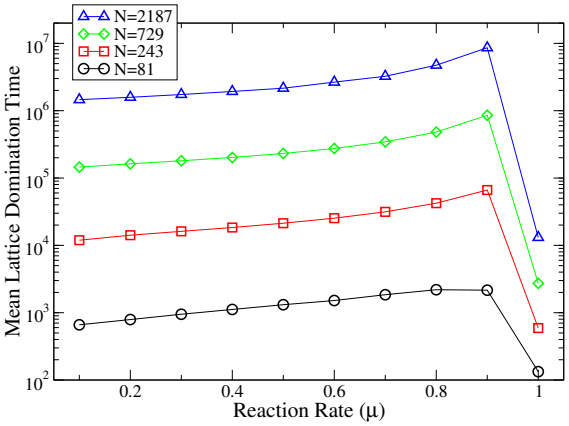

(b) 1D line.

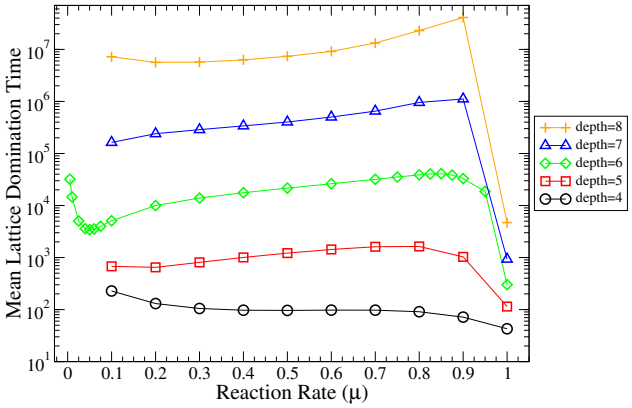

(c) Sierpinski Triangle.

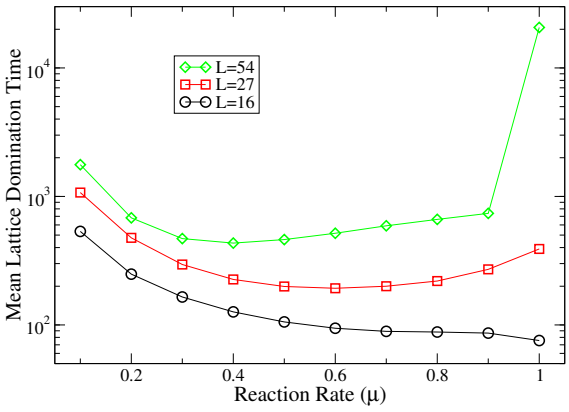

(d) 2D periodic with side length L.

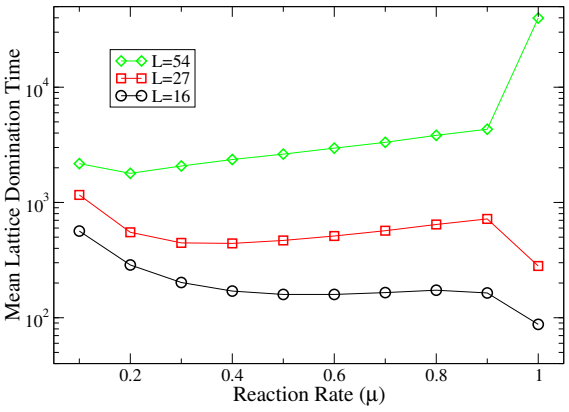

(e) 2D closed with side length L.

Figure 3.14: Lattice domination means for different lattice systems. We have fixed the system size and change the reaction rate. For the smaller system sizes the averages were done with around 10 million runs while the larger system sizes used at least half a million runs.

and 54 for the closed 2D lattice. In 1D with no swapping it is known that the interfaces eventually annihilate one another until there are no reactions possible [30], however this is not the case in 2D where the interfaces are now lines instead of points. A reason why this transition at $\mu_{\max}$ occurs is that in 2D, once the system size becomes large enough, it is possible for species to chase one another in species fronts and coexist, much like what is seen in coexistence states of the two species Lotka-Volterra model in 2D [71,122]. There has even been a paper on the relationship between the two models [43]. It is not known whether or not $\mu = 1$ is a local maxima/minima for the Sierpinski lattice, as the arguments used for 1D and 2D cannot be used for it. The only sure way to know would be to keep measuring lattice domination times for larger systems and seeing if a transition similar to that of figures 3.14d and 3.14e appears.

$\mu_{\min}$ most likely corresponds to the μ value that effectively makes the system well mixed. Since in our simulation μ is the probability of reaction and $\sigma = 1 - \mu$ is the probability of swapping, one can say that the probability of a particle reacting at lattice point k hops away from its current position is $(1-\mu)^k\mu$, which is a geometric distribution. With this probability we can easily find the average number of times a particle swaps before reacting. So a decent approximation for the spatial system to behave like that of a well mixed system would be when the mean hopping/swapping distance is about the same value as the largest distance across the lattice.

$$\sum_{k=0}^{\infty} k(1-\mu)^k\mu = \frac{1}{\mu} \sim d_{\max} \tag{3.10}$$

However this maximum distance is different for each lattice type. It is $L/2$ and L for the 1D periodic and closed lattices respectively, where L is the length of the circle/line, whereas for the Sierpinski Triangle lattice it is 2^m, where m is the depth as described in section 3.1. For the 2D periodic and closed lattices the maximum lattice point distances are L and $2L$ respectively, where L is the side length. From this reasoning it follows that the system size grows then $\mu_{\min}$ decreases, which is what we see in the data of our simulations. But equation 3.10 is a very rough approximation as it does not take the direction of hopping/swapping into account, nor does it take into account that if the particle fails to swap with a neutral species it lives on.

Another way to find when a system with a lattice structure behaves like the well mixed system is to study it at low values of μ. In figure 3.15 we plot a portion of the same data that is seen in figure 3.14 except that we have kept the system size (number of lattice points) fixed, changed the lattice structure of the system, and changed axis scales. In 3.15a we see the curves as they are portrayed in figure 3.14 on a log-linear plot, however in 3.15b we change the plot to a log-log plot and also add an extra curve depicting $1/\mu$. In section 3.2.1 we stated that we did not have to worry about our reaction and swapping rate parameters as all they did was rescale time, and that time rescale is exactly $1/\mu$. The argument is that the lattice systems behave like a well mixed system when the mean lattice domination times of the lattice systems start to scale like that of the well mixed system with respect to μ. As can seen in figure 3.15b, for some value μ all the lattice systems start to scale as $1/\mu$ and

follow the dashed line. This means that an excellent measure of when the lattice systems behave like a well mixed system is when they start to follow the dashed line and their lattice domination times start to go as $1/\mu$.

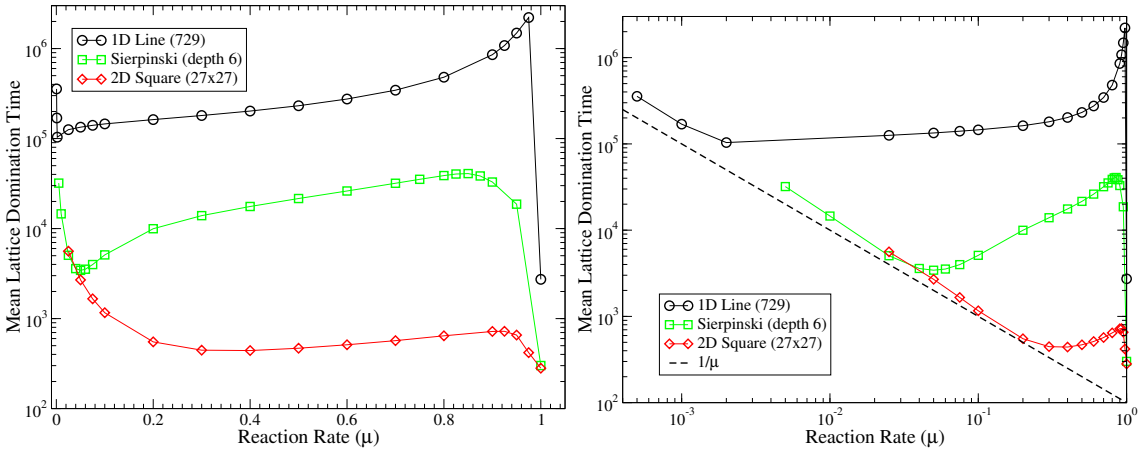

(a) Log-Linear **(b)** Log-Log

Figure 3.15: Average lattice domination times for different lattice structures in order to find when the systems look well mixed. Similar data shown in figure 3.14, but with different lattice structures (but same number of lattice points) and different axis scales.

3.3 Discussion and Summary

In this chapter we have studied the extinction processes that are encountered in a system of four species that compete in a cyclic way. In contrast to the much studied three species model where every species is in a predation-prey relationship with every other species, the four species cyclic competition is a simple case where some species are mutually neutral. As a result the four species tend to form two alliances that compete against each other. We study this model both in the well mixed case without any spatial dependence and on a variety of lattices: regular one- and two-dimensional lattices as well as the fractal Sierpinski triangle. In the lattice systems our individuals are mobile and they can swap places with their neighbors. These swappings can take place between predators and prey but also between mutually neutral partners.

Our study focuses on the probability distribution of the domination time, which is the time at which one of the teams completely fills the lattice. This probability distribution is a complicated function, with various regimes which can be related to different extinction processes. In the presence of neutral pair swapping the probability exhibits a crossover between two different exponential decays. The earlier regime corresponds to extinctions

taking place during the coarsening of domains that contain mostly one species. The second regime, characterized by very broad tails, results from extremely long-lived states that are due to the competition of a few very large domains where the members of one of the teams are very well mixed. This yields a stalemate as every domain is surrounded by domains that contain a mixture of prey and predators. We have verified this scenario through simulations where we prepared the system in an initial state where each half is occupied by one team, with the team members occupying the lattice in an alternate way. In the absence of swapping of neutral partners, which provide the efficient mixing mechanism inside the domains occupied by a single team, these long-lived states are absent and the probability distribution does not exhibit this marked crossover between different regimes.

It is worth pointing out that the most prominent features of the probability distribution are independent of the lattice type. Thus, in the presence of neutral partner swappings one observes for every lattice the emergence of long-lasting states characterized by well mixed large domains responsible of the crossover between the two different regimes with exponential decay.

As the probability distributions are rather complicated, important information can be lost when looking at averaged quantities. Thus, the mean domination time T as a function of the system size N behaves in a qualitatively similar way with or without neutral pair swapping; even so, the corresponding probability distributions are markedly different. For a fixed value of the predation and swapping rates a crossover is observed for larger systems to an algebraic increase $T \sim N^{\alpha}$ with an exponent $\alpha > 1$. The value of the exponent is found to depend on the dimension of the lattice and on the presence or absence of neutral partner swappings. From the domination times it is also possible to tell at what swapping rate the system starts to behave like a well mixed system given a fixed system size.

Chapter 4

Mixed Strategies in Cyclic Competition

Reported in this chapter are results from my recent research on mixed strategies. It is currently being reviewed for publication in Physical Review E [50].

4.1 Brief Introduction

As stated in the introduction of this thesis, in game theory, other than pure strategies, there is also the notion of mixed strategies [82]. A mixed strategy is when at every interaction an agent picks and plays one of the possible pure strategies using a probability distribution. Mixed strategies are sometimes encountered in nature [15, 65], but can be seen most readily in social systems where decision making is important [121, 127]. Economics is another area where game theory with either pure or mixed strategies has been studied. A series of economics papers focus on modifications of the three-species rock-paper-scissors model (see, for example, [6, 46, 62, 79, 93]), whereas others tie three-strategy cyclic domination to the Public Goods game [2, 102, 103, 108, 128, 129]. Some papers discuss spatial games in an economics setting, but usually only games with two pure strategies (Prisoner's Dilemma, Snowdrift, Hawk and Dove) are considered [39, 54, 96, 114].

In this chapter we study versions of the cyclic three- and four-strategy games where agents are selecting a strategy from a time-dependent probability distribution. Learning from a recent loss, an agent changes their probability distribution in such a way that it becomes less likely to play the losing strategy at the next interaction. As the emerging space-time properties in a spatial setting are of interest, we focus in this work on agents that live on a one-dimensional lattice and only interact with their two nearest neighbors. Some results are also presented for the well-mixed situation without an underlying spatial system.

In our implementation we describe every agent as an urn that contains β balls of three respectively four different types, corresponding to the different three respectively four strategies. At every interaction one of these β balls is chosen randomly and the related strategy is played. If that strategy loses, the ball is replaced by a different ball representing the winning strategy. In that way the losing agent is less likely to play at the next interaction the losing strategy again. It should be noted that the value β is a measure of discretization of the probability distribution, with the limit $\beta \to \infty$ yielding a continuous distribution. As we discuss in the following, changing the value of β has a strong impact on the properties of systems with cyclic domination. For example, for the three-species strategies we observe a transition from a neutrally stable system to a stable system when increasing β. In addition, in the limit of $\beta \gg 1$ the system synchronizes, yielding spatially extended coherent temporal waves. When considering four-strategies, one always has a neutrally stable system, but the average time for strategy extinction displays different regimes, depending on the value of β and on the system size.

4.2 Models

In the symmetric Lotka-Volterra model reactions are taking place in a cyclic way between M different species [29, 30]:

$$S_i + S_{i+1} \to S_i + S_i \tag{4.1}$$

where S_i is an agent of species i, with $i = 1, \cdots, M$ and the cyclic identification $M + 1 \equiv 1$. In the language of population dynamics, every species has one prey and is the prey of a single other species. The three-species case is special, as a reaction takes place whenever two agents of different types are selected. For cases with more than three species one has mutually neutral species that do not interact [10, 30]. Cyclic Lotka-Volterra games can be played in the well-mixed case as well as on lattices where a variety of situations have been considered. For example, one can impose a strict site restriction with exactly one agent occupying each lattice site and reactions taking place between neighboring sites [29, 30]. This can be coupled with exchanges of agents sitting on nearest neighbor sites, in order to provide a mechanism for mobility [85, 87]. Sometimes the site restriction is dropped so that every site can hold a variable number of agents that can diffuse and interact with agents on neighboring sites [41]. In the related systems with May-Leonard dynamics, the reactions in equation 4.1 is replaced by two separate reactions [68, 87]

$$\begin{aligned} S_i + S_{i+1} &\to S_i + \varnothing \\ S_i + \varnothing &\to S_i + S_i \end{aligned} \tag{4.2}$$

where $\varnothing$ indicates an empty site. In this scheme the number of agents in the system is a stochastic quantity that is only conserved on average.

We consider the following versions of the three- and four-strategy cyclic Lotka-Volterra game with mixed strategies where at every interaction agents play one of the possible strategies

using a time-dependent probability distribution. Imagine an agent as an urn that contains β balls of three (for the three-strategy version) or four (for the four-strategy case) different types. For a well-mixed system without a lattice structure we first choose two agents/urns at random out of a total of N agents/urns before choosing randomly a ball out of each selected urn. Depending on the types of balls selected, a reaction may take place following the reaction scheme of equation 4.1. If the strategy played by one of the agents is beaten, then the losing ball is replaced by a ball of the winning type before the balls are put back into the urns. The losing agent therefore changes the probability distribution as a result of the loss by increasing (decreasing) the probability to play the winning (losing) strategy at the next interaction. For a spatial game we only consider the case with exactly one agent at every lattice site. In order to start an interaction we select an agent and one of their neighbors at random and then proceed as for the well-mixed case. In our simulations we define one time step to be $N\beta$ proposed updates.

One can view this scheme in a spatial setting as a version of the spatial cyclic Lotka-Volterra model with multiple occupancy of each site, but there are important differences. In the model discussed in [41] in the context of population dynamics, individuals not only interact with agents on other lattice sites, they also diffuse by jumping with a given probability to one of the neighboring sites. As a result the number of individuals at each site fluctuates and only the average spatial density is constant. In our case, only interactions take place so that the number of balls at each site (which corresponds to the number of individuals at a given site in the model of [41]) is strictly conserved. As we will see in the following, this additional conservation law has a huge impact on the properties of our system.

4.3 The Mixing of Three Strategies

As already mentioned, the situation with three strategies is rather special, as every time two different strategies are played, there will be a losing strategy and a winning strategy. In the following we show, both in the well-mixed case as well as on the ring, that for continuous probability distributions a synchronization of the strategies played by the different agents takes place. For small number of balls per agent a transition in the stability properties of the lattice system is observed.

4.3.1 Mean-field Equations for the Well-mixed Case

We first consider the mixed three-strategies game in a well-mixed system without spatial structure. Agent j is characterized by the number of balls of each type at their possession: (a_j, b_j, c_j), with $a_j + b_j + c_j = \beta$, where a_j is the number of balls of type A. The state of each system of N agents is then given by the number of balls of each agent, i.e. by the

configuration:

$$\{(a_n, b_n, c_n)\} = \{(a_1, b_1, c_1), \cdots, (a_j, b_j, c_j), \cdots, (a_N, b_N, c_N)\} \tag{4.3}$$

The interaction scheme in equation 4.1 directly translates into the following Master equation for the probability that the system is in the state $\{(a_n, b_n, c_n)\}$ at time $\tau + 1$.

$$\begin{aligned} P(\{(a_n, b_n, c_n)\}; \tau + 1) = \\ & \frac{1}{\beta^2} \frac{2}{N(N-1)} \Big[\\ & + \sum_j \sum_{i \neq j} a_i (b_j + 1) P(\cdots, (a_i, b_i, c_i), \cdots, (a_j - 1, b_j + 1, c_j), \cdots; \tau) \\ & + \sum_j \sum_{i \neq j} b_i (c_j + 1) P(\cdots, (a_i, b_i, c_i), \cdots, (a_j, b_j - 1, c_j + 1), \cdots; \tau) \\ & + \sum_j \sum_{i \neq j} c_i (a_j + 1) P(\cdots, (a_i, b_i, c_i), \cdots, (a_j + 1, b_j, c_j - 1), \cdots; \tau) \Big] \\ & + [1 - \frac{1}{\beta^2} \frac{2}{N(N-1)} \sum_j \sum_{i \neq j} (a_i b_j + b_i c_j + c_i a_j)] P(\{(a_n, b_n, c_n)\}; \tau) \end{aligned} \tag{4.4}$$

where the factors $\frac{2}{N(N-1)}$ takes into account the number of combined choices of the two agents i and j. The first three sums represent the reaction in equation 4.1 through which the system enters the state $\{(a_n, b_n, c_n)\}$, while the last term represents the case where no reaction happens (when balls of the same type are pulled out for both agents) and the system stays in the same state.

We define the density of ball type A for agent j at time τ to be:

$$A_j(\tau) = \sum_{\{(a_n, b_n, c_n)\}} \frac{a_j}{\beta} P(\{(a_n, b_n, c_n)\}; \tau) \tag{4.5}$$

with similar equation for ball types B and C. Neglecting correlations, equations 4.4 and 4.5 yield the equation (with similar equations found for the other ball types through symmetry):

$$\begin{aligned} A_k(\tau + 1) - A_k(\tau) &= \sum_{\{(a_n, b_n, c_n)\}} \frac{a_k}{\beta} \left(P(\{(a_n, b_n, c_n)\}; \tau + 1) - P(\{(a_n, b_n, c_n)\}; \tau) \right) \\ &= \sum_{\{(a_n, b_n, c_n)\}} \frac{1}{\beta^3} \frac{2}{N(N-1)} \sum_{i \neq k} (a_i b_k - c_i a_k) P(\{(a_n, b_n, c_n)\}; \tau) \\ &= \frac{1}{N\beta} \left[2 \left(\frac{1}{N-1} \sum_{i \neq k} A_i(\tau) \right) B_k(\tau) - 2 \left(\frac{1}{N-1} \sum_{i \neq k} C_i(\tau) \right) A_k(\tau) \right] \end{aligned} \tag{4.6}$$

Letting $t = \frac{\tau}{N\beta}$ and taking the continuum limit $\beta \to \infty$ so that $A_k(\tau+1) - A_k(\tau) \to \frac{1}{N\beta}\partial_t A_k(t)$ finally leads to the mean-field equations:

$$\begin{aligned}
\partial_t A_k(t) = &\ 2\left(\frac{1}{N-1}\sum_{i\neq k} A_i(t)\right) B_k(t) - 2\left(\frac{1}{N-1}\sum_{i\neq k} C_i(t)\right) A_k(t) \\
\partial_t B_k(t) = &\ 2\left(\frac{1}{N-1}\sum_{i\neq k} B_i(t)\right) C_k(t) - 2\left(\frac{1}{N-1}\sum_{i\neq k} A_i(t)\right) B_k(t) \\
\partial_t C_k(t) = &\ 2\left(\frac{1}{N-1}\sum_{i\neq k} C_i(t)\right) A_k(t) - 2\left(\frac{1}{N-1}\sum_{i\neq k} B_i(t)\right) C_k(t)
\end{aligned} \tag{4.7}$$

Recovering the Well-mixed RPS Model

For the well-mixed case the first of the three equations in 4.7 can be rewritten as:

$$\begin{aligned}
\partial_t A_k(t) &= 2\left(\frac{1}{N-1}\sum_{i\neq k} A_i(t)\right) B_k(t) - 2\left(\frac{1}{N-1}\sum_{i\neq k} C_i(t)\right) A_k(t) \\
&= \frac{2}{N-1}\left(B_k \sum_i^N A_i - A_k \sum_i^N C_i - B_k A_k + A_k C_k\right) \\
&= \frac{2}{N-1}\left(B_k N\langle A\rangle_N - A_k N\langle C\rangle_N - B_k A_k + A_k C_k\right) \\
&= 2\left(B_k \frac{N}{N-1}\langle A\rangle_N - A_k \frac{N}{N-1}\langle C\rangle_N + \frac{A_k C_k - B_k A_k}{N}\right)
\end{aligned} \tag{4.8}$$

where $\langle\cdots\rangle_N$ denotes a mean over all agents/urns in the system. Taking $N \to \infty$ and making the index k to be continuous yields:

$$\partial_t A(x,t) = 2B(x,t)\langle A(x,t)\rangle_x - 2A(x,t)\langle C(x,t)\rangle_x \tag{4.9}$$

where $\langle\cdots\rangle_x = \frac{\int(\cdots)\,\mathrm{d}x}{\int \mathrm{d}x}$ indicates an average over the continuous index x. Finally, applying $\langle\cdots\rangle_x$ on both sides of equation 4.9 yields:

$$\begin{aligned}
\partial_t\langle A(x,t)\rangle_x = &\ 2\langle B(x,t)\rangle_x\langle A(x,t)\rangle_x - 2\langle A(x,t)\rangle_x\langle C(x,t)\rangle_x \\
\partial_t\langle B(x,t)\rangle_x = &\ 2\langle C(x,t)\rangle_x\langle B(x,t)\rangle_x - 2\langle B(x,t)\rangle_x\langle A(x,t)\rangle_x \\
\partial_t\langle C(x,t)\rangle_x = &\ 2\langle A(x,t)\rangle_x\langle C(x,t)\rangle_x - 2\langle C(x,t)\rangle_x\langle B(x,t)\rangle_x
\end{aligned} \tag{4.10}$$

where the second and third equations follow from symmetry. These are exactly the mean field equations for the three-species well-mixed case.

Case of Two Players ($N = 2$)

Let us have a closer look at the simple case of two agents $N = 2$. Equations 4.7 can be easily written as:

$$\begin{aligned} \partial_t A_1 &= 2(A_2B_1 - C_2A_1) \quad , \partial_t A_2 = 2(A_1B_2 - C_1A_2) \\ \partial_t B_1 &= 2(B_2C_1 - A_2B_1) \quad , \partial_t B_2 = 2(B_1C_2 - A_1B_2) \\ \partial_t C_1 &= 2(C_2A_1 - B_2C_1) \quad , \partial_t C_2 = 2(C_1A_2 - B_1C_2) \end{aligned} \tag{4.11}$$

From $\partial_t(A_1 - A_2)$ we find:

$$\partial_t(A_1 - A_2) = 2\left[(A_2B_1 - C_2A_1) - (A_1B_2 - C_1A_2)\right] = -2(A_1 - A_2) \tag{4.12}$$

as $A_i + B_i + C_i = 1$. Solving this differential equation yields:

$$A_1(t) - A_2(t) = (a_1 - a_2)e^{-2t} \tag{4.13}$$

where $a_1 = A_1(0)$ and $a_2 = A_2(0)$ are initial conditions. Similar equations are obtained for ball types B and C. It follows that whatever the initial conditions the difference in ball densities of the two agents vanish exponentially fast, yielding a synchronization of the two agents.

We can use the previous results to eliminate the densities of agent 2 and end up with the following three coupled non-autonomous differential equations for the ball densities of agent 1:

$$\begin{aligned} \partial_t A_1 &= 2(A_1B_1 - C_1A_1) + 2\left[(a_2 - a_1)B_1 - (c_2 - c_1)A_1\right]e^{-2t} \\ \partial_t B_1 &= 2(B_1C_1 - A_1B_1) + 2\left[(b_2 - b_1)C_1 - (a_2 - a_1)B_1\right]e^{-2t} \\ \partial_t C_1 &= 2(C_1A_1 - B_1C_1) + 2\left[(c_2 - c_1)A_1 - (b_2 - b_1)C_1\right]e^{-2t} \end{aligned} \tag{4.14}$$

We note that in the long time limit $t \to \infty$ we recover the mean field rate equations for the well-mixed rock-paper-scissors game.

In figure 4.1 we compare these theoretical results (lines in the figure), obtained through numerical integration of the equations 4.14, with results from stochastic simulations (symbols in the figure) for initial conditions $A_1(0) = 0.8$, $B_1(0) = 0.1$, $A_2(0) = 0.1$, and $B_2(0) = 0.8$. Even though the initial conditions are very different, the synchronization between the two agents is very rapid and the differences between the corresponding densities vanish exponentially, see figure 4.1d.

$\partial_t(A_l - A_m)$ in General

We find that in the simple case of two players that the synchronization is exponential. Here we attempt to derive that generally in the case of more than two players. For players l and

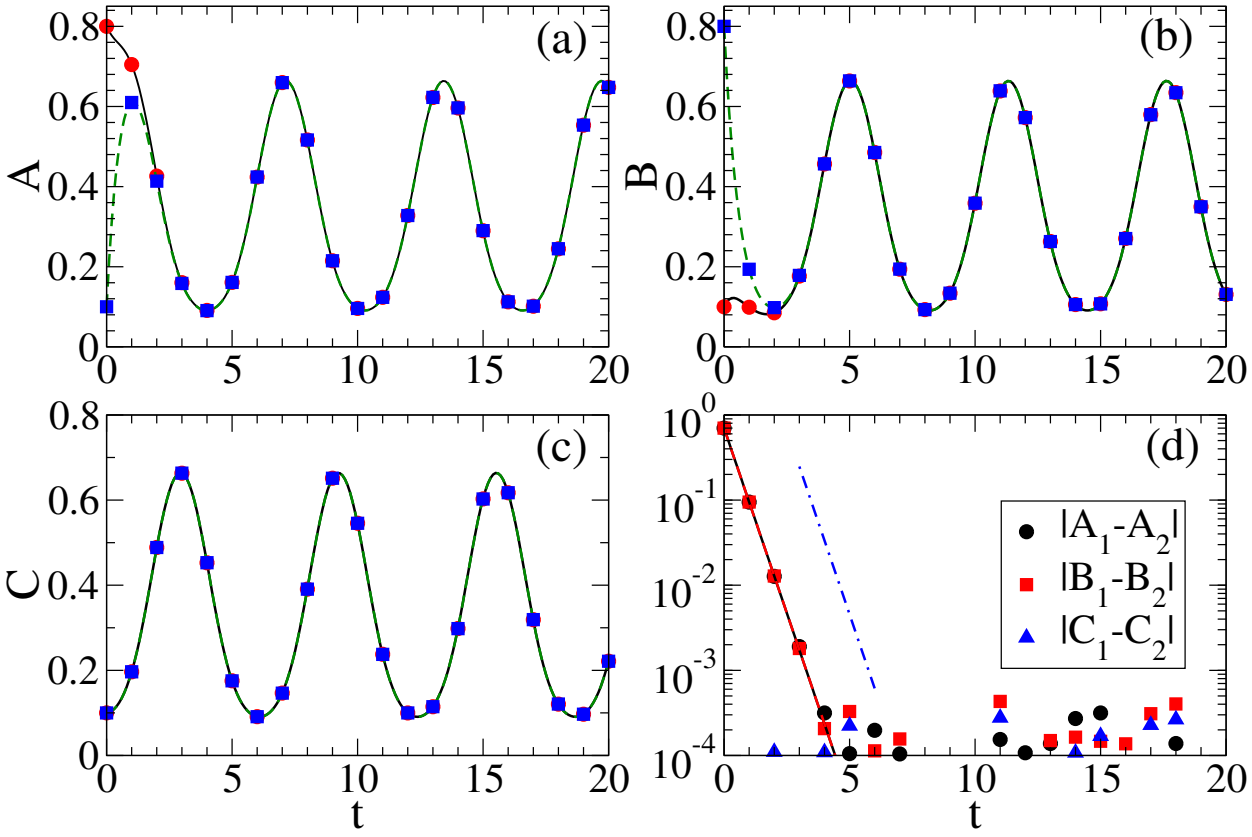

Figure 4.1: Time-dependent densities for a system of two agents obtained through numerical integration of equations 4.14 (full black line: agent 1, green dashed line: agent 2) and compared with results from stochastic simulations with $\beta = 10^7$ (red circles: agent 1, blue square: agent 2). The same initial conditions $A_1(0) = 0.8$, $B_1(0) = 0.1$, $A_2(0) = 0.1$, and $B_2(0) = 0.8$ are used for both methods. In (d) the symbols represent the the absolute values of the difference between strategy densities in the simulation data, while the lines are obtained from equations 4.14. An exponentially fast synchronization is observed. The dot-dashed blue line indicates an exponential slope of -2.

m look at the difference $\partial_t(A_l - A_m)$ and attempt to replicate the calculation in equation 4.12:

$$\begin{aligned}
\partial_t(A_l - A_m) &= \frac{2}{N-1}\left[\left(\sum_{i\neq l} A_iB_l - \sum_{i\neq l} C_iA_l\right) - \left(\sum_{i\neq m} A_iB_m - \sum_{i\neq m} C_iA_m\right)\right] \\
&= \frac{2}{N-1}\left[\sum_{i\neq l,m} (A_iB_l - C_iA_l - A_iB_m + C_iA_m) + B_lA_m - C_mA_l - A_lB_m + C_lA_m\right] \\
&= \frac{2}{N-1}\left[\sum_{i\neq l,m} (A_i(B_l - B_m) - C_i(A_l - A_m)) + A_m(B_l + C_l) - A_l(C_m + B_m)\right] \\
&= \frac{2}{N-1}\left[\sum_{i\neq l,m} (A_i(B_l - B_m) - C_i(A_l - A_m)) - (A_l - A_m)\right] \\
&= \frac{-2}{N-1}(A_l - A_m) + \frac{2}{N-1}\left[(B_l - B_m)\sum_{i\neq l,m} A_i - (A_l - A_m)\sum_{i\neq l,m} C_i\right]
\end{aligned} \tag{4.15}$$

So for a low number of players there seems to be a constant negative decay rate of $\frac{2}{N-1}$, however as the number of players increases the periodic non-constant terms dominate.

4.3.2 Numerical Simulations on the Ring

The simplest spatial system is the one-dimensional lattice with periodic boundary conditions. As discussed previously, every lattice site of the ring is occupied by one agent who has at their disposal β balls. In the initial state every ball is assigned with the same probability, one of three possible types corresponding to the three strategies A, B, and C. Once the system has been prepared in that way, pairs of neighboring sites are randomly selected and interactions take place following the scheme described above.

The dynamics can be readily visualized through space-time plots as those shown in figure 4.2. Inspection of these plots for various numbers of balls β reveals an interesting transition in the shape of the space-time patterns. Whereas for three balls or less the system behaves like the standard Lotka-Volterra rock-paper-scissors game on the ring with immobile agents (which corresponds to $\beta = 1$) and exhibits coarsening processes that end when only one strategy fills the complete lattice (see figure 4.2a), for $\beta \geq 4$ a tiling structure appears where a tile indicates that a part of the system is dominated by one of the three strategies for a finite amount of time, see figure 4.2b. It follows that every agent changes the most likely strategy after some time and that it becomes difficult for one strategy to dominate the system. This tiling structure, which persists for a long time, is reminiscent of very similar patterns that are encountered when allowing in the one-dimensional rock-paper-scissors model for swapping of particles as an efficient mechanism for mobility [116]. When we further increase β, the

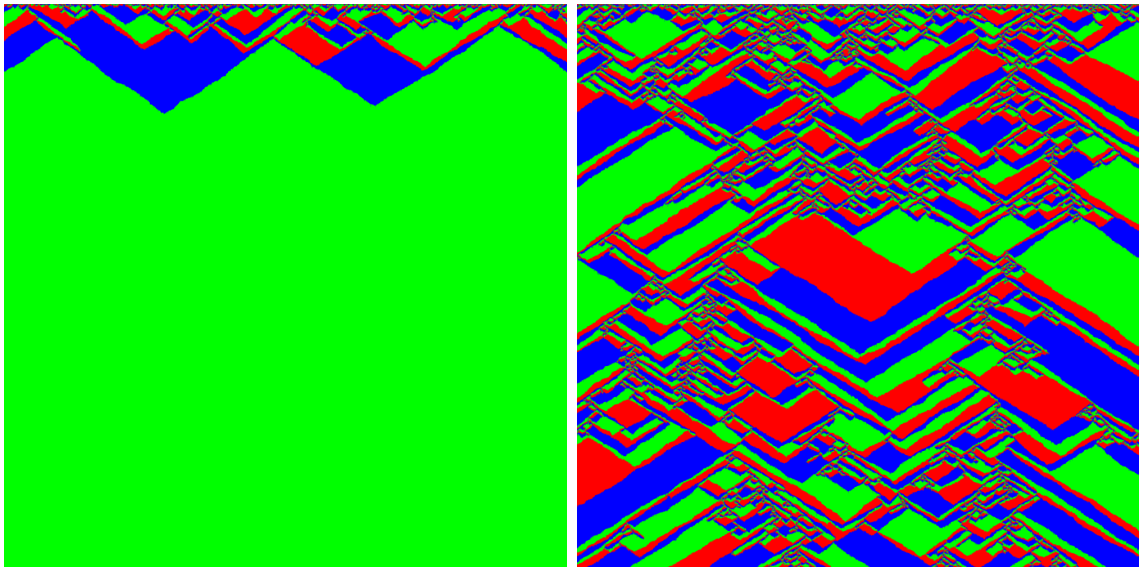

(a) $\beta = 3$ **(b)** $\beta = 4$

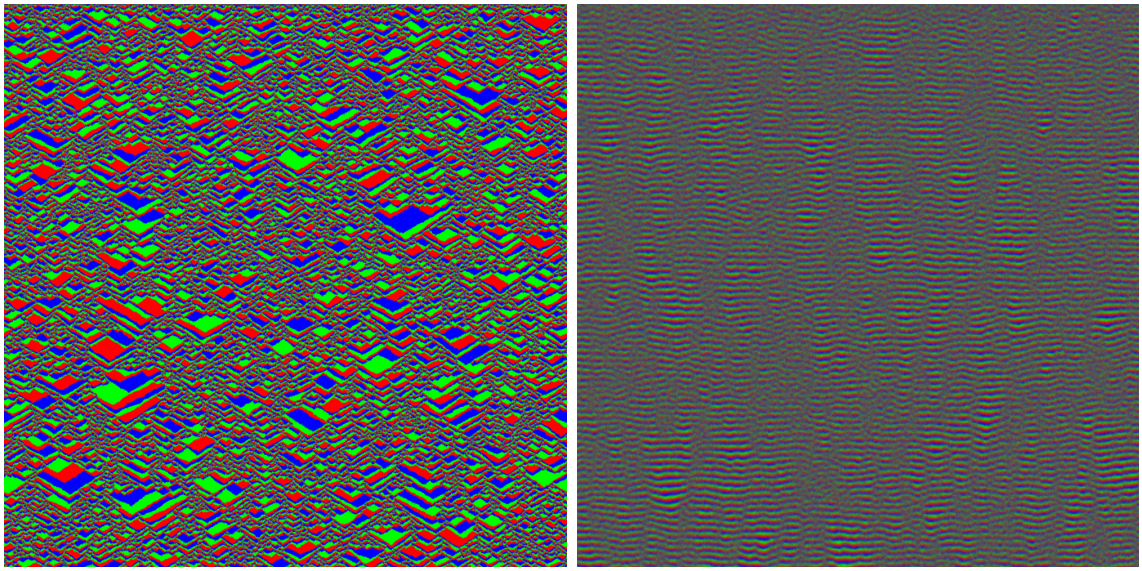

(c) $\beta = 6$ **(d)** $\beta = 100$

Figure 4.2: Space-time plots for three-strategies games on a ring with different numbers of balls β on each site: (a) $\beta = 3$, (b) $\beta = 4$, (c) $\beta = 6$, and (d) $\beta = 100$. Time progresses from top to bottom. For (a)-(c) 1000 time steps are shown for a system composed of 1000 sites, whereas for (d) we show 500 time steps for a system with 500 lattice points. To determine the color of a lattice site we use the RGB color model and map the percentage of A, B, and C to the percentage of the colors Red, Green, and Blue respectively. In this scheme a site that contains the same number of balls for all three species is assigned a grayish color.

tiles, corresponding to regions where one strategy dominates locally, decrease in size, see figure 4.2c for the case $\beta = 6$. This is accompanied by the emergence of grayish patches that indicate spatial regions where in the probability distribution the three strategies have similar weights. Finally for large values of β, corresponding to a probability distribution that approximates a continuous distribution, the system rapidly synchronizes and spatial extended coherent temporal was are formed, as shown in figure 4.2d for the example of $\beta = 100$ balls.

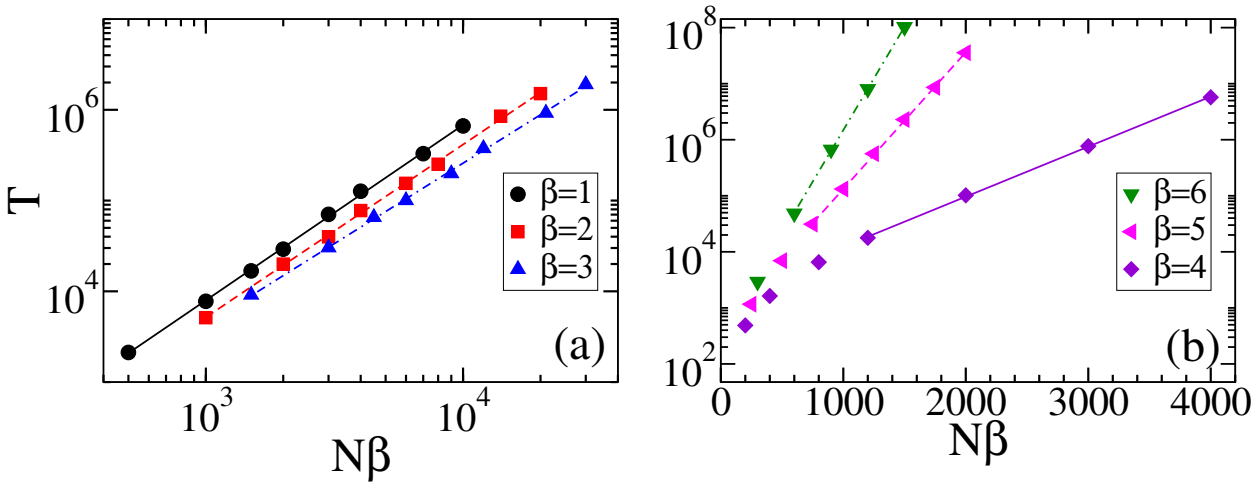

Figure 4.3: Average extinction time T as a function of the total number of balls $N\beta$ in the system. When changing the number of balls β per agent, a transition takes place between an algebraic dependence on the total number of balls in the system for $\beta \leq 3$, see panel (a), indicating a neutrally stable system, and an exponential dependence for $\beta \geq 4$, characterizing a stable system, see panel (b). Each data point results from an average over 2000 runs with different realizations of the noise. Error bars are smaller than the symbol sizes.

In order to quantitatively study the transition between coarsening and tiling we measure the average extinction time T, i.e. the average time at which only one of the strategies remains in the system. Figure 4.3 reveals that the average extinction time changes its dependence on the system size at the transition gleaned from the space-time plots. For $\beta \leq 3$ the average extinction time increases algebraically with the total number of balls, $T \sim (N\beta)^b$, as shown by the straight lines in the log-log plot in panel (a) of figure 4.3, with exponent $b = 1.93(2)$, $1.90(2)$, and $1.77(2)$ for $\beta = 1$, 2, and 3, respectively. In the language of population dynamics [24], this algebraic dependence means that the system is neutrally stable. We also note that the extinction time for a fixed value of $N\beta$ decreases for increasing β, indicating that the system becomes less stable. This trend is reversed when we enter the tiling regime, see figure 4.3b, as now for fixed $N\beta$ the extinction time strongly increases with β. In face, the dependence of T on $N\beta$ changes to an exponential dependence for $\beta \geq 4$, as the system becomes a stable system [24].

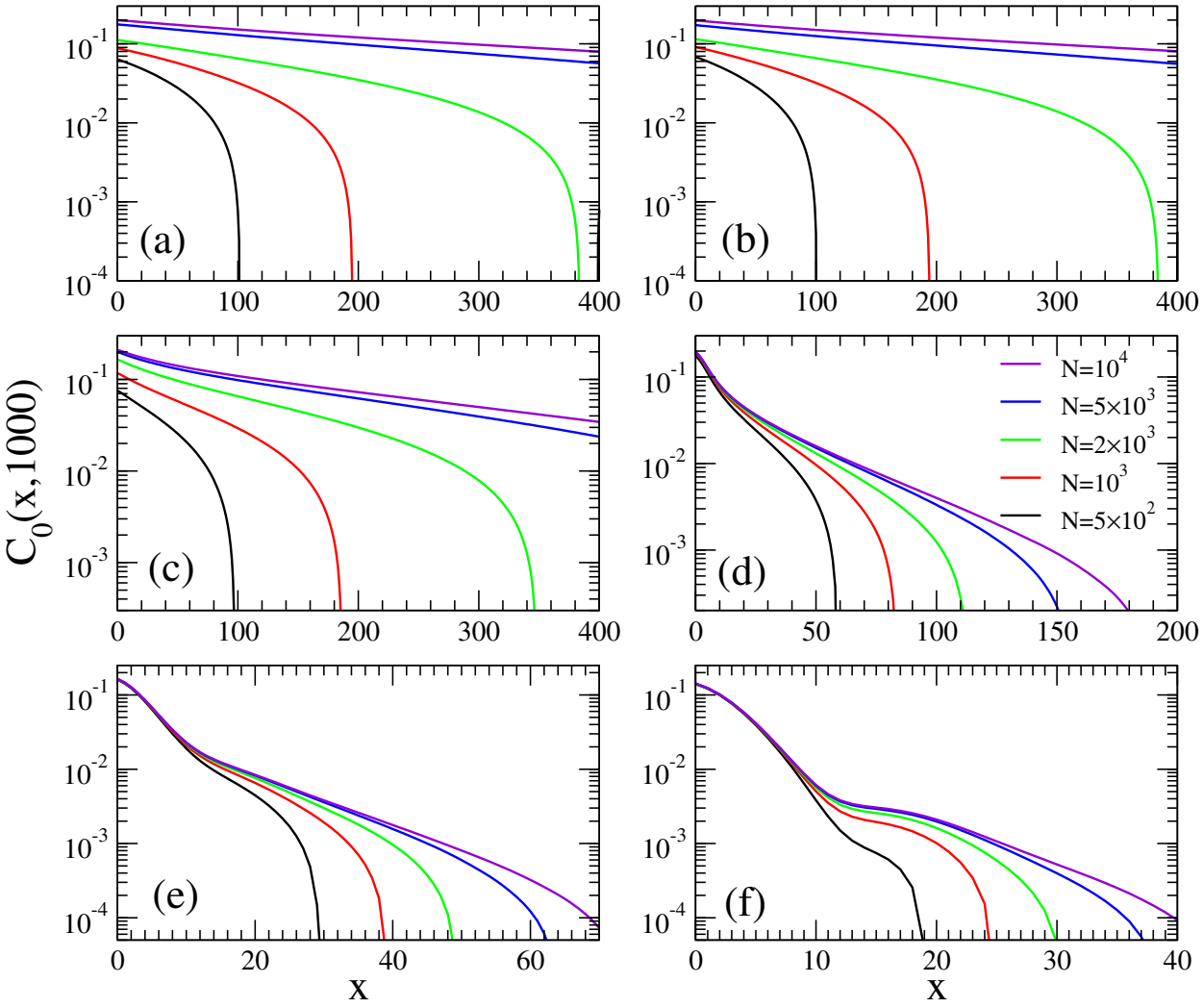

Figure 4.4: Spatial covariance at time $t = 1000$ for different numbers of balls β (increasing from 1 to 6 from (a) to (f)) and different system sizes. The data results from averaging over half a million independent runs.

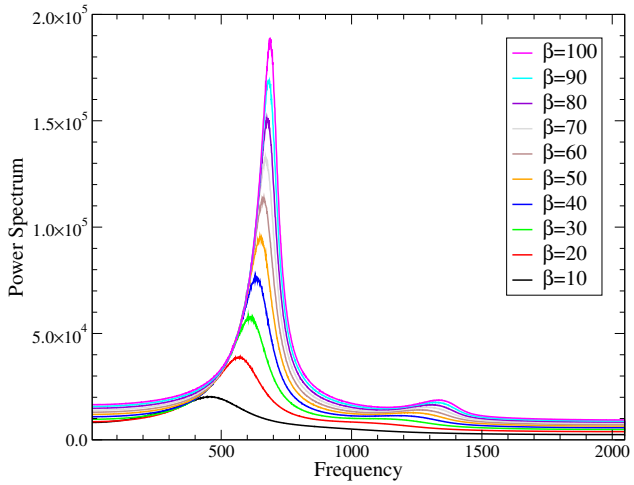

Figure 4.5: Temporal Fourier transform results for different numbers of balls β. The runs were done on a one-dimensional periodic lattice of length 1000. The systems started from a random initial condition, allowed to relax for 1000 time steps and the temporal Fourier transform of the strategy densities was done on the following 4096 time steps. The data results from averaging the Fourier transforms of 100 independent runs for each curve.

Another quantity that allows us to gain insights into this transition is the total space-time covariance

$$C_0(x,t) = \frac{C_{AA}(x,t) + C_{BB}(x,t) + C_{CC}(x,t)}{3} \tag{4.16}$$

with

$$C_{AA}(x,t) = \frac{1}{N}\sum_i A_i(t)A_{i+x}(t) - \mu_A(t)\mu_A(t) \tag{4.17}$$

and similar expressions for $C_{BB}(x,t)$ and $C_{CC}(x,t)$. Here $\mu_A(t) = \frac{1}{N}\sum_i A_i(t)$ and similarly for μ_B and μ_C. Figure 4.4 shows this quantity after 1000 time steps since the preparation of the system for β ranging from 1 to 6 and system sizes between $N = 500$ and $N = 10000$. For $\beta \leq 3$ the covariance displays the expected behavior for systems with domain ordering, with strong finite size effects for small systems, as in many instances runs have already reached their final state (with one strategy filling the whole system) at $t = 1000$, and an exponential decay with the distance x for larger sizes when the coarsening system is still far from its final state. After the transition to the tiling regime, see (d) and (f) in figure 4.4, the initial decay becomes system size independent and is followed by a shoulder (see the data for $\beta = 6$ in figure 4.4f). We relate this behavior to the typical sizes of the tiles whose spatial extensions are rather small and decrease with an increase of β.

In order to better understand the spatio-temporal patterns in the limit of large β in figure 4.5 we have also looked at the temporal Fourier transform of the strategies of the agents. Notice that as the number of balls β increases the prominent frequency asymptotes to some

value and a second peak also appears. We also see that the peaks become sharper as β increases. For smaller values of β the broader spectrum and lower frequencies can possibly be attributed to the spatial zig-zagging of the three species.

4.3.3 Reaction-Diffusion Equations and Synchronization

As we saw in figure 4.2d synchronization in space coupled with temporal oscillations sets in for large number of balls β. As in the limit $\beta \to \infty$ the probability distribution becomes continuous, we can capture this effect through spatial mean-field equations.

Our starting point are the mean-field equations 4.7 for N agents in the well-mixed case with $\beta \to \infty$ that need to be adapted to the spatial setting of a one-dimensional lattice where the agent on lattice site k interacts exclusively with the agents located on the neighboring sites $k-1$ and $k+1$. Each sum in equation 4.7 over $i \neq k$ then reduces to two terms, so that we obtain for $A_k(t)$ (with similar equations for $B_k(t)$ and $C_k(t)$):

$$\partial_t A_k = (A_{k+1} + A_{k-1})B_k - (C_{k+1} + C_{k-1})A_k \ . \tag{4.18}$$

Introducing the finite difference $\Delta^2 A_k = (A_{k+1} - A_k) - (A_k - A_{k-1})$ allows to recast this equation in the form:

$$\partial_t A_k = (\Delta^2 A_k)B_k - (\Delta^2 C_k)A_k + 2(B_k A_k - C_k A_k) \tag{4.19}$$

Taking the spatial continuum limit, where we approximate Δ by $a\partial_x$, yields the following set of partial differential equations:

$$\begin{aligned}
\partial_t A(x,t) &= \left(\partial_x^2 A(x,t)\right) B(x,t) - \left(\partial_x^2 C(x,t)\right) A(x,t) + 2\left(B(x,t)A(x,t) - C(x,t)A(x,t)\right) \\
\partial_t B(x,t) &= \left(\partial_x^2 B(x,t)\right) C(x,t) - \left(\partial_x^2 A(x,t)\right) B(x,t) + 2\left(C(x,t)B(x,t) - A(x,t)B(x,t)\right) \\
\partial_t C(x,t) &= \left(\partial_x^2 C(x,t)\right) A(x,t) - \left(\partial_x^2 B(x,t)\right) C(x,t) + 2\left(A(x,t)C(x,t) - B(x,t)C(x,t)\right)
\end{aligned} \tag{4.20}$$

where we set the length scale $a = 1$. This set of equations can straightforwardly be generalized to d dimensions, and will do so later in this section. The terms ∂_x^2 describe the diffusion of strategies through interactions, as the loser of an interaction changes their probability distribution in favor of the strategy against which they lost. The remaining terms are nothing else than the mean-field equations of the normal three-species cyclic game in the well-mixed case.

Comparison to 1D Numerical Simulation

In Fig. 4.6a we show the numerical solutions of this set of equations for the initial condition:

$$\begin{aligned} A(x,t=0) &= \frac{1}{2}\Theta[N/5 - |x - N/2|] \\ B(x,t=0) &= \frac{1}{2}\Theta[N/4 - |x - N/2|] \\ C(x,t=0) &= 1 - A(x,t=0) - B(x,t=0) \end{aligned} \tag{4.21}$$

where $\Theta[\cdots]$ is the Heaviside step function. In this initial state large segments of the system are occupied by agents that play the same initial strategy. For comparison we show in figure 4.6b a numerical simulation for $\beta = 10^6$ balls and the same initial condition. As expected a system with such a large number of balls is well described by the mean-field equations. The space-time plots in figure 4.6 show that the spatial system with a continuous probability distribution synchronizes very rapidly, yielding spatially extended regions where the probability distribution of every agent is very similar. As a result the strategies in the whole system coherently oscillate in time. This synchronization effect is readily understood from equations 4.20 by remarking that the diffusion terms efficiently smoothen out the spatial inhomogeneities in the probability distributions until only the well-mixed terms describing the standard rock-paper-scissors interactions matter.

Generalization to d Dimensions

From looking at the well mixed mean field equations 4.7 we can derive general mean field equations for when there is spatial structure:

$$\begin{aligned} \partial_t A_k(t) = &\ 2\left(\frac{1}{n.n.}\sum_{<ik>} A_i(t)\right) B_k(t) - 2\left(\frac{1}{n.n.}\sum_{<ik>} C_i(t)\right) A_k(t) \\ \partial_t B_k(t) = &\ 2\left(\frac{1}{n.n.}\sum_{<ik>} B_i(t)\right) C_k(t) - 2\left(\frac{1}{n.n.}\sum_{<ik>} A_i(t)\right) B_k(t) \\ \partial_t C_k(t) = &\ 2\left(\frac{1}{n.n.}\sum_{<ik>} C_i(t)\right) A_k(t) - 2\left(\frac{1}{n.n.}\sum_{<ik>} B_i(t)\right) C_k(t) \end{aligned} \tag{4.22}$$

where $n.n.$ is the number of neighbors and the sum with index $< ik >$ is the sum over the neighbors of site k.

On a d-dimensional grid lattice a site/player will be labeled with vector $\vec{k}$ and the number of nearest neighbors ($n.n.$) in equation 4.22 would be $2d$ since every player would get 2 neighbors per dimension. Here we only focus on one term because all the others can be

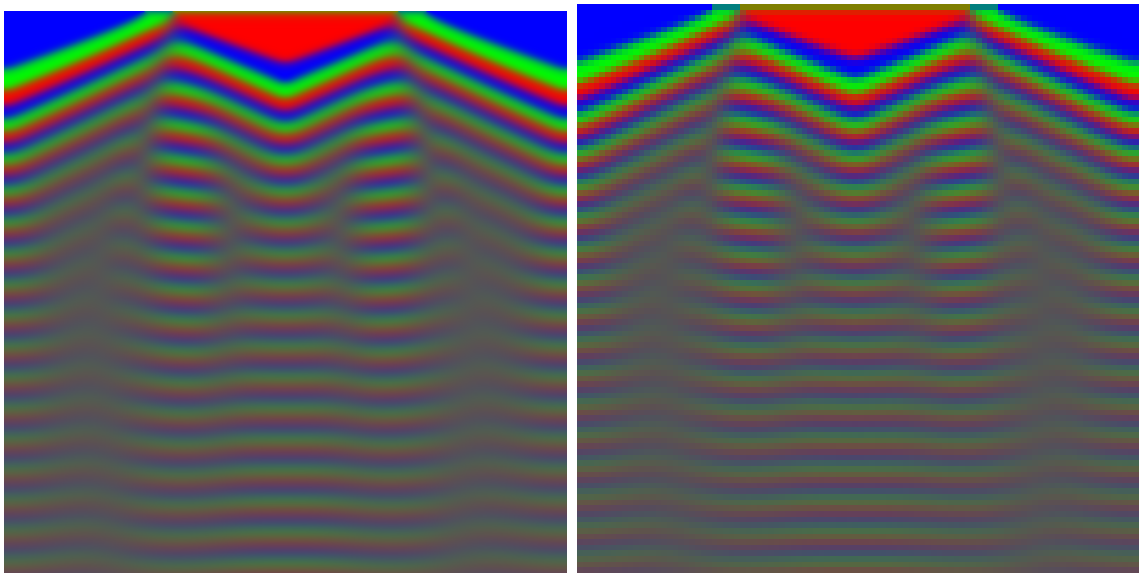

(a) Numerical Integration **(b)** Numerical Simulation

Figure 4.6: Space-time plots from (a) numerical integration of the spatial mean-field equations 4.20 and (b) the numerical simulation of a system of 100 lattice sites over 100 time steps with $\beta = 10^6$ balls at each site. In both cases the same initial condition 4.21 was used. Time increases in the downward direction. The system rapidly synchronizes and coherent waves are formed.

similarly manipulated. Rewriting the first term of $\partial_t A_k(t)$ from equation 4.22 yields:

$$2\left(\frac{1}{2d}\sum_{i=1}^{d}\left(A_{\vec{k}+\vec{e}_i}+A_{\vec{k}-\vec{e}_i}\right)\right)B_{\vec{k}} \tag{4.23}$$

where $\vec{e}_i$ is the unit vector for the ith dimension. In order to get two finite differences like in equation 4.19 we would need to subtract and add $2d$ multiples of either $A_{\vec{k}}$, $B_{\vec{k}}$, or $C_{\vec{k}}$.

$$\frac{1}{d}\left(\sum_{i=1}^{d}\left(A_{\vec{k}+\vec{e}_i}+A_{\vec{k}-\vec{e}_i}\right)-2dA_{\vec{k}}+2dA_{\vec{k}}\right)B_{\vec{k}} \tag{4.24}$$

We then use the $2d$ subtraction multiple to pair up with each $\vec{k}+\vec{e}_i$ and $\vec{k}-\vec{e}_i$ for every ith dimension. This yields the finite difference squared as seen in equation 4.19 for each dimension. The additional $2d$ multiple are then pulled outside the sum:

$$\begin{aligned}&\left(\frac{1}{d}\sum_{i=1}^{d}\left[\left(A_{\vec{k}+\vec{e}_i}-A_{\vec{k}}\right)-\left(A_{\vec{k}}-A_{\vec{k}-\vec{e}_i}\right)\right]+2A_{\vec{k}}\right)B_{\vec{k}}\\ &\qquad=\left(\frac{1}{d}\sum_{i=1}^{d}\Delta_i^2 A_{\vec{k}}\right)B_{\vec{k}}+2A_{\vec{k}}B_{\vec{k}}\end{aligned} \tag{4.25}$$

Then by letting space be continuous we go from a discretized $\vec{k}$ to a continuous vector $\vec{x}$, which yields:

$$\frac{1}{d}\left(\nabla^2 A(\vec{x},t)\right) B(\vec{x},t) + 2A(\vec{x},t)B(\vec{x},t) \tag{4.26}$$

We now finally have the spatial mean field partial differential equations for d dimensions:

$$\begin{aligned}
\partial_t A = &\ \frac{1}{d}\left[(\nabla^2 A)B - (\nabla^2 C)A\right] + 2\left(BA - CA\right) \\
\partial_t B = &\ \frac{1}{d}\left[(\nabla^2 B)C - (\nabla^2 A)B\right] + 2\left(CB - AB\right) \\
\partial_t C = &\ \frac{1}{d}\left[(\nabla^2 C)A - (\nabla^2 B)C\right] + 2\left(AC - BC\right)
\end{aligned} \tag{4.27}$$

Adding Self-interactions

We now look at the differences in the master equation, and consequently the mean field equations, when an agent performs a self-interaction with probability p and interacts with its neighbors with probability $(1-p)$ in one dimension. The following is the modified master

equation:

$$
\begin{aligned}
P(\{a_n,b_n,c_n\};\tau+1) = \\
&(1-p)\frac{1}{\beta^2}\frac{2}{N(n.n.)}\Big[\\
&\quad+\sum_j\sum_{<ij>} a_i(b_j+1)P(\cdots,\{a_i,b_i,c_i\},\{a_j-1,b_j+1,c_j\},\cdots;\tau) \\
&\quad+\sum_j\sum_{<ij>} b_i(c_j+1)P(\cdots,\{a_i,b_i,c_i\},\{a_j,b_j-1,c_j+1\},\cdots;\tau) \\
&\quad+\sum_j\sum_{<ij>} c_i(a_j+1)P(\cdots,\{a_i,b_i,c_i\},\{a_j+1,b_j,c_j-1\},\cdots;\tau) \\
&\quad\Big] \\
&+p\frac{1}{N}\frac{2}{\beta(\beta-1)}\Big[\\
&\quad+\sum_j (a_j-1)(b_j+1)P(\cdots,\{a_j-1,b_j+1,c_j\},\cdots;\tau) \\
&\quad+\sum_j (b_j-1)(c_j+1)P(\cdots,\{a_j,b_j-1,c_j+1\},\cdots;\tau) \\
&\quad+\sum_j (c_j-1)(a_j+1)P(\cdots,\{a_j+1,b_j,c_j-1\},\cdots;\tau) \\
&\quad\Big] \\
&+\Big[1-(1-p)\frac{1}{\beta^2}\frac{2}{N(n.n.)}\sum_j\sum_{<ij>}(a_ib_j+b_ic_j+c_ia_j) \\
&\qquad-p\frac{1}{N}\frac{2}{\beta(\beta-1)}\sum_j(a_jb_j+b_jc_j+c_ja_j)\Big]P(\{a_n,b_n,c_n\};\tau)
\end{aligned}
\tag{4.28}
$$

Where the notation used is the same as for equation 4.4 and equation 4.22. The only difference between the master equation above and the master equation 4.4 are the terms with the coefficient $\frac{2}{\beta(\beta-1)}$, as they are the self-interaction terms [26]. We then go through the same steps seen earlier in this subsection to derive the mean field equations:

$$
\partial_t A_k = 2(1-p)\left[\left(\frac{1}{n.n.}\sum_{<jk>}A_j\right)B_k-\left(\frac{1}{n.n.}\sum_{<jk>}C_j\right)A_k\right]+2p[A_kB_k-C_kA_k] \tag{4.29}
$$

Then following steps seen earlier in this section when adding spatial structure, equation 4.29 in d dimensions yields:

$$
\partial_t A = \frac{(1-p)}{d}\left[(\nabla^2 A)B-(\nabla^2 C)A\right]+2\left(BA-CA\right) \tag{4.30}
$$

So adding a self-interaction just rescales distance and can be seen as coarse graining the model. Also notice that p does not affect the self-interaction term.

4.4 The Mixing of Four Strategies

It results from the reactions in equation 4.1 that in the cyclic Lotka-Volterra scheme with four strategies, pairs of mutually neutral strategies are encountered, as the strategies A and C (B and D) do not compete against each other [10]. In the case of pure strategies, this partnership formation yields in a spatial game the formation of domains composed of neutral partners [91] as an agent with a given strategy takes advantage of the fact that its neutral partner plays a strategy that beats the strategy against which the agent would lose. This guiding principle also holds true when considering a four-strategies mixed game with time-dependent probability distributions. Still, remarkable changes in the domain structure and in the mean extinction time take place when changing the level of discretization of the probability distribution by increasing β.

In this section on four strategies we do not present any master equations or mean field equations. However the derivation and results would be very similar to those shown for three strategies.

4.4.1 Numerical Simulations on the Ring

A first impression of the changes that happen when the number of balls β is increased can be gained from the space-time plots shown in figure 4.7. For $\beta = 1$ we see the formation of regions dominated by neutral pairs (red and blue vs green and black). As there is no mechanism for mobility, red and blue (green and black) single-species regions become stuck within one another, forming superdomians of neutral partners [29,30]. As a results a winning strategy can invade the region of a losing strategy only until it hits a patch occupied by the partner the partner strategy of the losing strategy. This results in the zig-zag like structures where the different strategies (in order red, green, blue, black) dominate one after the other on a region of the lattice. These regions grow in extent after each change of strategy, yielding ultimately a lattice occupied by only one of the partnerships (either red and blue or green and black). As we increase β, domains of neutral pairs become effectively mixed, and a third strategy has a higher probability to invade a superdomain occupied by a given alliance. This results in a much slower growth of the neutral pair domains. Further increasing β causes the neutral species pairs to become very well mixed, resulting in two types of neutral-species domains that overall look purple and dark green. These neutral-species domains continue to compete against each other, yielding a slow coarsening process. Within these coarsening domains cyclic processes continue unabated, as revealed by the appearance of localized wave patterns for very large β, see figure 4.7. These waves are very much like those encountered in

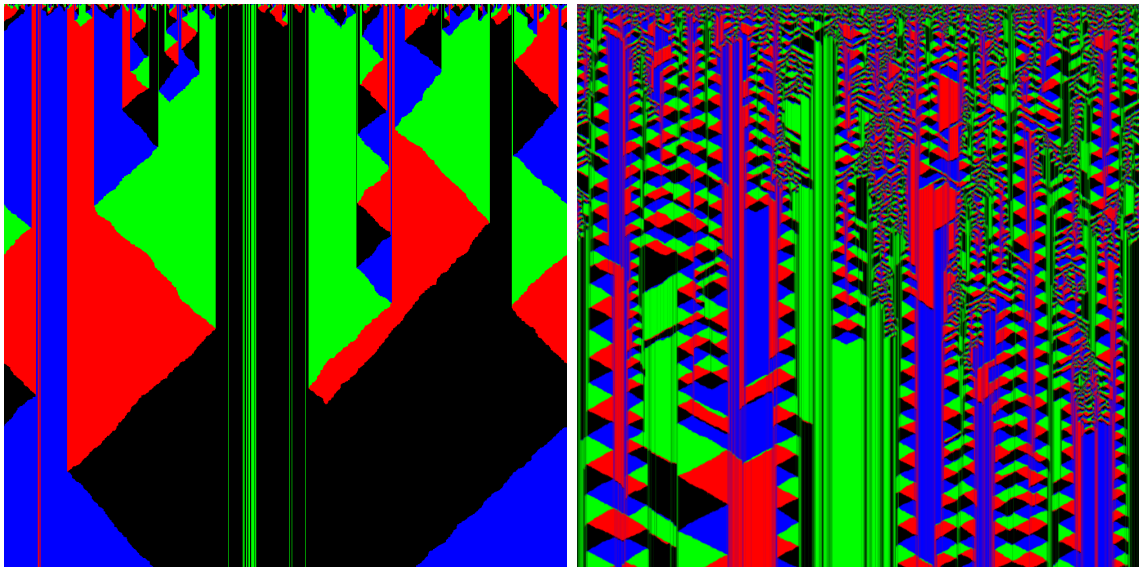

(a) $\beta = 1$ **(b)** $\beta = 10$

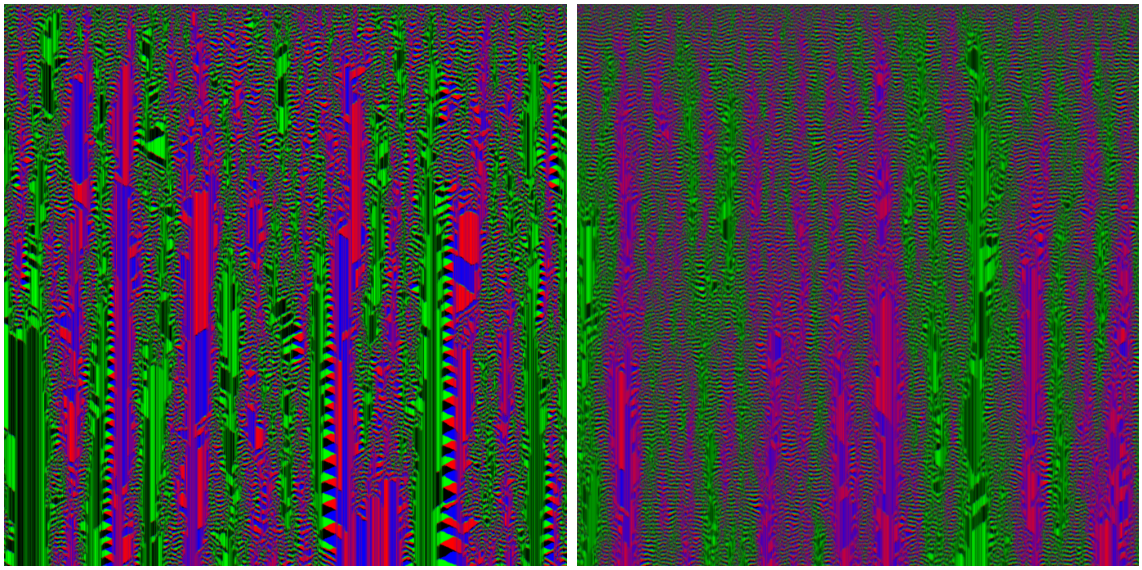

(c) $\beta = 20$ **(d)** $\beta = 50$

Figure 4.7: Space-time plots for four-strategies games on a ring with different numbers of balls β on each site: (a) $\beta = 1$, (b) $\beta = 10$, (c) $\beta = 20$, and (d) $\beta = 50$. Time progresses from top to bottom. 1000 time steps are shown for systems composed of 1000 sites. To determine the color of each lattice site we use the RGB color model and map the percentage of A, B, and C to the percentage of the colors Red, Green, and Blue respectively. This is adequate as the percentage of D is readily obtained from the fact that the sum over all densities is 1.

the three-species case, albeit of smaller extent, only that now one cycles through four types of balls instead of three.

For a more quantitative discussion we turn again to the space-time covariance of the form:

$$C_{XY}(x,t) = \frac{1}{N}\sum_i X_i(t)Y_{i+x}(t) - \mu_X(t)\mu_Y(t) \tag{4.31}$$

which yields the self-covariance if the species X and Y are the same (see equation 4.17) and the cross-covariance otherwise. We then define an *individual* spatial covariance through the equation:

$$C_i(x,t) = \frac{1}{4}\left(C_{AA}(x,t) + C_{BB}(x,t) + C_{CC}(x,t) + C_{DD}(x,t)\right) \tag{4.32}$$

A different spatial covariance can be obtained when we do not distinguish anymore between neutral strategies but consider them to form a unique group, i.e. strategies A and C together form the group denoted by $\mathcal{A}$, whereas B and D make up the group $\mathcal{B}$. We call the space-time covariance for these larger groups:

$$C_n(x,t) = \frac{1}{2}\left(C_{\mathcal{AA}}(x,t) + C_{\mathcal{BB}}(x,t)\right) \tag{4.33}$$

the *neutral* spatial covariance. From these two quantities we can extract two different time dependent length scales, $L_i(t)$ and $L_n(t)$, that provide some insights into the ordering of the super domains formed by neutral partners. These lengths are obtained from the intersection of the normalized covariance, $C_i(x,t)/C_i(0,t)$ and $C_n(x,t)/C_n(0,t)$, with a line of a constant value k, i.e. $C_i(x,t)/C_i(0,t) = k$ and similarly for $L_n(t)$. We use the following $k = 0.5$ after carefully checking that the qualitative features discussed below do not depend on the precise value of k.

Figure 4.8 shows the time evolution of these two lengths for different values of β. Let us first look at the pure case with $\beta = 1$, as we can compare for this case our lengths with those discussed previously in the literature. As shown by Frachebourg et al [30] one needs to consider two different types of domains for the four-species Lotka-Volterra model with immobile particles on a one-dimensional chain: the pure domains occupied by a single species and the super domains shared by two non-interacting species. Starting from a fully disordered state, the pure domains increase as $t^{1/3}$, whereas the superdomain size, i.e. the distance between active interfaces, is proportional to $t^{2/3}$. As seen in panel (a), for the case $\beta = 1$ both lengths $L_i(t)$ and $L_n(t)$ provide essentially the same information on the superdomains: they are proportional and both display an algebraic increase with an exponent 2/3 before saturating due to finite-size effects.

Increasing β yields a slowing down of the coarsening process as manifested by a gradual decrease of the exponent governing the growth of the two lengths. For $\beta = 5$, for example, the effective exponent before the transition to the saturation regime is close to 0.45, see panel (b). This decrease of the exponent describing the long-time regime before saturation

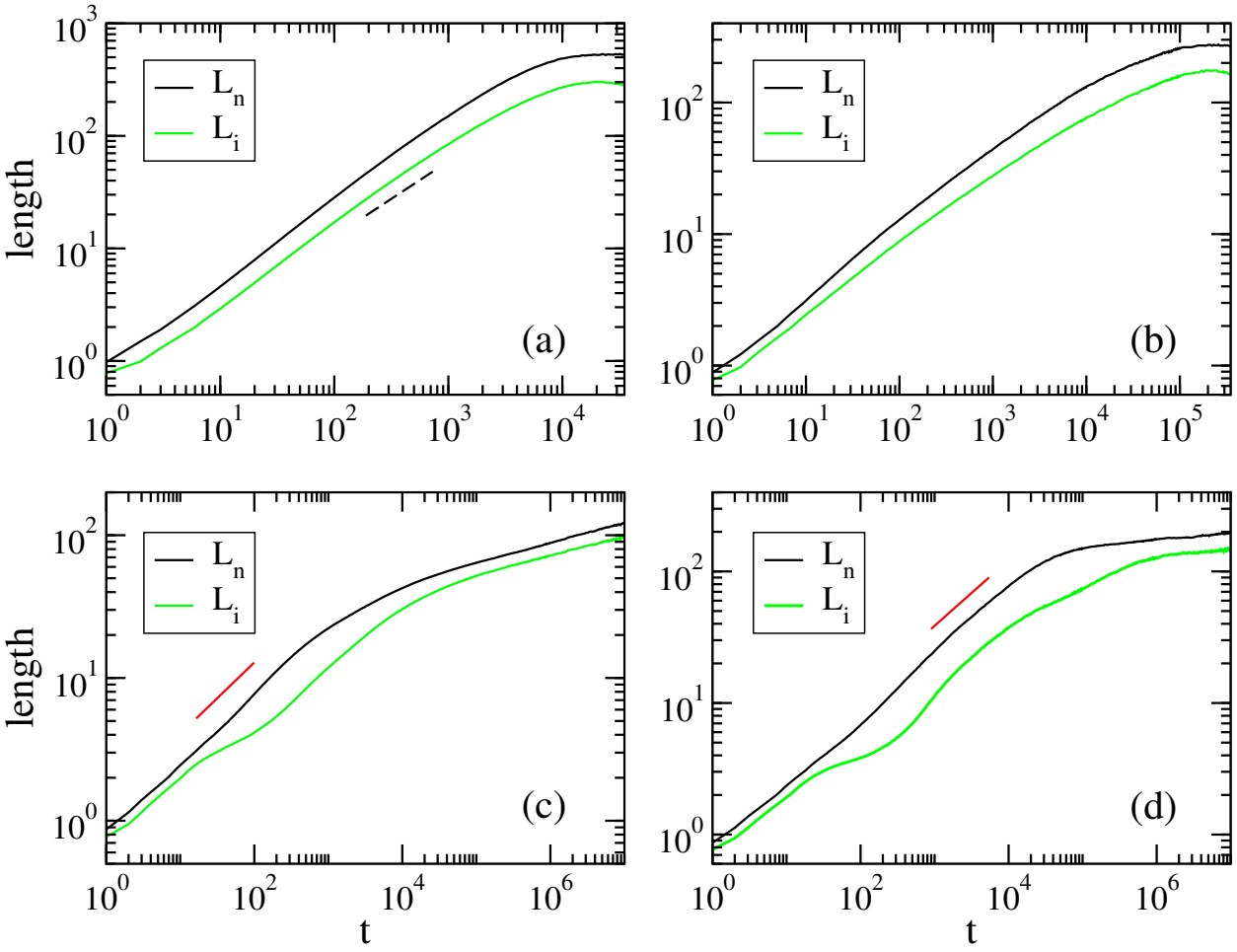

Figure 4.8: Time-dependent lengths extracted from the space-time covariance for the four-strategies mixed model on a one-dimensional lattice. The different panels show results for different of β: (a) $\beta = 1$, (b) $\beta = 5$, (c) $\beta = 15$, and (d) $\beta = 30$. L_i respectevily L_n is obtained from the individual respectively neutral spatial covariance. In (a) the system size is $N = 5000$, whereas in all other panels data for system of 2500 sites are shown. The data result from averaging over typically a few thousand independent runs. In (a) the dashed line indicates an exponent of 2/3 whereas in (c) and (d) the short red lines indicate an algebraic growth with an exponent of 1/2.

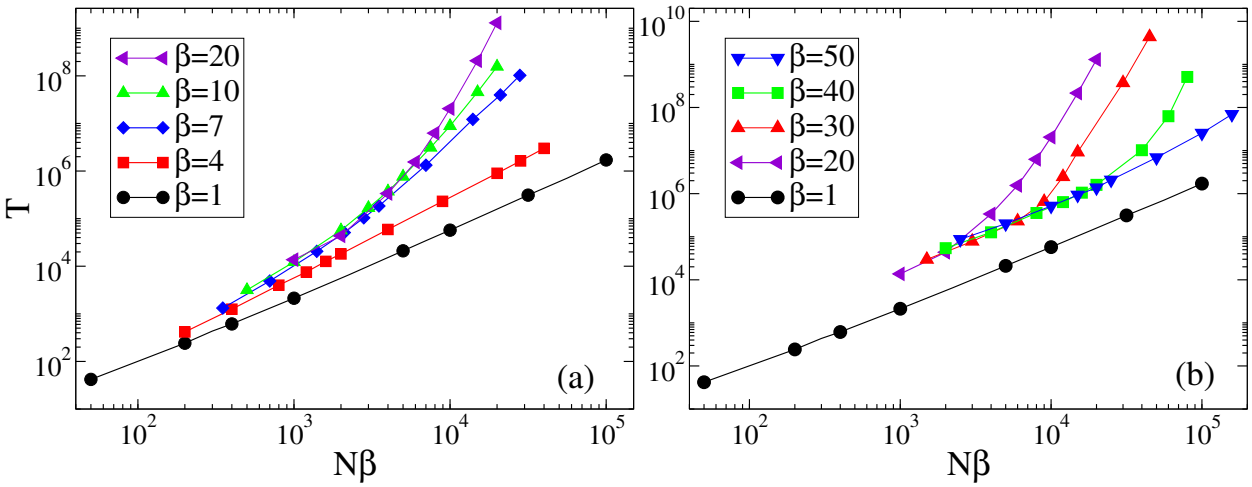

Figure 4.9: Average lattice domination time as a function of the total number of balls $N\beta$ in the system. Each data point results from an average over 2000 runs, the standard error being smaller than the sizes of the symbols.

continues when further increasing β, with a value of 0.14 for $\beta = 15$ and 0.05 for $\beta = 30$, see panels (c) and (d). This very slow increase for large β is not size-dependent and should therefore not be confused with the finite-size plateau seen for example in (a) for $\beta = 1$. The very weak increase of the correlation length for large β and large t instead indicates that domain growth almost comes to a standstill due to strong mixing effects. Interestingly, for large β the long-term regime is preceded by another regime where L_n increases as a square-root of time (indicated by the red segments in (c) and (d)), whereas L_i displays some non-trivial features that reflect the complicated ordering processes seen in the space-time plots. We tentatively identify this regime with the initial formation and growth of the neutral-species super domains followed by a coarsening process where essentially only two types of domains compete against each other.

Another way to characterize these systems is through the study of extinction events. The lattice domination time shown in figure 4.9 is the mean number of time steps needed until only one neutral species pair remains in the system. Interestingly, different regimes also show up in the lattice domination time when changing the value of β. For $\beta = 1$, i.e. the case of pure strategies the lattice domination time increases with the system size as $N^{1.40}$ [49], making this a neutrally stable system. Increasing β slightly changes the exponent (for $\beta = 4$ its value is 1.68), but has no other effect on the lattice domination time. For $\beta \geq 5$, however, different regimes emerge as a function of the system size, as shown in Fig. 4.9a. Plotting the lattice domination time against the total number of balls in the system, $N\beta$, reveals a first regime where the lattice domination time increases algebraically with an exponent close to 2. This is followed by a crossover to a second algebraic regime with a much larger exponent (for example, for $\beta = 30$ the exponent is 5.60). For β not too large, this crossover takes place at rather similar values of $N\beta$, i.e. the larger β is, the smaller the needed system size is to

enter the second algebraic regime. Fig. 4.9b displays another change of behavior for values of $\beta > 20$, as the crossover is then shifted to larger values of $N\beta$ when increasing β. For the smaller sizes, i.e. before the crossover, the data for different β values fall on one common curve with an exponent of approximately 1.5.

The emergence of two regimes in the lattice domination time for $\beta \geq 5$ can be related to different types of extinction events linked to the prevailing domain structure. On the one hand, in small systems extinction can take place at rather short times since the preparation of the system, due to the formation of a few super domains followed by a coarsening of these domains. For larger N many such domains are formed, resulting in complicated processes dominated by triangular (zig-zag) space-time patterns as those seen in figure 4.7b for $\beta = 10$. This periodic cycling through triangles of all four ball types yields a very slow coarsening process. A further increase of β results in the replacement in this second regime of the triangular structures by very long-lived wave patterns, due to some spatially localized synchronization, that dominate the purplish and dark green domains in figure 4.7d. Domains grow very slowly in that regime, see the late-time behavior of the growth length shown in figure 4.8d, and extinction events are only encountered at very late times.

In [49] we showed for the four-species model with pure strategies ($\beta = 1$) that much can be learned about extinction events when studying the probability distribution of the lattice domination time. We expect this to be also true for the more complicated cases with β large. However, the extremely large values of the domination times make it impossible with the resources at our disposal to perform enough runs for a reliable computation of this probability distribution.

Case with Swapping

We have also looked briefly into the case where we have allowed the swapping of neutral strategies. In figure 4.10 we show space-time plots of the four mixed strategy game where we have allowed swapping between neutral strategies/balls with rate 1. We find, much like in [49], that neutral species domains form and, due to the high swap rate, become very well mixed and homogenous. These domains then coarsen, creating slowly growing domains of purplish and dark green color, the best example being 4.10c. However unlike 4.7 the zig-zags as well as the wave patterns are not as prominent for a low value of β. For large values of β though the systems with and without swapping are indistinguishable.

4.5 Discussion and Summary

In this chapter we discussed a version of the three- and four-species Lotka-Volterra model where the agents are using a mixed strategy, i.e. agents play a pure strategy using probability distribution every time they interact. Taking into account that agents, both in ecology

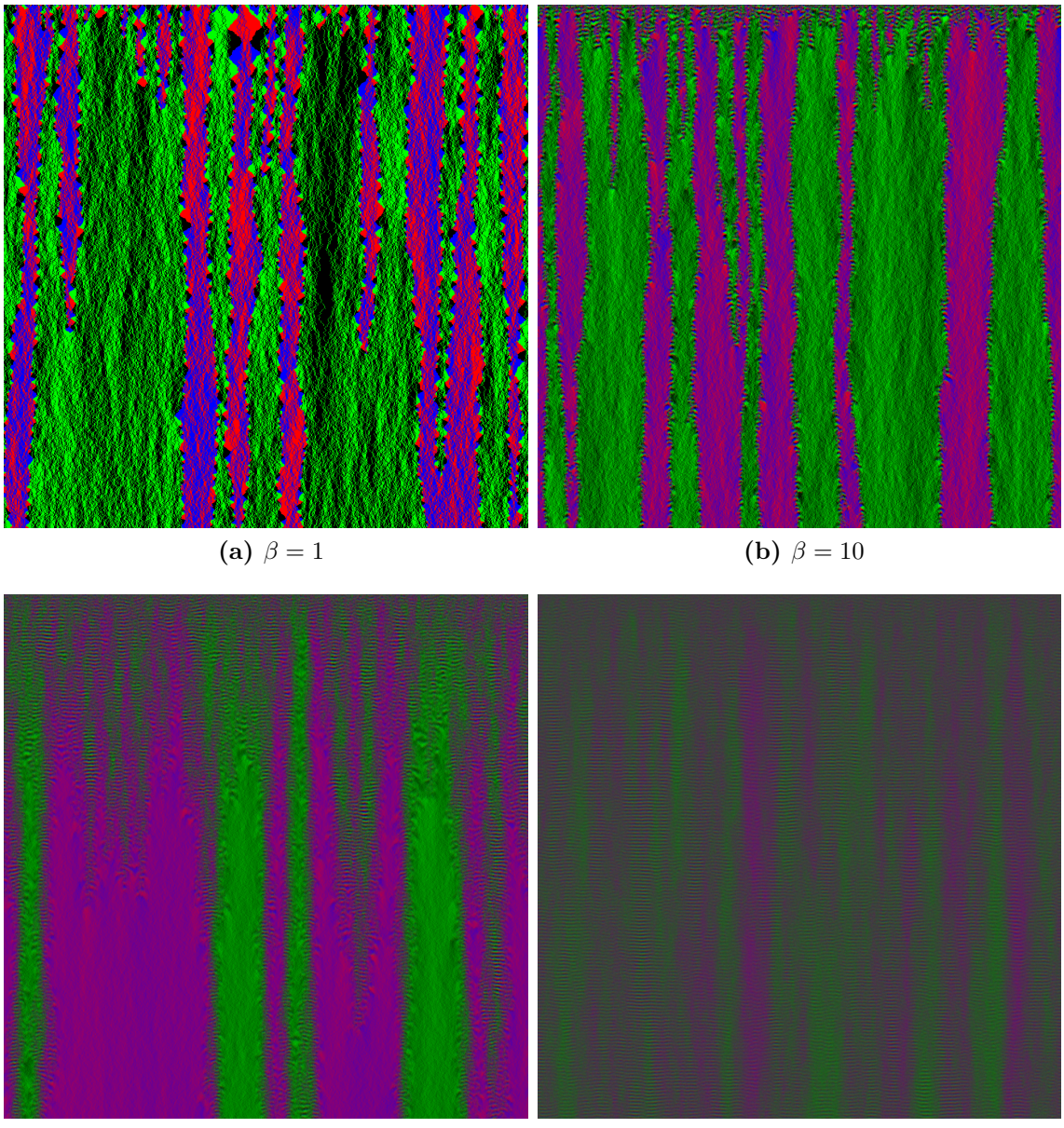

(a) $\beta = 1$ **(b)** $\beta = 10$

(c) $\beta = 100$ **(d)** $\beta = 1000$

Figure 4.10: Space-time plots for four-strategies games on a ring where we have allowed neutral strategy swapping with different numbers of balls β on each site: (a) $\beta = 1$, (b) $\beta = 10$, (c) $\beta = 100$, and (d) $\beta = 1000$. Time progresses from top to bottom. 1000 time steps are shown for systems composed of 1000 sites. We use the same coloring seen in figure 4.7.

and economics, tend to learn from past experience, we consider time-dependent probability distributions where a losing agent decreases the probability to play a losing strategy at the next interaction. In order to do so, we treat an agent as an urn containing β balls of three respectively four types, where each type corresponds to one of the three respectively four strategies. If a strategy loses, a ball of the corresponding type is replaced by a ball with the winning strategy. The number of balls β in the urn therefore measure the level of discretization of the probability distribution, with the limit $\beta \to \infty$ corresponding to a continuous distribution.

As our study revealed, some remarkable changes take place when changing the level of discretization. For the three-strategy case on a one-dimensional lattice we observe a transition between neutrally stable for $\beta \leq 3$, where the average time needed for one strategy to completely pervade the system grows algebraically with the system size, to stable for $\beta > 3$, where this time increases exponentially with the extent of the system. This transition gives rise to a change of space-time patterns and the emergence of a tiling structure where strategies dominate for a finite amount of time over certain regions of the lattice. In the limit $\beta \gg 1$, when the probability distribution approximates a continuous distribution, this tiling structure evolves into spatially extended waves where the dominating strategies changes periodically. Synchronization throughout the system is also encountered in the case without spatial dependence and can be understood in the mean-field limit of an infinite number of agents using continuous probability distributions by analyzing the corresponding rate equations.

The four-strategy case is characterized by the existence of pairs of non-interacting strategies. As a result agents in a spatial setting with $\beta = 1$ want to ally themselves with agents that play the complementary strategy in order to fight off the competing pair of strategies. A direct consequence of this rivalry between competing alliances is the formation and coarsening of superdomains occupied by a single alliance. In contrast to the three-strategy case, an increase of β does not yield a stable system. Instead, the mean lattice domination time, i.e. the average time needed for one alliance to completely fill the system, always increases algebraically with $N\beta$. Still, different regimes can be identified as a function of N and β. For example for large values of these parameters a very slow coarsening process is observed, with local synchronized waves within the competing domains.

Besides some results for the well-mixed case without spatial setting, we focus in this chapter on the one-dimensional lattice. It is well known from cases with $\beta = 1$ that the dimensionality of the lattice can have a huge impact on the properties of the system. Taking into account the already complex behavior observed in our study of the ring, we expect the appearance of additional intriguing features, especially for the four-strategy case, when considering systems with time-dependent probability distributions in two space dimensions.

We have restricted us to the simple three- and four-species Lotka-Volterra models with time-dependent probability distribution, as for these situations the properties for the case $\beta = 1$ are well understood and provide a case against which we can study changes that emerge

when using a time-dependent probability distribution to play a strategy. Recently there has been a strong focus on more complicated situations, with more species and/or more complex interaction schemes. It is an interesting question how the properties of these systems change when considering a mixed strategy game with a time-dependent probability distribution.

Chapter 5

Conclusions

In this thesis we have studied game theoretic ecological models. Specifically we studied finite systems with cyclic competition and pure and mixed strategies. Cyclic competition has gained a lot of popularity in the physics community and has applications to lizards and bacteria, as described in the introduction of this thesis. A plethora of publications on the topic of cyclic competition has even been produced from Virginia Tech [10, 26, 27, 40–43, 49, 50, 74, 90, 91, 116, 130]. Most of these are for the case of pure strategies. The case of pure strategies has been extensively studied and is used to model biological and ecological systems where a strategy represents a genotype. In chapter 3 the case of four cyclically competing species, specifically the lattice domination time, is extensively studied. However, in social and economics systems it is possible for an agent to choose a strategy out of a distribution. In chapter 4 we introduce a model that attempts to bridge population dynamics to decision theory. Mean field approximations for all models studied in this thesis give coexistence in the form of oscillations for all strategies, but for finite systems this is not the case as extinction can readily occur.

5.1 Extinction in Four Species

Stochastic evolution of a finite population of predators and prey eventually ends in species extinctions and loss of biodiversity. In many instances very different routes to species extinctions are possible, where the different extinction scenarios might prevail at different stages of the time evolution.

It is found that even though mean field equations predict ever-lasting coexistence for four cyclically competing species, when the system has a finite size it is possible for one of the species to become extinct due to stochastic fluctuations, in the well mixed case, or coarsening, when there is spatial structure. In a well mixed system the probability distributions of what we call the lattice domination time are shaped much like that of a shifted exponential with a

characteristic slope and can be scaled onto a master curve through scaling by the system size. However by adding space to the model we see that the probability distribution drastically changes, and now contains two characteristic slopes. The first slope is from systems that die out quickly, which we attribute to individual domains dying out and the system effectively behaving well mixed. The second slope is for long lived systems, which we attribute to neutral species pair domain formation and slow coarsening.

The takeaway message we wish to convey to the reader for that chapter is that spatial structure promotes cooperation and that looking at probability distributions for extinction times may convey more information than looking at averages.

5.2 Mixed Strategies in Cyclic Competition

Systems composed of multiple species that interact in a cyclic way have been at the center of a multitude of studies in recent years. Mostly discussed in the context of evolutionary game theory and population dynamics, these systems allow us to understand some of the generic properties arising from non-trivial interactions in ecological systems.

We find that in the mixed strategy model different stabilities occur depending on how discretized the probability distributions are with the parameter β. For three strategies in one dimension we find that the stability transitions from neutrally stable to stable when β goes from three to four. This transition can also be seen in space-time plots when tiles of pure strategies form for $\beta \geq 4$. Interesting steps are also seen in the spatial covariance, which is attributed to the size of the pure strategy tiles. However, this sudden transition is not seen with four strategies, where we instead observe a transition between two neutrally stable regimes. This neutral stability is attributed to the fact that with four strategies there are now neutral strategies which form domains with one another. These neutral domains coarsen slowly, giving a long lived system which is neutrally stable. In the case of both the three and four strategies systems we found that with a large enough value of β all of the agents strategies synchronize, causing temporal patterns and oscillations through the system.

For the reader we wish to convey that by allowing agents to choose their strategy from a distribution, rather than playing a pure strategy, it is possible to change the stability of the system. Also, depending on how discretized the distribution is, we get intriguing behavior, such as changes in stability and synchronization.

5.3 Future and Prospective Work

In this thesis we have only looked into the cases of three and four strategies/species. More interesting behavior might be found if one extends the model(s) to more species. We have

also restricted ourselves to using Lotka-Volterra dynamics, and it would be interesting to instead use May-Leonard dynamics to see differences. In the mixed strategy project we have only looked into the one-dimensional case, and it is possible that there could be interesting dynamics happening in higher dimensions. We have also only looked into the average extinction/domination times in that project and it would also be interesting to look at probability distribution of those quantities.

5.4 Research Acknowledgements

I would like to thank Sven Dorosz for sharing his preliminary results of simulations on the Sierpinski lattice and useful discussions that were helpful in the results of the third chapter of this thesis. I also thank Qian He and Professor Uwe Täuber for sharing and discussing results of their previous publications.

In no particular order I would also like to thank Johannes Knebel, Richard Blythe, Darka Labavic, Hildegard Meyer-Ortmanns, and Malte Henkel for useful discussions.

Appendix A

Well Mixed Always Changing Pair Periods

When simulating well mixed systems it is possible to speed up the computational run time by using schemes to rescale time. In reference [27] for the well mixed system two algorithmic schemes are used. The first is the pick random pair (PRP) scheme in which two agents were chosen from the system and react if possible. The second is what is called the always changing pair (ACP) scheme which is similar to that of a Gillespie algorithm. For the ACP scheme 'time' is measured in terms of interaction steps.

Table A.1 is an example of how ACP is used for three species (RPS) Lotka Volterra model. Note that one reaction time step is $1/Z$ in system time, and also that the k_i values can be greater than one due to the normalization of the probabilities. A similar scheme can be used for four species. In figure A.1 we show a density plots and corresponding power spectrum

Reaction	**Probability**
$A + B \xrightarrow{k_a} A + A$	$k_a N_a N_b / Z$
$B + C \xrightarrow{k_b} B + B$	$k_b N_b N_c / Z$
$C + A \xrightarrow{k_c} C + C$	$k_c N_c N_a / Z$

Table A.1: Description of how to model the RPS ACP Scheme, where $Z \equiv k_a N_a N_b + k_b N_b N_c + k_c N_c N_a$.

for RPS and four species. We find that using the scheme shown in table A.1 gives sharp peaks in the power spectra when the parameters yield oscillations for the mean field theory (please see references [10, 26, 27] for details). From the peaks in the power spectra we can calculate the period by dividing the number of Monte Carlo time steps by the local maxima of the power spectra.

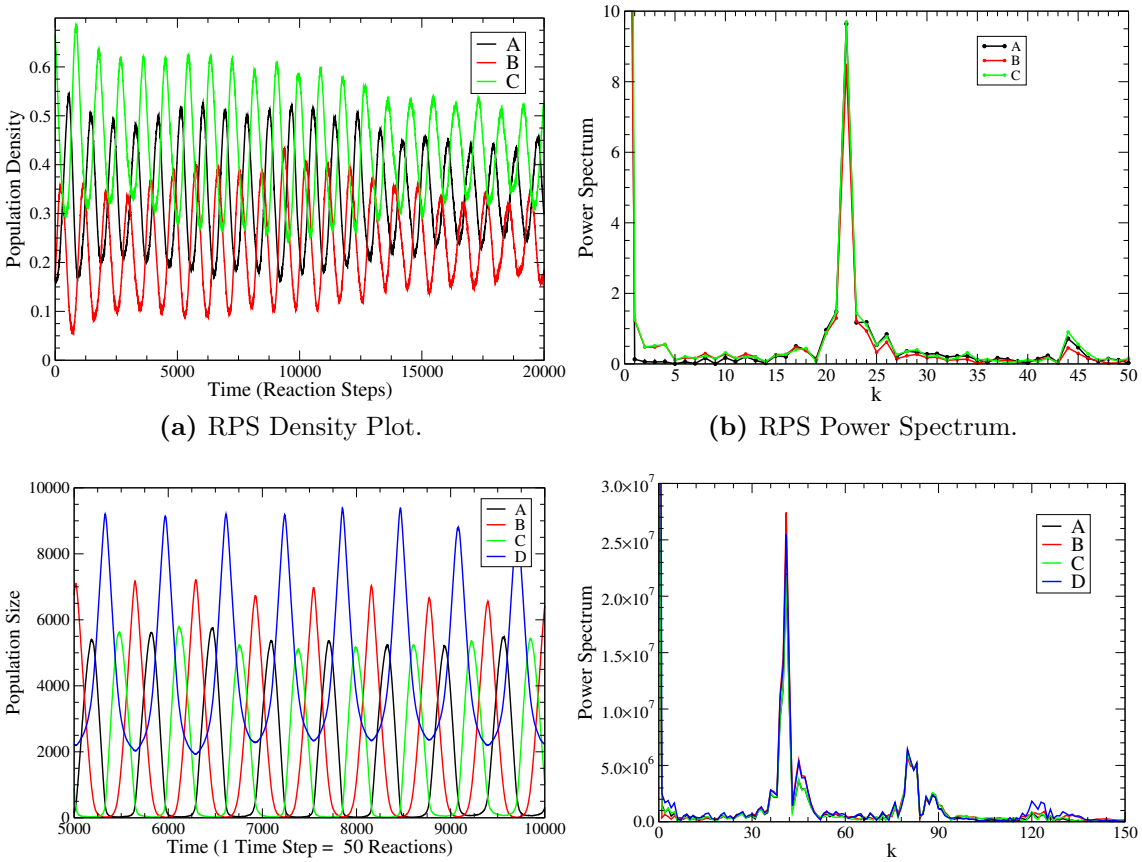

(a) RPS Density Plot.

(b) RPS Power Spectrum.

(c) Four Species Densities.

(d) Four Species Power Spectrum.

Figure A.1: Density and power spectra using the ACP scheme. Plot (a) ran for 20 000 reactions with reaction rates $k_a = 3$, $k_b = 2$, $k_c = 1$ and initial conditions $N_a = 50$, $N_b = 50$, and $N_c = 200$. (b) is the power spectrum of plot (a) with a prominent peak at value 22 with another at around 44. Plot (c) ran for 24 939 x 50 reactions and had reaction rates $k_a = 0.4$, $k_b = 0.4$, $k_c = 0.1$, $k_d = 0.1$, and initial conditions $N_a = 200$, $N_b = 1000$, $N_c = 4800$, and $N_d = 4000$. (d) is the power spectrum of plot (c) with a prominent peak at value 41 and others at values around 80 and 120. The code to generate the data for plot (c) courtesy of Sara Case.

In table A.2 we show the approximate period for different system sizes and reaction rates for the RPS well mixed system. Notice that in all cases the period (T) is roughly three times the system size (N). We do the same for four species in table A.3 and find again that the period (T) is roughly three times the system size (N).

Rates			**Ini. Pop.**			**Tot. Pop.**	**Period**
k_a	k_b	k_c	N_a	N_b	N_c	N	T
3	2	1	100	100	100	300	909
3	2	1	50	50	200	300	909
3	2	1	150	150	150	450	1333
3	2	1	200	200	200	600	1818
3	2	1	250	250	250	750	2222
2	1	1	100	100	100	300	909
2	1	1	150	150	150	450	1428
2	1	1	25	25	400	450	1379
2	1	1	200	200	200	600	1818
1	1	1	100	100	100	300	952
1	1	1	150	150	150	450	1428
1	1	1	50	50	500	600	1818

Table A.2: Table of calculated periods with different rates and initial conditions for the well mixed RPS system. Each measurement used 30 ensembles.

Rates				**Ini. Pop.**				**Tot. Pop.**	**Period**
k_a	k_b	k_c	k_d	N_a	N_b	N_c	N_d	N	T
0.5	0.5	0.5	0.5	1000	1500	500	2000	5000	15439
0.5	0.5	0.5	0.5	2500	2500	2500	2500	10000	32125
0.4	0.4	0.1	0.1	1875	1875	1875	1875	7500	21365
0.4	0.4	0.1	0.1	200	1000	4800	4000	10000	30413
0.4	0.4	0.1	0.1	2500	2500	2500	2500	10000	30255
0.3	0.3	0.2	0.2	1250	1250	1250	1250	5000	16530
0.3	0.3	0.2	0.2	1000	1250	1750	3500	7500	20101
0.3	0.3	0.2	0.2	4000	1000	4000	1000	10000	29247

Table A.3: Table of calculated periods with different rates and initial conditions for the well mixed four species system. Each measurement used a single run. The code to generate the data courtesy of Sara Case.

Appendix B

Spatial Covariance Relations

In this appendix we exploit a quantity that is conserved on each lattice site, the maximal occupancy, to form a relation between self and cross covariances for models that have cyclic symmetry across species. We derive relations for the cases when reactions conserve particle number (Lotka-Volterra dynamics) and when it does not (May-Leonard dynamics, treating empty sites as a separate species).

B.1 Lotka-Volterra Dynamics

Assuming a fully occupied lattice and cyclic Lotka-Volterra dynamics (which conserves total particle number) with all species symmetric, for the Rock-Paper-Scissors (RPS) model each lattice site has a density of either A,B, or C, which means that there is a conservation law:

$$a_k(t) + b_k(t) + c_k(t) = 1 \tag{B.1}$$

where $a_k(t)$ is the density of particle A at site k at time t, and similarly for $b_k(t)$ and $c_k(t)$. Summing over all sites k in equation B.1 and dividing by the total number of lattice sites (N) yields the sum of the spatial means:

$$\mu_a(t) + \mu_b(t) + \mu_c(t) = 1 \tag{B.2}$$

where $\mu_a(t) = \frac{1}{N}\sum_i a_i(t)$. We can rewrite $1 = 1$ as:

$$\begin{aligned} \frac{1}{N}\sum_i \left[a_i(t) + b_i(t) + c_i(t)\right]\left[a_{i+x}(t) + b_{i+x}(t) + c_{i+x}(t)\right] = \\ = \left[\mu_a(t) + \mu_b(t) + \mu_c(t)\right]\left[\mu_a(t) + \mu_b(t) + \mu_c(t)\right] \end{aligned} \tag{B.3}$$

Now expand the polynomials on each side of equation B.3, subtract the right side (the means) from the left to get some equation that equals zero, and focus on the covariance terms which

look like:

$$C_{aa}(x,t) = \frac{1}{N}\sum_i a_i(t)a_{i+x}(t) - \mu_a(t)\mu_a(t) \tag{B.4}$$

and cross-covariance terms:

$$C_{ab}(x,t) = \frac{1}{N}\sum_i a_i(t)b_{i+x}(t) - \mu_a(t)\mu_b(t) \tag{B.5}$$

One of the assumptions about the cross-covariances that is made is that it is spatially and particle symmetric, which in equation form is:

$$C_{ab}(x,t) = C_{ab}(-x,t) = C_{ba}(x,t) = C_{ba}(-x,t) \tag{B.6}$$

Mathematically the only equality in equation(s) B.6 is $C_{ab}(x,t) = C_{ba}(-x,t)$, however the rest of equalities are true for physics reasons as long as there are no asymmetries on the lattice (and enough ensembles to get rid of noise).

Now combining equations B.4, B.5, and B.6 into equation B.3 yields:

$$C_{aa}(x,t) + C_{bb}(x,t) + C_{cc}(x,t) + 2\left[C_{ab}(x,t) + C_{bc}(x,t) + C_{ca}(x,t)\right] = 0 \tag{B.7}$$

Now let us define:

$$C_0(x,t) = \frac{C_{aa}(x,t) + C_{bb}(x,t) + C_{cc}(x,t)}{3} \tag{B.8}$$

to be the total spatial covariance and:

$$C_1(x,t) = \frac{C_{ab}(x,t) + C_{bc}(x,t) + C_{ca}(x,t)}{3} \tag{B.9}$$

to be the total spatial cross-covariance. Finally combining equations B.8 and B.9 into equation B.7 yields:

$$C_0(x,t) + 2C_1(x,t) = 0 \tag{B.10}$$

So if C_0 and C_1 were to be exponential/power law in x at a fixed time t they would have to have the same slope on a linear-log / log-log plot. Notice that in the derivation of B.10 no specific lattice structure was assumed other than it having reflection symmetry. Empirical evidence is shown in figure B.1.

Although the calculation were done with three species (RPS) it is possible to extend it to many species, as long as there is cyclic symmetry across the species. A prime example would be the reaction scheme seen in [74]. This scheme is a generalization of cyclic competition and has n cyclically competing species who predate on r species in a cyclic way. In their model they have Lotka-Volterra and May-Leonard reactions, however for this section we disregard the May-Leonard reactions. We have to define the covariance between any two species. This is done by using similar notation for species and interactions as in [74]. If we have n species

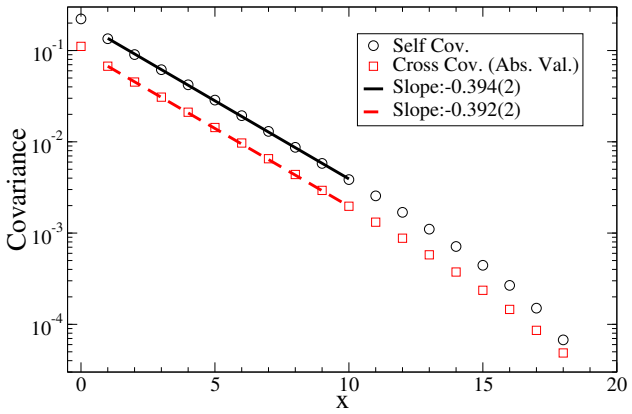

Figure B.1: The self (C_0) and cross (C_1) spatial covariance at time step 200 as a function of distance x for a 2D periodic lattice system with length 256 with 5000 ensembles. Exponential fits are also shown. Notice that the slopes are very similar (by up to 2 digits). These are improved statistics of the results of [41].

and define $S_i(x,t)$ to be the number of species i at lattice site x at time t, we define the covariance between two species to be:

$$C_{i,j}(x,t) = \frac{1}{N}\sum_y S_i(y,t)S_j(y+x,t) - \left(\frac{1}{N}\sum_y S_i(y,t)\right)\left(\frac{1}{N}\sum_y S_j(y,t)\right) \tag{B.11}$$

where the sum over y is over the lattice points of which there are N. This equation is very similar to that of equations B.4 and B.5 and we exactly get B.4 for $i = j$. We now define the symmetric covariance to be:

$$C_j(x,t) = \frac{1}{n}\sum_{i=1}^{n} C_{i,i+j}(x,t) \tag{B.12}$$

where j takes integer values between and including 0 and $\lfloor n/2 \rfloor$. If the quantity $i+j$ is bigger than n it is modulo by n. Using these generalized definitions, equations B.8 and B.9 are recovered for $n = 3$. We can now generate the relations between different symmetric covariances, like in equation B.10, for an arbitrary number of species. Some sample calculations of what the symmetric covariance relations would look like for different numbers of species are listed in table B.1.

B.2 May-Leonard Dynamics

It is also possible to perform the same calculations for the full model given in [74] with May-Leonard reactions. However we need to take into account empty sites. For a model with

Number of Species (n)	Symmetric Covariance Relation
1	$C_0 = 0$
2	$C_0 + C_1 = 0$
3	$C_0 + 2C_1 = 0$
4	$C_0 + 2C_1 + C_2 = 0$
5	$C_0 + 2C_1 + 2C_2 = 0$
6	$C_0 + 2C_1 + 2C_2 + C_3 = 0$
7	$C_0 + 2C_1 + 2C_2 + 2C_3 = 0$

Table B.1: Symmetric covariance relations for different numbers of species (n) in the Lotka-Volterra reaction scheme and fully occupied lattice.

single occupancy or with multiple occupancy with a maximum occupation size we still have a conserved quantity. Reusing our RPS notation from equation B.1 and B.2 the conserved quantities are now:

$$a_k(t) + b_k(t) + c_k(t) + \varnothing_k(t) = 1 \tag{B.13}$$

$$\mu_a(t) + \mu_b(t) + \mu_c(t) + \mu_\varnothing(t) = 1 \tag{B.14}$$

where $\varnothing$ represents empty sites. with the introduction of empty sites we now have to define two new covariances, the covariance between species and empty sites and the self covariance of empty sites, which are respectively:

$$C_E = \frac{C_{a\varnothing} + C_{b\varnothing} + C_{c\varnothing}}{3} \tag{B.15}$$

$$C_\varnothing = C_{\varnothing\varnothing} \tag{B.16}$$

where we have used the notation of equations B.5 and B.11 for the double indexed covariances. Following the same steps seen in section B.1 for equations B.13 and B.14 we arrive at the spatial covariance relation:

$$C_0 + 2C_1 + 2C_E + \frac{1}{3}C_\varnothing = 0 \tag{B.17}$$

where we have reused the symmetric covariance as defined in equation B.12. Notice that the only difference between B.10 and B.17 is the term $2C_E + \frac{1}{3}C_\varnothing$. Like in section B.1 we again create a table of the covariance relations for May-Leonard type dynamics in table B.2. Notice that the entries in the table are almost identical to those in table B.1 except for the term $2C_E + \frac{1}{n}C_\varnothing$.

Number of Species (n)	Symmetric Covariance Relation
1	$C_0 + 2C_E + C_\varnothing = 0$
2	$C_0 + C_1 + 2C_E + \frac{1}{2}C_\varnothing = 0$
3	$C_0 + 2C_1 + 2C_E + \frac{1}{3}C_\varnothing = 0$
4	$C_0 + 2C_1 + C_2 + 2C_E + \frac{1}{4}C_\varnothing = 0$
5	$C_0 + 2C_1 + 2C_2 + 2C_E + \frac{1}{5}C_\varnothing = 0$
6	$C_0 + 2C_1 + 2C_2 + C_3 + 2C_E + \frac{1}{6}C_\varnothing = 0$
7	$C_0 + 2C_1 + 2C_2 + 2C_3 + 2C_E + \frac{1}{7}C_\varnothing = 0$

Table B.2: Symmetric covariance relations for different numbers of species (n) in the May-Leonard reaction scheme with a maximum occupancy.

Bibliography

[1] D. Aerts, M. Czachor, B. D'Hooghe, M. Kuna, B. Sinervo, and S. Sozzo. Quantum probabilities in competing lizard communities. *Nature Publishing Group*, 2012. (Cited on page 11.)

[2] A. Arenas, J. Camacho, J. a. Cuesta, and R. J. Requejo. The joker effect: cooperation driven by destructive agents. *Journal of Theoretical Biology*, 279(1):113, June 2011. (Cited on pages 7 and 37.)

[3] R. Axelrod. Effective choice in the prisoner's dilemma. *Journal of Conflict Resolution*, 24(1):3, 1980. (Cited on page 3.)

[4] R. Axelrod and W. D. Hamilton. The evolution of cooperation. *Science*, 211(4489):1390, 1981. (Cited on page 3.)

[5] R. M. Axelrod. *The evolution of cooperation*. Basic books, 2006. (Cited on page 3.)

[6] E. Bahel. Rock–paper–scissors and cycle-based games. *Economics Letters*, 115(3):401, 2012. (Cited on pages 6 and 37.)

[7] A. Blasi. On a random walk between a reflecting and an absorbing barrier. *The Annals of Probability*, 4(4):695, 1976. (Cited on page 22.)

[8] D. D. Cameron, A. White, and J. Antonovics. Parasite-grass-forb interactions and rock-paper-scissor dynamics: predicting the effects of the parasitic plant Rhinanthus minor on host plant communities. *Journal of Ecology*, 97(6):1311, Nov. 2009. (Cited on page 4.)

[9] R. S. Cantrell and C. Cosner. *Spatial ecology via reaction-diffusion equations*. John Wiley & Sons, 2004. (Cited on page 10.)

[10] S. O. Case, C. H. Durney, M. Pleimling, and R. K. P. Zia. Cyclic competition of four species: Mean-field theory and stochastic evolution. *EPL (Europhysics Letters)*, 92(5):58003, Dec. 2010. (Cited on pages 13, 18, 38, 54, 63, and 66.)

[11] A. M. Chammah and A. Rapoport. *Prisoner's Dilemma: a Study in Conflict and Cooperation*. Ann Arbor, University of Michigan Press, 1965. (Cited on page 3.)

[12] L. Cronk and B. L. Leech. *Meeting at Grand Central: understanding the social and evolutionary roots of cooperation*. Princeton University Press, 2012. (Cited on page 6.)

[13] M. Cross and H. Greenside. *Pattern formation and dynamics in nonequilibrium systems*. Cambridge University Press, 2009. (Cited on page 13.)

[14] M. C. Cross and P. C. Hohenberg. Pattern formation outside of equilibrium. *Reviews of Modern Physics*, 65(3):851, 1993. (Cited on page 13.)

[15] P. H. Crowley. Hawks, doves, and mixed-symmetry games. *Journal of Theoretical Biology*, 204(4):543, 2000. (Cited on page 37.)

[16] L. Dai, K. S. Korolev, and J. Gore. Slower recovery in space before collapse of connected populations. *Nature*, 496(7445):355, 2013. (Cited on page 17.)

[17] L. Dai, D. Vorselen, K. S. Korolev, and J. Gore. Generic indicators for loss of resilience before a tipping point leading to population collapse. *Science*, 336(6085):1175, 2012. (Cited on page 17.)

[18] D. F. de Souza, H. C. Carneiro, F. M. Franca, and P. Lima. Rock-paper-scissors wisard. In *Computational Intelligence and 11th Brazilian Congress on Computational Intelligence (BRICS-CCI & CBIC), 2013 BRICS Congress on*, page 178. IEEE, 2013. (Cited on page 6.)

[19] A. Deutsch and S. Dormann. *Cellular automaton modeling of biological pattern formation*. Springer Science and Business Media, 2005. (Cited on page 13.)

[20] U. Dobramysl. *On the Relaxation Dynamics of Disordered Systems*. PhD thesis, Virginia Tech, 2013. (Cited on page 1.)

[21] U. Dobramysl and U. Täuber. Spatial variability enhances species fitness in stochastic predator-prey interactions. *Physical Review Letters*, 101(25):258102, Dec. 2008. (Cited on page 1.)

[22] U. Dobramysl and U. C. Täuber. Environmental versus demographic variability in stochastic predator–prey models. *Journal of Statistical Mechanics: Theory and Experiment*, 2013(10):P10001, Oct. 2013. (Cited on pages 1 and 13.)

[23] U. Dobramysl and U. C. Täuber. Environmental versus demographic variability in two-species predator-prey models. *Physical Review Letters*, 110(4):048105, Jan. 2013. (Cited on page 1.)

[24] A. Dobrinevski and E. Frey. Extinction in neutrally stable stochastic Lotka-Volterra models. *Physical Review E*, 85(5):051903, 2012. (Cited on pages ix, 13, 16, 19, 22, and 46.)

[25] L. A. Dugatkin and H. K. Reeve. *Game theory and animal behavior*. Oxford University Press, 1998. (Cited on page 4.)

[26] C. H. Durney, S. O. Case, M. Pleimling, and R. K. P. Zia. Saddles, arrows, and spirals: Deterministic trajectories in cyclic competition of four species. *Physical Review E*, 83(5):051108, May 2011. (Cited on pages 10, 18, 53, 63, and 66.)

[27] C. H. Durney, S. O. Case, M. Pleimling, and R. K. P. Zia. Stochastic evolution of four species in cyclic competition. *Journal of Statistical Mechanics: Theory and Experiment*, 2012(06):P06014, June 2012. (Cited on pages 13, 18, 63, and 66.)

[28] D. Easley and J. Kleinberg. *Networks, crowds, and markets: Reasoning about a highly connected world*. Cambridge University Press, 2010. (Cited on page 4.)

[29] L. Frachebourg, P. Krapivsky, and E. Ben-Naim. Segregation in a one-dimensional model of interacting species. *Physical Review Letters*, 77(10):2125, 1996. (Cited on pages 38 and 54.)

[30] L. Frachebourg, P. L. Krapivsky, and E. Ben-Naim. Spatial organization in cyclic Lotka-Volterra systems. *Physical Review E*, 54(6):6186, 1996. (Cited on pages 34, 38, 54, and 56.)

[31] E. Frey. Evolutionary game theory: Theoretical concepts and applications to microbial communities. *Physica A: Statistical Mechanics and its Applications*, 389(20):4265, Oct. 2010. (Cited on page 11.)

[32] D. Fundenberg and E. Maskin. Evolution and cooperation in noisy repeated games. *The American Economic Review*, page 274, 1990. (Cited on page 3.)

[33] C. Gavin, A. Pokrovskii, M. Prentice, and V. Sobolev. Dynamics of a Lotka-Volterra type model with applications to marine phage population dynamics. In *Journal of Physics: Conference Series*, volume 55, page 80. IOP Publishing, 2006. (Cited on page 1.)

[34] J. P. Gollub and J. Langer. Pattern formation in nonequilibrium physics. *Reviews of Modern Physics*, 71(2):S396, 1999. (Cited on page 13.)

[35] G. Hardin. The tragedy of the commons. *Science*, 162(3859):1243, 1968. (Cited on page 6.)

[36] J. C. Hardin and A. L. Sweet. A note on absorption probabilities for a random walk between a reflecting and an absorbing barrier. *Journal of Applied Probability*, 6(1):224, 1969. (Cited on pages 22 and 23.)

[37] J. C. Hardin and A. L. Sweet. Moments of the time to absorption in the random walk between a reflecting and an absorbing barrier. *Society of Industrial and Applied Mathematics Review*, 12(1):140, 1970. (Cited on pages 22 and 23.)

[38] C. Hauert, S. De Monte, J. Hofbauer, and K. Sigmund. Volunteering as Red Queen mechanism for cooperation in public goods games. *Science (New York, N.Y.)*, 296(5570):1129, May 2002. (Cited on page 7.)

[39] C. Hauert and M. Doebeli. Spatial structure often inhibits the evolution of cooperation in the snowdrift game. *Nature*, 428(6983):643, 2004. (Cited on page 37.)

[40] Q. He. *Spatio – Temporal Patterns , Correlations , and Disorder in Evolutionary Game Theory*. PhD Thesis, Virginia Tech, November 2011. (Cited on pages 9 and 63.)

[41] Q. He, M. Mobilia, and U. C. Täuber. Spatial rock-paper-scissors models with inhomogeneous reaction rates. *Physical Review E*, 82:051909, Nov 2010. (Cited on pages xiii, 38, 39, 63, and 72.)

[42] Q. He, M. Mobilia, and U. C. Täuber. Coexistence in the two-dimensional May-Leonard model with random rates. *The European Physical Journal B-Condensed Matter and Complex Systems*, 82(1):97, 2011. (Cited on pages 15 and 63.)

[43] Q. He, U. C. Täuber, and R. K. P. Zia. On the relationship between cyclic and hierarchical three-species predator-prey systems and the two-species Lotka-Volterra model. *The European Physical Journal B-Condensed Matter and Complex Systems*, 85(4):1, 2012. (Cited on pages 34 and 63.)

[44] D. J. Hoare, J. Krause, N. Peuhkuri, and J.-G. J. Godin. Body size and shoaling in fish. *Journal of Fish Biology*, 57(6):1351, 2000. (Cited on page 16.)

[45] J. Hofbauer and K. Sigmund. *Evolutionary games and population dynamics*. Cambridge University Press, 1998. (Cited on pages 10 and 11.)

[46] C. H. Hommes and M. I. Ochea. Multiple equilibria and limit cycles in evolutionary games with logit dynamics. *Games and Economic Behavior*, 74(1):434, 2012. (Cited on pages 6 and 37.)

[47] R. B. Hoyle. *Pattern formation: an introduction to methods*. Cambridge University Press, 2006. (Cited on page 13.)

[48] B. Intoy. Sierpinski simulations playlist. `http://www.youtube.com/playlist?list=PL5nkmS7zmdjyOa2viedeZttP-LCeC9jnP`, December 2014. (Cited on pages ix and 26.)

[49] B. Intoy and M. Pleimling. Extinction in four species cyclic competition. *Journal of Statistical Mechanics: Theory and Experiment*, 2013(08):P08011, 2013. (Cited on pages iii, 8, 18, 19, 58, 59, and 63.)

[50] B. Intoy and M. Pleimling. Synchronization and extinction in cyclic games with mixed strategies, March 2015. arXiv:1503.00058. (Cited on pages iii, 8, 37, and 63.)

[51] L.-L. Jiang, T. Zhou, M. Perc, and B.-H. Wang. Effects of competition on pattern formation in the rock-paper-scissors game. *Physical Review E*, 84(2):021912, 2011. (Cited on page 15.)

[52] B. Kerr, C. Neuhauser, B. J. Bohannan, and A. M. Dean. Local migration promotes competitive restraint in a host–pathogen 'tragedy of the commons'. *Nature*, 442(7098):75, 2006. (Cited on page 4.)

[53] B. Kerr, M. A. Riley, M. W. Feldman, and B. J. Bohannan. Local dispersal promotes biodiversity in a real-life game of rock–paper–scissors. *Nature*, 418(6894):171, 2002. (Cited on pages 4 and 5.)

[54] T. Killingback and M. Doebeli. Spatial evolutionary game theory: Hawks and doves revisited. *Proceedings of the Royal Society of London. Series B: Biological Sciences*, 263(1374):1135, 1996. (Cited on page 37.)

[55] B. C. Kirkup and M. A. Riley. Antibiotic-mediated antagonism leads to a bacterial game of rock-paper-scissors in vivo. *Nature*, 428(6981):412, Mar. 2004. (Cited on page 4.)

[56] J. Knebel, T. Krüger, M. F. Weber, and E. Frey. Coexistence and survival in conservative Lotka-Volterra networks. *Physical Review Letters*, 110(16):168106, 2013. (Cited on pages 10 and 11.)

[57] P. Kollock. Social dilemmas: The anatomy of cooperation. *Annual Review of Sociology*, page 183, 1998. (Cited on pages 3, 6, and 7.)

[58] K. S. Korolev, J. B. Xavier, and J. Gore. Turning ecology and evolution against cancer. *Nature Reviews Cancer*, 14(5):371, 2014. (Cited on page 9.)

[59] E. Kussell and M. Vucelja. Non-equilibrium physics and evolution—adaptation, extinction, and ecology: a key issues review. *Reports on Progress in Physics*, 77(10):102602, 2014. (Cited on page 9.)

[60] R. A. Lankau and S. Y. Strauss. Mutual feedbacks maintain both genetic and species diversity in a plant community. *Science*, 317(5844):1561, 2007. (Cited on page 4.)

[61] E. G. Leigh. *Ecological role of Volterra's equations*. Princeton University, 19, 1968. (Cited on page 1.)

[62] S. Loertscher. Rock–scissors–paper and evolutionarily stable strategies. *Economics Letters*, 118(3):473, 2013. (Cited on pages 6 and 37.)

[63] A. J. Lotka. Analytical note on certain rhythmic relations in organic systems. *Proceedings of the National Academy of Sciences of the United States of America*, 6(7):410, 1920. (Cited on page 1.)

[64] A. J. Lotka. *Elements of physical biology*. Baltimore: Williams & Wilkins, 1925. (Cited on page 1.)

[65] S. M Flaxman. The evolutionary stability of mixed strategies. *Trends in Ecology & Evolution*, 15(12):482, 2000. (Cited on page 37.)

[66] T. R. Malthus. *An essay on the principle of population*, volume 1. Cosimo, Inc., 2013. (Cited on page 1.)

[67] R. M. May. *Stability and complexity in model ecosystems*, volume 6. Princeton University Press, 2001. (Cited on page 10.)

[68] R. M. May and W. J. Leonard. Nonlinear aspects of competition between three species. *SIAM Journal on Applied Mathematics*, 29(2):243, 1975. (Cited on pages 13 and 38.)

[69] L. M. Merlo, J. W. Pepper, B. J. Reid, and C. C. Maley. Cancer as an evolutionary and ecological process. *Nature Reviews Cancer*, 6(12):924, 2006. (Cited on page 9.)

[70] M. Mobilia, I. Georgiev, and U. Täuber. Fluctuations and correlations in lattice models for predator-prey interaction. *Physical Review E*, 73(4):040903, 2006. (Cited on page 1.)

[71] M. Mobilia, I. T. Georgiev, and U. C. Täuber. Phase transitions and spatio-temporal fluctuations in stochastic lattice Lotka–Volterra models. *Journal of Statistical Physics*, 128(1-2):447, 2007. (Cited on pages viii, 1, 13, 14, and 34.)

[72] M. Mobilia, I. T. Georgiev, and U. C. Täuber. Spatial stochastic predator-prey models. In *Stochastic Models in Biological Sciences*, volume 7 of *Banach Center Publications*, page 253, Warsaw, Sept. 2008. Institute of Mathematics Polish Academy of Sciences. (Cited on page 1.)

[73] H. Morlon. Microbiology. Microbial cooperative warfare. *Science (New York, N.Y.)*, 337(6099):1184, Sept. 2012. (Cited on pages 4 and 5.)

[74] S. Mowlaei, A. Roman, and M. Pleimling. Spirals and coarsening patterns in the competition of many species: a complex ginzburg–landau approach. *Journal of Physics A: Mathematical and Theoretical*, 47(16):165001, 2014. (Cited on pages 11, 63, 71, and 72.)

[75] J. D. Murray. *Mathematical Biology I: An Introduction, vol. 17 of Interdisciplinary Applied Mathematics*. Springer, New York, NY, USA,, 2002. (Cited on page 10.)

[76] J. R. Nahum, B. N. Harding, and B. Kerr. Evolution of restraint in a structured rock-paper-scissors community. *Proceedings of the National Academy of Sciences of the United States of America*, 108 Suppl:10831, June 2011. (Cited on page 4.)

[77] J. v. Neumann. Zur Theorie der Gesellschaftsspiele. *Mathematische Annalen*, 100(1):295, 1928. (Cited on page 2.)

[78] M. F. Neuts. Absorption probabilities for a random walk between a reflecting and an absorbing barrier. *Bulletin of the Belgian Mathematical Society*, 15:253, 1963. (Cited on page 22.)

[79] T. W. Norman. Cycles versus equilibrium in evolutionary games. *Theory and Decision*, 69(2):167, 2010. (Cited on pages 6 and 37.)

[80] M. A. Nowak and K. Sigmund. Bacterial game dynamics. *Nature*, 418(6894):138, July 2002. (Cited on page 4.)

[81] M. Olson. *The logic of collective action; public goods and the theory of groups*. Harvard University Press, 1965. (Cited on page 6.)

[82] M. J. Osborne and A. Rubinstein. *A course in game theory*. MIT Press, 1994. (Cited on pages 3 and 37.)

[83] W. Poundstone. *Prisoner's dilemma*. Anchor, 2011. (Cited on page 2.)

[84] S. Rajarajeshwari, R. Kumar, and S. Sankaranarayanan. Chaotic time series prediction for rock-paper-scissors using adaptive social behaviour optimization (asbo). *International Journal of Computer Applications*, 74(11):30, 2013. (Cited on page 6.)

[85] T. Reichenbach and E. Frey. Instability of spatial patterns and its ambiguous impact on species diversity. *Physical Review Letters*, 101(5):058102, 2008. (Cited on page 38.)

[86] T. Reichenbach, M. Mobilia, and E. Frey. Coexistence versus extinction in the stochastic cyclic Lotka-Volterra model. *Physical Review E*, 74(5):051907, Nov. 2006. (Cited on pages 12 and 21.)

[87] T. Reichenbach, M. Mobilia, and E. Frey. Mobility promotes and jeopardizes biodiversity in rock–paper–scissors games. *Nature*, 448(7157):1046, 2007. (Cited on pages 15 and 38.)

[88] T. Reichenbach, M. Mobilia, and E. Frey. Self-organization of mobile populations in cyclic competition. *Journal of Theoretical Biology*, 254(2):368, 2008. (Cited on page 15.)

[89] R. J. Requejo, J. Camacho, J. A. Cuesta, and A. Arenas. Stability and robustness analysis of cooperation cycles driven by destructive agents in finite populations. *Physical Review E*, 86(2):026105, 2012. (Cited on page 7.)

[90] A. Roman, D. Dasgupta, and M. Pleimling. Interplay between partnership formation and competition in generalized May-Leonard games. *Physical Review E*, 87(3):032148, 2013. (Cited on pages 15 and 63.)

[91] A. Roman, D. Konrad, and M. Pleimling. Cyclic competition of four species: domains and interfaces. *Journal of Statistical Mechanics: Theory and Experiment*, 2012(07):P07014, 2012. (Cited on pages 15, 19, 25, 54, and 63.)

[92] J. Roughgarden. *Evolution's rainbow: Diversity, gender, and sexuality in nature and people*, page 90. University of California Press, 2013. (Cited on page 5.)

[93] F. Salvetti, P. Patelli, and S. Nicolo. Chaotic time series prediction for the game, rock-paper-scissors. *Applied Soft Computing*, 7(4):1188, 2007. (Cited on pages 6 and 37.)

[94] A. Sanchez and J. Gore. Feedback between population and evolutionary dynamics determines the fate of social microbial populations. *Public Libary of Science Biology*, 11(4):e1001547, 2013. (Cited on page 17.)

[95] H.-Y. Shih and N. Goldenfeld. Path-integral calculation for the emergence of rapid evolution from demographic stochasticity. *Physical Review E*, 90(5):050702, 2014. (Cited on page 11.)

[96] E. A. Sicardi, H. Fort, M. H. Vainstein, and J. J. Arenzon. Random mobility and spatial structure often enhance cooperation. *Journal of Theoretical Biology*, 256(2):240, 2009. (Cited on page 37.)

[97] B. Sinervo and C. M. Lively. The rock-paper-scissors game and the evolution of alternative male strategies. *Nature*, 380(6571):240, 1996. (Cited on pages 4 and 5.)

[98] B. Sinervo, D. B. Miles, W. A. Frankino, M. Klukowski, and D. F. DeNardo. Testosterone, endurance, and Darwinian fitness: natural and sexual selection on the physiological bases of alternative male behaviors in side-blotched lizards. *Hormones and Behavior*, 38(4):222, Dec. 2000. (Cited on page 4.)

[99] J. M. Smith. *Evolution and the Theory of Games*. Cambridge University Press, 1982. (Cited on pages 3 and 4.)

[100] J. M. Smith. The games lizards play. *Nature*, 380(6571):198, Mar. 1996. (Cited on page 4.)

[101] J. M. Smith and G. R. Price. The logic of animal conflict. *Nature*, 246:15, 1973. (Cited on page 3.)

[102] G. Szabó and C. Hauert. Evolutionary prisoner's dilemma games with voluntary participation. *Physical Review E*, 66(6):062903, 2002. (Cited on page 37.)

[103] G. Szabó and C. Hauert. Phase transitions and volunteering in spatial public goods games. *Physical Review Letters*, 89(11):118101, Aug. 2002. (Cited on pages 7 and 37.)

[104] B. Szczesny. *Coevolutionary Dynamics in Structured Populations of Three Species*. PhD Thesis, University of Leeds, May 2014. (Cited on page 9.)

[105] B. Szczesny, M. Mobilia, and A. M. Rucklidge. When does cyclic dominance lead to stable spiral waves? *EPL (Europhysics Letters)*, 102(2):28012, 2013. (Cited on page 15.)

[106] A. Szolnoki, M. Mobilia, L.-L. Jiang, B. Szczesny, A. M. Rucklidge, and M. Perc. Cyclic dominance in evolutionary games: a review. *Journal of The Royal Society Interface*, 11(100), 2014. (Cited on pages 9 and 11.)

[107] A. Szolnoki and M. Perc. Reward and cooperation in the spatial public goods game. *EPL (Europhysics Letters)*, 92(3):38003, 2010. (Cited on page 7.)

[108] A. Szolnoki, G. Szabó, and M. c. v. Perc. Phase diagrams for the spatial public goods game with pool punishment. *Physical Review E*, 83:036101, March 2011. (Cited on page 37.)

[109] U. C. Täuber. Stochastic population oscillations in spatial predator-prey models. *Journal of Physics: Conference Series*, 319:012019, Sept. 2011. (Cited on page 1.)

[110] U. C. Täuber. Population oscillations in spatial stochastic Lotka–Volterra models: a field-theoretic perturbational analysis. *Journal of Physics A: Mathematical and Theoretical*, 45(40):405002, 2012. (Cited on pages 1 and 11.)

[111] U. C. Täuber, M. Howard, and B. P. Vollmayr-Lee. Applications of field-theoretic renormalization group methods to reaction–diffusion problems. *Journal of Physics A: Mathematical and General*, 38(17):R79, 2005. (Cited on page 11.)

[112] D. R. Taylor and L. W. Aarssen. Complex competitive relationships among genotypes of three perennial grasses: implications for species coexistence. *American Naturalist*, page 305, 1990. (Cited on page 4.)

[113] P. Thomas, C. Fleck, R. Grima, and N. Popović. System size expansion using feynman rules and diagrams. *Journal of Physics A: Mathematical and Theoretical*, 47(45):455007, 2014. (Cited on page 11.)

[114] M. H. Vainstein and J. J. Arenzon. Disordered environments in spatial games. *Physical Review E*, 64:051905, October 2001. (Cited on page 37.)

[115] A. van den Nouweland. Rock-paper-scissors; a new and elegant proof. Department of Economics - Working Papers Series 1003, The University of Melbourne, 2007. (Cited on page 6.)

[116] S. Venkat and M. Pleimling. Mobility and asymmetry effects in one-dimensional rock-paper-scissors games. *Physical Review E*, 81(2):021917, 2010. (Cited on pages 44 and 63.)

[117] T. L. Vincent and J. S. Brown. *Evolutionary game theory, natural selection, and Darwinian dynamics*. Cambridge University Press, 2005. (Cited on page 4.)

[118] V. Volterra. Variations and fluctuations of the number of individuals in animal species living together. *Journal du Conseil*, 3(1):3, 1928. (Cited on page 1.)

[119] J. Von Neumann and O. Morgenstern. *Theory of games and economic behavior*. Princeton University Press, 1944. (Cited on page 2.)

[120] Z. Wang and B. Xu. Incentive and stability in the Rock-Paper-Scissors game: an experimental investigation, July 2014. Arxiv: 1407.1170. (Cited on page 6.)

[121] Z. Wang, B. Xu, and H.-j. Zhou. Social cycling and conditional responses in the Rock-Paper-Scissors game. *Scientific Reports*, 4:5830, 2014. (Cited on pages 6 and 37.)

[122] M. J. Washenberger, M. Mobilia, and U. C. Täuber. Influence of local carrying capacity restrictions on stochastic predator–prey models. *Journal of Physics: Condensed Matter*, 19(6):065139, 2007. (Cited on pages 1 and 34.)

[123] B. Weesakul. The random walk between a reflecting and an absorbing barrier. *The Annals of Mathematical Statistics*, page 765, 1961. (Cited on page 22.)

[124] Wikipedia. Rock-paper-scissors — wikipedia, the free encyclopedia, 2015. [Online; accessed 22-January-2015] `http://en.wikipedia.org/w/index.php?title=Rock-paper-scissors&oldid=642995095`. (Cited on page 6.)

[125] A. Winkler. *Analytic Approaches to Stochastic Many-Particle Systems: Scaling and Renormalization in Microbial Communities and in Chemical Kinetics*. PhD thesis, München, Ludwig-Maximilians-Universität, Diss., 2012, 2012. (Cited on page 9.)

[126] B. Xu. Cycles of strategies and changes of distribution in public goods game: An experimental investigation. *arXiv:1307.2064v2*, 2014. (Cited on page 7.)

[127] B. Xu, H. J. Zhou, and Z. Wang. Cycle frequency in standard Rock-Paper-Scissors games: Evidence from experimental economics. *Physica A: Statistical Mechanics and its Applications*, 392(20):4997, Oct. 2013. (Cited on pages 6 and 37.)

[128] Z. Xu, Z. Wang, and L. Zhang. Bounded rationality leads to equilibrium of public goods games. *Phys. Rev. E*, 80:061104, Dec 2009. (Cited on page 37.)

[129] L.-X. Zhong, W.-J. Xu, Y.-D. Shi, and T. Qiu. Coupled dynamics of mobility and pattern formation in optional public goods games. *Chaos, Solitons and Fractals*, 47(0):18, 2013. (Cited on page 37.)

[130] R. K. P. Zia. General properties of a system of s species competing pairwise. *arXiv:1101.0018*, 2011. (Cited on pages 11 and 63.)